UNIVERSITÉ DU QUÉBEC

THESIS

SUBMITTED TO

THE INSTITUT ARMAND-FRAPPIER

IN PARTIAL FULFILLMENT OF THE REQUIREMENTS

FOR THE DEGREE OF MASTER OF SCIENCE

IN VIROLOGY AND IMMUNOLOGY

BY

AURELIO BONAVIA

INFECTABILITY OF PRIMARY HUMAN NEURAL CELLS BY HUMAN CORONAVIRUSES 229E AND OC43

JUNE 1995

To Herb (Dr. Eling) and Solveig (Dr. Turpin) that made this happen...

To Dr. Makino who made me discover the field...

TABLE OF CONTENTS

TABLES

FIGURES

LIST OF ABBREVIATIONS

Ab	:	Antibody
ATCC	:	American Type Culture Collection
BCV	:	Bovine coronavirus
bp	:	Base pairs
cDNA	:	Complementary DNA
CMV	:	Cytomegalovirus
CNP	:	Cyclic nucleotide phosphodiesterase
CNS	:	Central nervous system
DEPC	:	Diethylpyrocarbonate
DIF	:	Double immunofluorescence
DNA	:	Deoxyribonucleic acid
EBV	:	Epstein-Barr virus
EDTA	:	Ethylenediaminetetraacetic acid
EM	:	Electron microscopy
FBS	:	Fetal bovine serum
FIPV	:	Feline infectious peritonitis virus
FITC	:	Fluorescein-conjugated antibody
GFAP	:	Glial fibrillary acidic protein
gp	:	Guinea pig
HCV	:	Human coronavirus
HEV	:	Hemagglutinating encephalomyelitis virus
HEPES	:	N-2-Hydroxyethylpiperazine-N'-2-ethanesulfonic acid
HIV	:	Human immunodeficiency virus

HTLV-I	:	Human lymphotropic virus type 1
HSV	:	Herpes simplex virus
IBV	:	Infectious bronchitis virus
IF	:	Immunofluorescence
Ig	:	Immunoglobulin
ISH	:	*In situ* hybridization
LFA	:	Lymphocyte function antigen
m	:	Mouse
mAb	:	Monoclonal antibody
mRNA	:	Messenger RNA
MHV	:	Murine hepatitis virus
MS	:	Multiple sclerosis
NSE	:	Neuron specific enolase
NY	:	Nuclear yellow
ORF	:	Open reading frame
PBS	:	Phosphate buffered saline
PCR	:	Polymerase chain reaction
PFU	:	Plaque-forming unit
r	:	Rabbit
RER	:	Rough endoplasmic reticulum
RNA	:	Ribonucleic acid
RT	:	Reverse transcription
SDS	:	Sodium dodecyl sulfate
SDS-PAGE	:	SDS-Polyacrylamide gel electrophoresis
SIF	:	Simple immunofluorescence
$TCID_{50}$	:	Lethal tissue culture infective dose

TEMED	:	N,N,N',N'-tetramethyl-ethylenediamine
TGEV	:	Porcine transmissible gastroenteritis virus
TRITC	:	Rhodamine-conjugated antibody

SOMMAIRE

Les coronavirus humains se regroupent en deux souches sérotypiques, 229E et OC43, et causent des maladies respiratoires (Myint, 1994), gastro-intestinales (Resta *et al.*, 1985), et ont été associés à des myocardites (Riski and Hovi, 1980). Plusieurs observations suggérent que les coronavirus humains pourraient aussi être neurotropes. Des particules coronavirales furent observées dans des échantillons provenant de cerveaux de patients atteints de sclérose en plaques (Tanaka *et al.*, 1976). Des taux d'anticorps anti-coronavirus humains élevés ont aussi été trouvés dans le liquide céphalo-rachidien de patients atteints de sclérose en plaques, ce qui suggère une implication possible de ce virus dans l'étiologie de la maladie (Salmi *et al.*, 1982). Deux souches de coronavirus ont été isolées a partir d'échantillons provenant du cerveau de patient atteints de sclérose en plaques (Burks *et al.*, 1980) et l'inoculation intracérebrale de ces virus à des primates a provoqué une maladie démyélinisante (Murray *et al.*, 1992). En plus, le génome du coronavirus humain 229E (HCV-229E) a été amplifié à partir d'échantillons de patients atteints de sclérose en plaque mais pas de témoins (Stewart *et al.*, 1992).

Ces études sont en accord avec l'hypothèse que les coronavirus humains pourraient être impliqués dans l'étiologie de maladies neurologiques comme la sclérose en plaques. Par contre, le neurotropisme comme tel n'a pas été prouvé jusqu'à date. Des études

avec des lignées continues ont démontré que les coronavirus humains peuvent infecter des cellules nerveuses murines et humaines, et que l'infection est productive (Pearson and Mims, 1985; Talbot *et al.*, 1994; Talbot, communication personnelle). Toutefois, ces lignées cellulaires étant immortalisées, il est possible que leur infection ne reflète pas correctement le contexte naturel. Le but du projet de maîtrise était, donc de déterminer l'infectabilité des cellules nerveuses humaines en culture primaire par les coronavirus humains 229E et OC43, une étape importante dans la démonstration du neurotropisme des coronavirus humains, les cultures primaires se rapprochant le plus de la situation *in vivo*.

Pour détecter les antigènes viraux exprimés dans les cellules infectées, nous avons utilisé la méthode d'immunofluorescence indirecte. Pour détecter les antigènes produits par HCV-229E, nous avons utilisé l'anticorps monoclonal 5-11H.6 et un anticorps polyclonal de lapin, les deux dirigés contre 229E. Nous n'avons pas pu détecter la présence d'antigènes viraux, ni dans les cellules humaines neuronales et astrocytaires fœtales, ni dans les microglies, oligodendrocytes ou astrocytes adultes humains. Pour détecter les antigènes d'HCV-OC43, nous avons utilisé l'anticorps monoclonal 4-E11.3 anti-HEV et un anticorps polyclonal de cobaye anti-OC43. Ce dernier anticorps fut produit expressément pour les expériences présentées ici. Des antigènes de HCV-OC43 ont été détectés dans des cellules humaines astrocytaires fœtales, microglies et astrocytes adultes, mais n'ont pas

été détectés dans les neurones fœtaux ni dans les oligodendrocytes adultes.

Étant donné les résultats négatifs en immunofluorescence dans le cas de HCV-229E, nous avons utilisé une technique beaucoup plus sensible, le RT-PCR/Southern blotting, qui permet de détecter l'ARN viral dans des cellules infectées. Avec cette technique, nous avons pu détecter l'ARN de 229E dans des cellules humaines astrocytaires fœtales, microglies adultes et dans un mélange d'oligodendrocytes et astrocytes adultes. Les échantillons de neurones étant très difficiles à obtenir, ils n'ont pas pu être testés avec cette technique.

Nous avons aussi pu détecter par microscopie électronique la présence d'HCV-OC43 dans des astrocytes fœtaux infectées en utilisant la méthode des coupes ultra-minces.

Nous avons détecté et quantifié les particules virales infectieuses produites après l'infection des cultures primaires par la méthode d'immunoperoxydase indirecte. Des particules infectieuses d'HCV-229E et d'HCV-OC43 ont ainsi été détectées dans des cultures d'astrocytes fœtaux infectés. Également, un taux très bas de particules infectieuses d'HCV-OC43 a été détecté dans les cultures de microglies et d'oligodendrocytes/astrocytes adultes. La différence dans les titres de virus produits pourrait être due à la différence dans la concentration de cellules dans chaque échantillon. Étant donné que

nous avons travaillé avec des cultures primaires, nous ne pouvions pas contrôler ce paramètre.

Finalement, nous avons produit cinq hybridomes sécrétant des anticorps monoclonaux anti-OC43.

Les résultats de ce projet de recherche montrent l'infectabilité de certains types de cellules gliales humaines par les deux souches prototypes du coronavirus humain.

La différence dans les degrés d'infectabilité par les deux souches du coronavirus humain n'est pas surprenante car ce phénomène a été montré dans le modèle de souris (Dubois-Dalcq *et al.*, 1982; Gagneten *et al.*, 1995). Le type de cellules qui sont infectables est similaire à celui observé dans l'étude fait avec HCV-OC43 et les cellules nerveuses primaires de souris et dans celui fait avec des cultures primaires foetales humaines (Pearson et Mims, 1985). Il est intéressant de constater que les résultats dans le modèle de souris concordent avec les résultats chez l'humain. Par contre, les résultats obtenus en culture primaire ne correspondent pas tout à fait avec ceux en lignées continues où les deux souches virales, 229E et OC43 montrent une haute infectabilité, un grand taux de production virale et où tous les types de cellules nerveuses sont infectables (Talbot, communication personnelle). Même si notre étude présente de l'information plus détaillée dans la caractérisation de l'infection des cellules nerveuses humaines par les coronavirus humains, il y encore beaucoup à faire

dans le domaine pour comprendre le neurotropisme des coronavirus, et faire le lien avec des maladies neurologiques. Finalement, il est intéressant de noter que les coronavirus humains semblent infecter les mêmes types de cellules nerveuses que le virus de l'immunodéficience humaine, soit les astrocytes et les microglies (Sharpless *et al.*, 1992)

SUMMARY

The goal of this project was to determine the infectability of human primary cultured neural cells by human coronaviruses (HCV) 229E and OC43.

To detect viral antigens expressed in infected cells we used an indirect immunofluorescence technique. To detect antigens of HCV-229E we used monoclonal antibody 5-11H.6 and a rabbit polyclonal antiserum, both anti-229E. We could not detect the presence of viral antigens in infected human fetal neurons, fetal astrocytes, adult microglia, adult oligodendrocytes or adult astrocytes. To detect antigens of HCV-OC43 we used monoclonal antibody 4-E11.3 anti-HEV and a guinea pig polyclonal antibody to OC43. The latter reagent was produced for these experiments. Viral antigens were detected in infected human fetal astrocytes, adult microglia and adult astrocytes but not in fetal neurons and adult oligodendrocytes.

To verify the negative results obtained with HCV-229E we used a more sensitive technique, RT-PCR/Southern-blotting, to detect viral RNA in infected cells. With this method, we could detect HCV-229E RNA in fetal astrocytes, adult microglia and in a mix of adult oligodendrocytes and astrocytes. The neuron samples were scarce so we could not test them with this technique.

Also, we have detected the presence of HCV-OC43 in infected cells by electron microscopy of ultra-thin sections. This was not possible for HCV-229E.

We have detected and quantified the infectious particles produced after infection of the primary cultures using the indirect immunoperoxidase method. Infectious HCV-229E and HCV-OC43 particles were detected in cultures of infected fetal astrocytes. Low amounts of infectious OC43 were also detected in infected adult astrocytes, oligodendrocytes and microglial cultures.

Finally, five hybridomas secreting monoclonal antibodies directed against HCV-OC43 were produced.

INTRODUCTION

Human coronaviruses are known to cause respiratory (Myint, 1994) and gastrointestinal (Resta *et al.*, 1985) diseases, and have been associated with myocarditis (Riski and Hovi, 1980). Human coronaviruses may also be neurotropic. The study of neurotropic human coronaviruses arose when coronavirus-like particles were observed in samples from the brain of a multiple sclerosis patient (Tanaka *et al.*, 1976). Since then, high titers of anti-human coronaviral antibodies were found in the cerebrospinal fluid of multiple sclerosis patients, suggesting a possible implication of this virus in the etiology of the disease (Salmi *et al.*, 1982). Two coronaviral strains were isolated from brain samples of MS patients (Burks *et al.*, 1980) and their intracerebral inoculation in primates caused a demyelinating disease (Murray *et al.*, 1992a). Furthermore, HCV-229E genome was amplified from brain samples of MS patients (Stewart *et al.*, 1992).

These studies are consistent with the hypothesis implicating coronaviruses in neurological diseases. However, the neurotropism of human coronaviruses has not yet been proven. Studies in continuous cell lines have shown that human coronaviruses can infect mouse and human neural cells and that the infection can be productive and persistent (Pearson and Mims, 1985; Talbot *et al.*, 1994; Talbot, personal communication). The project described here was designed to study the infectability of primary human neural cells by the two known strains of human coronaviruses, 229E and OC43. To support the hypothesis of a possible neurotropism, we wanted to determine which cell type was infectable and if the infection was productive.

LITERATURE REVIEW

1. Coronaviruses

1.1 Isolation of coronaviruses from humans

Human coronaviruses (HCV) belong to the family *Coronaviridae* (Tyrrell *et al.*, 1975). Two serogroups are known, and only one strain per group has been well characterized (Myint, 1994). These strains are HCV-229E for group 1 and HCV-OC43 for group 2. Other human strains can be found in the literature. Among them are B814, EVS, LP, 692, and other OC strains (Kendall *et al.*, 1962; Kapikian *et al.*, 1973; McIntosh *et al.*, 1967b).

In 1962, a study was carried out to isolate viruses from patients with common colds (Kendall *et al.*, 1962). This study yielded the first isolation of the B814 strain. It was not until 1965 that it was reported that B814 was an ether labile virus that failed to be maintained in tissue culture and eggs. It could only be propagated in organ cultures of human fetal tracheal epithelium (Tyrrell and Bynoe, 1965). The same year, strain 229E was isolated from a patient with an upper respiratory tract infection. The virus was characterized as an ether-labile particle with a diameter of 89 nm. The virus was unrelated to the known human respiratory myxoviruses and had an RNA genome (Hamre and Procknow, 1966). In 1967, strains 229E and B814 were detected by electron microscopy and were shown to be related to avian infectious bronchitis virus (Almeida and Tyrrell, 1967). Other studies determined that it was possible to identify infectious bronchitis virus (IBV)-like or mouse hepatitis virus (MHV)-

like particles in specimens obtained from patients with a common cold (McIntosh *et al.*, 1967a). Later in 1967, the previously isolated strains OC38 and OC43 (OC for organ culture) were successfully grown in suckling-mouse brains (McIntosh *et al.*, 1967b). In 1968, more viral isolations from patients with upper respiratory infections were reported: of these, nine samples were characterized and matched to 229E (Kapikian *et al.*, 1969). For the first time, some epidemiological data was provided, including incidence of viral infection in the population according to age and also some serological studies.

In 1969 the Coronaviruses were classified as a new group by an informal group of virologists composed of J.D. Almeida, D.M. Berry, C.H. Cunningham, D. Hamre, M.S. Hofstad, L. Mallucci, K. McIntosh, and D.A.J. Tyrrell (Almeida *et al.*, 1969). Later in 1969, it was reported that 229E could be grown in L132 cells (Bradburne, 1969). More epidemiological studies for OC strains and for 229E followed that report. A strong correlation was found between coronavirus infection and LRTD (lower respiratory tract disease) in infants and no correlation was found with upper respiratory infections. A difference in serum titers of 229E was also found in adults and in children (McIntosh *et al.*, 1970a). In 1970, strains OC38 and OC43 were successfully adapted to grow in cell monolayers of monkey origin (Bruckova *et al.*, 1970). In 1972, strain 692 was detected by immune electron microscopy, and serological studies revealed that is was not related to either 229E or OC43 (Kapikian *et al.*, 1973).

Currently more than a dozen coronaviruses have been isolated from patients and the existence of HCV is well accepted among the scientific community. Recent studies focus on the characterization of the viruses and understanding their replication mechanisms and pathogenesis. The two serologically different strains, HCV-229E and HCV-OC43, are adapted to cell culture, and were chosen as the prototypes for further studies.

1.2 Physical description

Human coronaviruses are large enveloped viruses. They can be detected by electron microscopy and show pleomorphic forms of about 80 to 200 nm in diameter. Their non-segmented genome is composed of an infectious single-stranded positive RNA of 27-30 kb. The buoyant density in sucrose is 1.18 g/ml (Pokorny *et al.*, 1975). Human coronaviruses are heat labile: they can be inactivated at 33°C or at 37°C (Bucknall *et al.*, 1972). Strain 229E is more labile but retains more infectability after freeze-thawing. Both strains are susceptible to pH changes, but OC43 is more stable (Bucknall *et al.*, 1972). Strain 229E requires a pH of about 6 for optimal growth (Lamarre and Talbot, 1989). Both strains are also sensitive to liposolvents. Growth of 229E in L132 cells can be inhibited by actinomycin D (Kennedy and Johnson-Lussenburg, 1978). Strain OC43 can hemagglutinate human group O erythrocytes, while 229E cannot (Kapikian *et al.*, 1972). Strain OC43 may induce fusion of susceptible cells (Bruckova *et al.*, 1970).

Each coronavirus particle contains approximately 200 peplomers of 10 to 20 nm embedded in its lipid bi-layered surface which gives them the appearance of a crown ("corona"). Human coronaviruses have at least three structural proteins: S, M, and N (spike, membrane associated protein and nucleocapsid respectively), with HE (hemagglutinin esterase) being an additional structural protein in HCV-OC43. The coronavirus genome also codes for several non-structural proteins that appear to be essential for viral genome replication.

1.2.1 Surface protein (S)

The peplomers on the surface of coronaviruses are formed by dimers or trimers of the S glycoprotein, previously named E2, (Myint, 1994). The S protein has a molecular mass of 160-200 kDa and is formed by two dissimilar portions called S1 and S2 that can be separated by digestion with trypsin (Sturman *et al.*, 1985). The S protein has been implicated in the recognition of the cellular receptor, cell mediated cytotoxicity, and cell fusion (Sturman *et al.*, 1985), pH dependent thermolability, inhibition of hemagglutination and also neutralization (Collins *et al.*, 1982; Schmidt and Kenny, 1982; Daniel and Talbot, 1990). The S protein bears different post-translational modifications such as acylation and glycosylation (Ricard *et al.*, 1985; Cavanagh, 1983). These modifications may be responsible for the different roles of the S protein.

1.2.2 Membrane protein (M)

The M protein, previously named E1, is the most abundant protein in the membrane and has a molecular mass of 25-26 kDa. Proteins of approximately 20 , 24 , 27, and 40 kDa, bearing different levels of glycosylation, are observed and are probably linked by disulfide bonds (Jouvenne *et al.*, 1994). The M protein varies in the extent of glycosylation, the type of linkage (N-link and O-link), and the degree to which N-linked high-mannose glycans have been converted to complex glycans (Spaan *et al.*, 1990). The M protein is highly hydrophobic and bears three α-helical transmembrane domains (Jouvenne *et al.*, 1990; Mounir and Talbot, 1992). The N-terminal half is exposed at the outer surface of the membrane (Rottier *et al.*, 1986), while the C-terminal half is located in the interior of the virus (Spaan *et al.*, 1990). The protein was also found to interact with the nucleocapsid (Sturman *et al.*, 1980; Spaan *et al.*, 1988). The M protein apparently supports the structure of the envelope and is essential for virus budding (Mounir and Talbot, 1992). Antibodies against the M protein require complement to neutralize viral infectivity (Collins *et al.*, 1982).

1.2.3 Nucleocapsid protein (N)

The N protein has a molecular mass of 47-55 kDa. It is a basic non-glycosylated protein that encapsidates the RNA genome in a flexible nucleocapsid with helical symmetry (Kennedy and

Johnson-Lussenburg, 1975). It combines three structural, and most likely functional, domains, designated I, II and III. Domains I and II contribute to the basic character of the protein, having a large amount of positively charged residues while domain III has negatively charged residues (Masters *et al.*, 1990). This protein is thought to have an important role in the replication cycle of the virus. Variation in the concentration of the N protein might be responsible for the switch from transcription to replication (Stohlman and Lai, 1979). It has been reported that this protein may be involved in the immune response against coronaviruses (Korner *et al.*, 1991; Lecomte *et al.*, 1987).

1.2.4 Hemagglutinin-esterase (HE)

The HE protein, previously called E3, is only found in the OC43 strain of HCV. It has a molecular mass of 130-140 kDa and is composed of two subunits of 65 kDa linked by disulfide bonds (King and Brian, 1982; Hogue and Brian, 1986). The HE protein recognizes sialic acid-containing receptors similar to those for influenza C viruses (Vlasak *et al.*, 1988).

1.2.5 Non-structural proteins

The non-structural proteins are proteins that are not packaged in the virion and are only synthesized and found in an infected host cell. Human coronaviruses have specific ORFs for the non-structural

proteins. The gene coding for the RNA dependent RNA polymerase occupies the 5' two thirds of the viral genome and is called mRNA 1. Strain 229E contains two ORFs in mRNA 4 and one ORF in mRNA 5 (Jouvenne *et al.*, 1992). Strain OC43 contains two ORFs between the genes of the S protein and the M protein (Mounir and Talbot, 1992). The functions of these non-structural proteins are still unknown but they are probably implicated in the synthesis of RNA or in the encapsidation process.

1.3 Cellular receptor

In the murine model, the S protein has been implicated in the recognition of the cellular receptor (Sturman *et al.*, 1985). Two glycoproteins of 110 kDa and 58 kDa have been found to bind MHV (Boyle *et al.*, 1987; Holmes *et al.*, 1994). These glycoproteins belong to the carcinoembryonic antigen family and are present on the surface of liver, intestinal epithelium, respiratory epithelium, brain and spleen cells. Holmes *et al.*, have shown that different strains of MHV shared this cellular receptor (Holmes *et al.*, 1989).

In humans, the cellular receptor for HCV-229E is aminopeptidase N, a cell-surface metalloprotease present on intestinal, lung and kidney epithelial cells (Yeager *et al.*, 1992). The cellular receptor for HCV-OC43 is still unknown.

1.4 Genome sequence

The complete nucleotide sequence of the HCV-229E RNA is now known: mRNA 1 (Herold *et al.*, 1993), mRNA 3 (S protein) (Raabe *et al.*, 1990), mRNA 4 and mRNA 5 (Raabe and Siddell, 1989b; Jouvenne *et al.*, 1992), mRNA 6 (M protein) (Raabe and Siddell, 1989a; Jouvenne *et al.*, 1990), mRNA 7 (N protein) (Schreiber *et al.*, 1989; Myint *et al.*, 1990). For OC43, sequences are known for the N protein (Kamahora *et al.*, 1989), M protein (Mounir and Talbot, 1992), S protein (Mounir and Talbot, 1993b; Künkel and Herrler, 1993), HE (Zhang *et al.*, 1992), and mRNA 4 (Mounir and Talbot, 1993a).

For HCV-229E, it has been reported that the gene sequence for the N protein is highly homologous to the N protein of porcine transmissible gastroenteritis virus, TGEV, (Schreiber *et al.*, 1989), and that the gene for the S protein is highly homologous to the S protein of IBV, feline infectious peritonitis virus (FIPV), TGEV, and MHV-JHM (Raabe *et al.*, 1990). For HCV-OC43, it has been determined that there is high level of identity between the gene for the N protein with the homologous one of bovine coronavirus (BCV). Similarly, there is relatedness between the leader sequence with MHV (Kamahora *et al.*, 1989), the M protein with BCV (Mounir and Talbot, 1992), HE with BCV (Zhang *et al.*, 1992), and the S protein with BCV (Mounir *et al.*, 1994). A phylogenetic relation has also been established between OC43 and influenza C virus, due to high homology between their HE protein (Zhang *et al.*, 1992).

1.5 Replication

The steps of adsorption, penetration and uncoating of coronaviruses are not well understood. It is thought that virus attaches to the cellular receptor through the S protein, or the HE protein if present (Boyle *et al.*, 1987; Talbot *et al.*, 1984). It is not clear if penetration occurs by fusion of the virus envelope with the plasma membrane or with endosomal membranes (Krzystyniak and Dupuy, 1984; Mizzen *et al.*, 1985; Kooi *et al.*, 1991). Once the virus uncoats, its genomic RNA, which is capped and poly-adenylated, attaches to ribosomes leading to the synthesis of the virus-specific RNA-dependent RNA polymerase (Strauss and Strauss, 1983). This polymerase may be distinct from the polymerase responsible for the production of subgenomic mRNAs. The newly synthesized polymerase transcribes the positive RNA into a full length negative strand RNA (Lai *et al.*, 1982a). While the exact mechanism is not understood, the minus strand then serves as the template for transcription of a nested set of 5 to 7 positive stranded subgenomic RNAs which are 3' coterminal (Lai *et al.*, 1982a; Stern and Kennedy, 1980). These mRNA are capped and polyadenylated (Siddell *et al.*, 1983; Spaan *et al.*, 1988; Stern and Kennedy, 1980). The translated ORF in each mRNA is situated at the non-common 5' end (Siddell *et al.*, 1982; Sturman and Holmes, 1983).

The 5' end of the plus-strand genomic and subgenomic RNAs contains an identical leader sequence of 60-70 bases (Baric *et al.*, 1983; Brown *et al.*, 1984; Lai *et al.*, 1982b). This leader sequence is important in the replication of coronaviruses, although how the leader functions is not clear. One model for coronavirus RNA transcription is the discontinuous, leader-primed transcription mechanism. The leader sequence, after being transcribed from the 3' end of the minus strand, disassociates from its template and moves downstream, reattaching to the template by means of a recognition signal which is complementary to the leader. Transcription then restarts. This process is repeated several times at the initiation site for each subgenomic RNA (Baric *et al.*, 1985; Budzilowicz *et al.*, 1985; Lai, 1986; Shieh *et al.*, 1987). This leader primed transcription may explain the high frequency of recombination found in coronaviruses and also the existence of defective interfering particles (Makino *et al.*, 1988). Because of their genome, coronaviruses are sensitive to a high frequency of mutation.

Most coronavirus proteins are translated in polysomes either attached to the RER or in the cytoplasmic matrix. Some proteins (S, HE) are co-translationally N-glycosylated whereas the M protein of HCV-OC43 is post-translationally O-glycosylated. Virion assembly takes place in the cytoplasm. The genome is encapsidated by the N protein which starts the process by binding to the leader sequence (Stohlman *et al.*, 1988). The virion then buds from the RER or Golgi apparatus (Tooze *et al.*, 1984), where the cellular proteins are excluded. Coronavirus budding only occurs where there is a high

concentration of the M protein (Holmes *et al.*, 1981; Holmes *et al.*, 1984). The life cycle is therefore entirely cytoplasmic.

1.6 Pathogenesis

Coronaviruses are in general host specific. Various strains infect a vast spectrum of animals including cat, cattle, chicken, dog, horse, monkey, mouse, pig, rabbit, rat, sheep, and turkey, causing different diseases (Table 1).

Human coronaviruses cause up to 30% of common colds in humans (Myint, 1994). The incubation period is 2 to 4 days and the symptoms include malaise, headache, profuse rhinorrhoea, nasal blockage, sneezing, fever and abdominal pain. Studies done on adult sera show a high frequency of neutralizing antibodies to HCV-229E and also high titers of antibodies against HCV-OC43. Infections by the 229E and OC43 strains of HCV seem to fluctuate from year to year (McIntosh *et al.*, 1970b; Bradburne and Somerset, 1972). A study spanning 4 years on more than four hundred patients showed that 90% of adults were seropositive for HCV (Chambon *et al.*, 1987). Other studies in infants with acute lower respiratory tract disease revealed that 8.2% of patients aged under 18 months were HCV-seropositive (McIntosh *et al.*, 1974). The geographical distribution of coronavirus infections is very wide, HCV respiratory infections have been detected in North and South America, and in Europe. Human coronaviruses have also been linked to other diseases. For example coronavirus-like

Table 1: Hosts and associated pathogenesis of coronaviruses. Other: Infectious peritonitis, runting, nephritis, pancreatitis, parotitis, and adenitis.
Abbreviations: HCV, human coronavirus; TGEV porcine transmissible gastroenteritic; CCV, canine coronavirus; FECV, feline enteric coronavirus; FIPV, feline infectious peritonitis virus; MHV, murine coronavirus; SDAV, sialodacryadenitis virus; HEV, porcine hemagglutinating encephalomyelitis virus; BCV, bovine coronavirus; RbCV, rabbit coronavirus; IBV, avian infectious bronchitis virus; TCV, turkey coronavirus.
From Holmes, 1990

Group	Virus	Host	Respiratory infection	Enteric infection	Hepatitis	CNS infection	Other
I	229E	Human	X			?	
	TGEV	Pig	X	X			X
	CCV	Dog		X			
	FBCV	Cat		X			
	FIPV	Cat	X	X	X	X	X
II	OC43	Human	X	?		?	
	MHV	Mouse	X	X	X	X	
	SDAV	Rat					X
	HEV	Pig	X	X		X	
	BCV	Cow		X			
	RbCV	Rabbit		X			X
III	IBV	Chicken	X				X
IV	TCV	Turkey	X	X			

particles were observed by electron microscopy in stools of patients with necrotizing enterocolitis. Stool samples were passaged in cultures of human fetal intestinal organs and coronaviral-like particles were produced (Resta *et al.*, 1985). It has also been associated with myocarditis (Riski and Hovi, 1980). Riski and Hovi described a patient with a common cold who developed myocarditis. High titers of antibodies against OC43 were detected in this patient. No other virus could be detected and all the bacterial tests were negative. Upon recovery, the serum titer of antibodies against OC43 declined, suggesting a link between HCV and myocarditis. There is also strong evidence to suggest that HCV may be a neurotropic virus and that it could be involved in neurological diseases, such as multiple sclerosis, as discussed below.

2. Multiple sclerosis

2.1 Pathology

Multiple Sclerosis is a neurologic demyelinating disease. It is characterized by chronic demyelination, inflammation and gliosis. In North America, it represents the most important neurological illness in early to middle adulthood. There are 50,000 people affected in Canada (Talbot, 1995), and as many as 350,000 in the United States (Hauser, 1994). The exact cause is still unknown but there is substantial evidence to believe that an environmental agent, perhaps a virus, could trigger the illness in a genetically susceptible host (Johnson, 1985).

Examination of the brain of patients at autopsy reveals sclerotic plaques or scar tissue areas visible in the white and, exceptionally, in the gray matter. Other histopathologic characteristics are perivenular cuffing, tissue infiltration by mononuclear cells, T lymphocytes or macrophages. There is a substantial loss of myelin sheaths and a clear symptom of astrocyte growth (gliosis). It seems that at the initial state of demyelination there is also oligodendrocyte proliferation (Hauser, 1994). About 35% of MS patients present no clinical signs and diagnosis of the disease is only possible at autopsy (Hauser, 1994). The symptoms of the disease vary from patient to patient. The first symptoms are either very mild, with no need to consult a physician, or very severe. Some of these include weakness in the limbs, visual blurring, sensory disturbances, diplopia, ataxia, and loss of dexterity.

Three classes of disease have been identified: relapsing-remitting MS, where the patient experiences recurrent attacks during short or extended periods of time, followed by complete, partial or no recovery; chronic progressive MS, where the patient undergoes a gradual progressive worsening form of the disease, the patient may also have some acute relapsing attacks; and benign MS, where the patient presents a fixed neurologic deficit that can vary in magnitude (Hauser, 1994).

2.2 Demographic and geographical data

Even though multiple sclerosis has been detected in different areas of the globe, it seems to follow a definite geographical pattern. Epidemiological studies show that the disease follows a North-South gradient in the Northern Hemisphere, with higher incidence further from the equator (Kurtzke, 1980). There is also a clearly increased risk of women developing MS, with a two fold preponderance in women (Duquette *et al.*, 1992). The disease shows a higher prevalence in some races: it has a high incidence in Caucasians, is extremely rare in Japan, and is unknown in black Africa (Ebers and Sadovnick, 1993). The highest prevalence was detected in the Orkney islands, north of Scotland, with a ratio of 250/100,000 (1 in 400). Multiple sclerosis is not seen in early childhood. The disease manifests itself in patients 20 to 50 years-old, with the highest onset at about 30 years of age.

2.3 Genetics

The results of epidemiological studies determining that specific ethnic groups where at higher risk suggest that a genetic factor could be involved in the etiology of multiple sclerosis. It has been reported that major histocompatibility alleles A3, B7, DR2, and DW2 on chromosome 6 are frequently found in white Caucasian MS patients (Oger *et al.*, 1987). Other alleles like DR15, and DQ6 have also been reported as high risk (Hillert and Olerup, 1993). On the other hand

alleles A2, B12, DR7, and DW7 are infrequently found in MS (Oger *et al.*, 1987). It is generally accepted that the disease susceptibility trait is in the HLA-DR-DQ subregion. Other genetic traits have been linked to MS, such as the S and SS allotype of properdine (Stewart *et al.*, 1979), and some Gm allotypes of IgG (Salier *et al.*, 1981).

Family studies have also provided interesting data. Children of MS patients have 1% more probability of getting the disease, and this percentage is increased to 3% among brothers and sisters (Sadovnick and MacLeod, 1981). Twin studies revealed that monozygote twins are 25% and dizygote twin are 8% more likely to develop the illness. These values are less than would be expected of a typical hereditary disease (McKay and Myrianthoroulos, 1966).

2.4 Environmental hypothesis

The geographic distribution of MS has led many scientists to postulate why people are more susceptible to the disease in specific areas. Besides the possible genetic component mentioned above, it has been established that people who migrate from a high to low risk area after late adolescence are still at high risk (Alter *et al.*, 1966a; Alter *et al.*, 1966b; Dean and Kurtzke, 1971; Kurtzke, 1991). A very interesting, extensive study in the Faröe islands clearly showed this "transmission" of the disease. Multiple sclerosis was undocumented in the islands prior to World War II. Contact with mainland Europe was limited until the end of World War II, when British troops arrived in

the islands to establish a military base. Interestingly, after the war, and up to twenty years later, an epidemic of MS was observed (Kurtzke and Hyllested, 1986). This strongly suggests that the British troops brought with them an environmental agent that causes multiple sclerosis.

2.5 Other viruses implicated in MS

It is now generally accepted that an environmental agent like an infectious pathogen could be linked to the development of MS. Among these infectious agents, viruses are important candidates. Not only do data in humans support this idea but there are well described demyelinating diseases caused by viruses in animals as well (e.g. coronavirus (Wang, *et al.*, 1990), and Theiler's virus (Welsh et al., 1990) in mice and Visna virus (Panitch *et al.*, 1976) in sheep. Viruses are also known to cause illnesses in the central nervous system of humans. For example, measles virus causes subacute sclerosing panencephalitis (SSPE) (Swoveland, 1991), JC virus causes multifocal leukoencephalopathy (Sweeny *et al.*, 1993), and HTLV-I induces tropical spastic paraparesis/HTLV-I associated myelopathy (TSP-HAM) (Rodgers-Johnson, 1994). The viral hypothesis is also supported by the fact that many studies revealed high antiviral antibodies titers in the sera and cerebrospinal fluid of MS patients, suggesting a viral infection of the central nervous system (Salmi *et al.*, 1982; Allen and Brankin, 1993; Sindic *et al.*, 1994; Conrad *et al.*, 1994). Several studies

have been designed to identify candidate viruses. Viral isolation or detection experiments have been performed for several viruses.

2.5.1 Measles virus

An association of measles virus to a neurological pathology was reported in 1972 when an unusual subacute encephalitis in an infant seemed to be caused by this virus (Bell *et al.*, 1972). Viral sequences have been detected in brain sections of MS and SSPE patients by *in situ* hybridization (Haase *et al.*, 1981a; Haase *et al.*, 1981b), by dot blot hybridization (Dowling *et al.*, 1986), and by PCR (Godec *et al.*, 1990).

2.5.2 Epstein-Barr virus (EBV)

An epidemiological study of 214 MS patients measured how the relative risk of developing MS correlated with EBV-induced infectious mononucleosis. It was found that patients that had infectious mononucleosis showed a 2.9 fold increased risk for MS and patients who were infected before the age of 18 years had a 7.9 fold increased risk of developing MS, suggesting a possible age-dependent host response to the virus (Martyn *et al.*, 1993). High antibody titers for EBV have also been found in serological studies of MS patients (Haahr *et al.*, 1994). However, a study using brain sections of 10 MS patients failed to detect EBV RNA using *in situ* hybridization (Hilton *et al.*, 1994).

2.5.3 JC virus

An extrapolation was proposed from an animal model of progressive multifocal leukoencephalopathy caused by the JC polyomavirus to human multiple sclerosis. It was suggested that the virus is latent in human brains and the antigens produced induce an aberrant immune response in the host (Stoner, 1993). However, JC viral genomic sequences could not be detected in brain tissues of MS patients (Buckle *et al.*, 1992), and there was no evidence of JC virus infection of MS patients (Boerman *et al.*, 1993).

2.5.4 Cytomegalovirus (CMV)

Cytomegalovirus was isolated from the brain and lymph node of a chimpanzee with acute demyelinating disease. The disease occurred more than three years after intracerebral inoculation of brain cells from a MS patient. In order to isolate the virus, several passages in cell culture had to be assessed. This suggested that the virus was present in the brain of the animal in a latent form. This was then corroborated when similar studies were performed in asymptomatic chimpanzees in the colony of origin, and it was established that they were also CMV carriers (Wroblewska *et al.*, 1979).

2.5.5 Human lymphotropic virus type 1 (HTLV-I)

This virus has been studied extensively in conjunction with MS. Several research groups have reported contradictory data in looking at HTLV-I genome in peripheral blood cells or in brains of MS patients (Reddy *et al.*, 1989; Oksenberg *et al.*, 1990; Myhr *et al.*, 1994; Kira *et al.*, 1994).

2.5.6 Retrovirus

Reverse transcriptase activity was detected in cultures of cells obtained from lumbar-punctured cerebrospinal fluid from an MS patient (Perron *et al.*, 1989), and in long-term peripheral blood mononuclear cells of patients (Hollsberg *et al.*, 1989). However, a PCR study reported that it was not possible to detect retroviral sequences in brain capillaries, brain tissue and peripheral blood mononuclear cells from MS patients (Rasmussen and Claussen, 1992). A recent study reported the presence of retroviral particles, using electron microscopy, in long-term cultures of cerebrospinal fluid and peripheral blood mononuclear cells of MS patients (Haar *et al.*, 1994).

2.5.7 Herpes simplex viruses (HSV)

This virus has repeatedly being linked to MS because a high percentage of the population is latently infected before adolescence but there is still no evidence of its implication in MS. A study using PCR to amplify the HSV genome in brain samples of 77 MS patients showed that only one was positive for HSV-1, and none was positive for HSV-2 (Nicoll *et al.*, 1992).

2.5.8 Other viruses

Other viruses such as tick-borne encephalitis virus (Vagabov *et al.*, 1982), rabies virus, scrapie, and parainfluenza virus 1 (Johnson, 1985) have been isolated from MS patients. Other reports show no detection of spumavirus, oncoviruses (Svenningsson *et al.*, 1992), and canine distemper virus (Cosby *et al.*, 1989) in MS patients. Serum antibodies also failed to recognize HIV-1, HIV-2 and, simian immunodefiency virus (SIV), (Brokstad *et al.*, 1994).

3. Coronaviruses and multiple sclerosis

3.1 HCV found in MS patients

The first report linking coronaviruses to MS was published in 1976. Coronavirus-like particles were detected by electron microscopy in a brain sample extracted at autopsy from a plaque near

the white matter of an MS patient (Tanaka *et al.*, 1976). Even though there was no immunological information or virus isolation, the finding opened a new door in the viral etiology of MS. Four years later, two coronaviruses were isolated from MS patients (Burks *et al.*, 1980). Brain homogenates from patients were cultured in suckling mice and in *in vitro* cell cultures known to be sensitive to coronavirus infection. Coronaviruses S.D. and S.K. were isolated from two MS patients. This was the first report of a coronavirus present in the human CNS.

The S.D. and S.K. strains were subsequently inoculated into mice. S.K. did not cause disease in inoculated animals, but S.D. proved to be lethal. Brain homogenates were infectious upon inoculation of other mice. However, it was not certain that these coronavirus strains were human, especially because they could only be cultured in murine cell lines. They also show striking genomic identity to murine coronavirus (Gerdes *et al.*, 1981). It is important to remember that human coronaviruses are difficult to culture in human cell lines and in fact OC43 failed to be cultured in the human lines tested with S.D. and S.K. The cultures were sampled by electron microscopy and by antibody testing and it was suggested that the viruses were not murine hepatitis virus (MHV). Further testing of the serum and spinal fluid of the patients revealed that antibodies against S.K. were present in the cerebrospinal fluid of both patients. The serum antibody concentrations against the respective isolates were elevated in the patient from whom the isolate was obtained. Antibodies to S.K. were found in 97% of MS patients and in 85% of the normal controls (Burks

et al., 1980). The two strains were then compared to other coronaviruses and it was determined that S.K. and S.D. cross react with HCV-OC43 but not with HCV-229E, MHV-A59 or MHV-JHM in a plaque neutralization assay. Both strains cross react by immunoprecipitation to HCV-OC43 and MHV-A59, suggesting a possible relatedness of these strains (Gerdes *et al.*, 1981).

Serologic studies on MS patients support the hypothesis of the implication of the virus in the etiology of this illness. One study showed a significant difference of anti-coronavirus antibody titers in the cerebrospinal fluid between MS patients and controls (Salmi *et al.*, 1982). On the other hand, the analysis of sera showed no significant difference between patients and controls. Similar findings with sera were already published by Madden *et al.*, (Madden *et al.*, 1981) and were later corroborated by a study with a large number of patients (Hovanec and Flanagan, 1983).

Further studies on detection of coronavirus RNA in the brain of MS patients were pursued. A first study failed to detect OC43 RNA in tissues from autopsies of 4 MS patients and in biopsies from one MS patient, using a cDNA probe and classical hybridization (Sorensen *et al.*, 1986). Murine-like coronavirus RNA was found in 11 out of 21 MS patients, and in 2 out of 21 controls (16 with non-neurological disease and 5 with other neurological diseases) using a S.D. coronavirus cDNA probe in *in situ* hybridization (ISH). The results were similar upon reassessment with a MHV-A59 cDNA probe.

A study was then done using cDNA probes from different species of coronavirus to determine which virus was present in positive patient samples. Samples were also tested on 9 extra negative control patients. All of the MS patients were positive for S.D., and the controls were negative; 5 out of 12 MS patients were positive for OC43, and the controls were negative. There was no positive results for HCV-229E (Murray *et al.*, 1990; 1992b). The negative results with HCV-229E were not surprising since the samples were screened with a cDNA probe of coronavirus S.D. which has been established to be unrelated to 229E. Another study used brain samples from autopsies of MS patients, neurologic controls and normal subjects. The RNA was extracted from white and gray matter and RT-PCR was performed for 229E and OC43. The results revealed the presence of 229E RNA in 4 out of 11 MS patients, and not in the 11 controls. There were no positive results for OC43 (Stewart *et al.*, 1992).

3.2 Infection of mice with HCV

Human coronavirus OC43 was lethal when inoculated intracerebrally or extraneurally into sucling CD1 mice. Resistance to infection was observed with increasing age of the animal. Animals greater than 20 days-old were not susceptible to disease after intracerebral inoculation. Transfer of immune or non-immune spleen cells from resistant animals did not protect newborn animals from OC43 infection (Pearson and Mims, 1983).

3.3 Infection of primates with HCV

Some *in vivo* tests have been conducted in primates. Owl and African green monkeys (different species) were inoculated intracerebrally with the coronavirus S.D. strain, an MS isolate. The monkeys were susceptible to infection, and showed a subacute panencephalitis. Brain autopsies showed focal areas of demyelination and pathological signs of neurological disease. Viral RNA was detected by ISH in certain areas of the brain (depending on the species), but viral antigen could not be detected (Murray *et al.*, 1992a).

3.4 Infection of human neural continuous cell lines with HCV

Two cell lines, human rhabdomyosarcoma (RD) and human glioblastoma (U-87 MG) can be infected with OC43. At 28 days post-infection, infectious virus and hemagglutinating activity were observed in both cell lines (Collins and Sorensen, 1986). Other studies of infection of continuous cell lines by human coronaviruses used the 229E strain. The L132 human embryonic lung cell line, SK-N-SH neuroblastoma cell line; H4 neuroglioma cell line; U-87 MG and U-373 MG astrocytoma cell lines, and MO3.13 immortalized human oligodendrocytes cell line were all infectable by HCV-229E, as shown by immunofluorescence detection of viral antigen using a monoclonal antibody (Talbot *et al.*, 1994), as well as by detection of infectious

viral particles (Talbot, personal communication). Similar results have now been obtained with the OC43 strain of HCV (Talbot, personal communication).

3.5 Infection of primary CNS cells with HCV

Primary cultures of neural mouse cells were infected with HCV-OC43. Using double immunofluorescence, it was determined that oligodendrocytes and Schwann cells were not infectable. The same technique revealed that astrocytes, neurons and fibroblasts were infectable but no cytopathic effects were observed. The only cell type that produced infectious virus was the neuron. A primary human embryo brain cell culture was also infected with the virus and immunofluorescence revealed that astrocytes were infectable. No cytopathic effects were observed, and no infectious virus was present. (Pearson and Mims, 1985).

3.6 Infection of primary human CNS with other viruses

Thwo studies have reported *in vitro* viral infections of human fetal cell cultures. The first study using double immunofluorescence, showed that astrocytes and fibroblasts, but not neurons, were infectable by Herpes simplex virus, types 1 and 2 (Kennedy *et al.*, 1983). The second study showed that microglia, but not astrocytes, were infectable and could produce infectious virus after infection with human immunodeficiency virus type 1 (HIV-1) (Lee *et al.*, 1993). A

related study described the infection of an adult human brain cell culture (AHB) with JC virus and the detection by double immunofluorescence of infected astrocytes and fibroblasts (Wroblewska *et al.*, 1982). Similar experiments were performed with HIV-1 and HIV-2 (Brynmor *et al.*, 1990) where they demonstrated that only one strain of HIV-1 adapted to a macrophage cell line could productively infect microglia, inducing cytophatic effects. Another report showed infection with HTLV-I in astrocytes and oligodendrocytes in a mixed glial cell culture (Watabe *et al.*, 1989). It is important to note that all these studies, including the one performed with HCV, used a mixed population cell culture system. This is an important issue when interpreting infectious virus titers because you cannot predict which cell type produced them. Also in some reports no negative controls were provided. There is only two reports where primary adult human enriched neural cells have been infected *in vitro* . The first one was a study with HIV-1 (Sharpless *et al.*, 1992), where astrocytes, oligodendrocytes and microglia cell cultures were infected with HIV-1, the only susceptible cells were the microglia, suggesting a restricted tropism for HIV-1. Similarly enriched oligodendrocytes, microglia and a mixture of microglia and astrocytes were infected with HTLV-I founding that only microglia were infectable (Hoffman *et al.*, 1992). Is interest to note that the results with astrocytes and oligodendrocytes do not match Watabe's previous study with mixed cultures.

MATERIALS AND METHODS

1. Primary cultures of cells from human brain

Primary cultures of cell mixtures or enriched preparations of oligodendrocytes, astrocytes and microglia from human brain tissue were provided by Dr. Voon Wee Yong (Montreal Neurological Institute, McGill University, Montreal, Quebec, Canada). Cells were obtained from brain biopsies performed on epileptic patients in an attempt to ameliorate an intractable form of the disease. Cells were then put in culture in Dr. Yong's laboratory following his own protocol (Yong and Antel, 1992). Brain tissue extracted either *en bloc* or by Cavitron™ ultrasonic aspiration were washed in phosphate buffered saline (PBS). Tissue was diced with scalpels and washed a few times in PBS. The tissue was then trypsinized in 0.25% (w/v) trypsin with 50 µg/ml DNase in a water bath at 37°C on a magnetic plate. After 30 min. to 1 hr the solution was passed through a Büchner funnel nylon mesh, and 1 ml of fetal bovine serum (FBS) was added to inactivate the trypsin; PBS was added to recover the cells trapped in the mesh. The filtrate was then centrifuged at 1,200 rpm for 10 min. The supernatant was discarded, leaving 2 ml to resuspend the pellet. Phosphate buffered saline was added, and the solution was transferred to a 40 ml polycarbonate tube with 9 ml of Percoll to obtain a 30% (v/v) final concentration. The tube was then centrifuged at 15,000 rpm for 30 min. The viable cell layer was transferred to a 50 ml plastic tube and diluted with PBS. The cells were recentrifuged at 2,000 rpm for 10 min. The supernatant was discarded, leaving 1 ml to resuspend the pellet. Dulbecco's modified Eagle medium (DMEM) was added to a final

volume of 45 ml and centrifuged at 1,000 rpm for 10 min. The supernatant was discarded, leaving 1 ml to resuspend the pellet. Culture medium was added to bring up the volume to 25 ml and centrifuged at 600 rpm for 10 min. This last procedure was performed twice. The cells were resuspended at a concentration of $2x10^6$ to $4x10^6$ cells/ml and plated onto 10 µg/ml poly-L-lysine coated coverslips or Falcon flasks in feeding medium; DMEM high glucose (Gibco, Grand Island, New York, USA) supplemented with 5% (v/v) FBS (Gibco), and 10 µg/ml gentamicin (Gibco). The cells were incubated in a humidified incubator at 37°C and 5% (v/v) CO_2. Due to the age of the patients (mostly adults), neurons did not survive the procedure. Therefore, neuron preparations were obtained from brain tissue samples from therapeutic abortions. Fetal cultures were performed as described by Yong V W *et al.*, (1992). These procedures have official approval from the Human Ethics Committee. After transportation to our laboratory, all cells were kept in culture in glass or plastic poly-L-lysine coated micro discs or 16 well Lab-Tek® dishes (Nunc Inc., Naperville, Illinois, USA). The culture medium used was DMEM high clucose (Gibco) supplemented with 5% (v/v) FBS (Gibco), and 10 µg/ml gentamicin (Gibco). Incubation was at 37 °C and 5% (v/v) CO_2 in a humidified chamber incubator.

2. Continuous cell lines

Human coronavirus 229E stocks were grown and tested in a human embryonic lung cell line, L132, from the American Type Culture Collection (ATTC), Rockville, Maryland, USA. Human coronavirus OC43 stocks were grown and tested in a human colorectal adenocarcinoma cell line (HRT-18). This cell line was graciously provided by Dr. David Brian (Department of Microbiology, University of Tennessee, Knoxville, Tennessee, USA). Both cell lines were kept in culture in MEM Earle: M199 Hanks (1:1, v/v) media supplemented with 10% (v/v) FBS (Gibco), 50 µg/ml gentamicin (Gibco) and 0.13% (w/v) of sodium bicarbonate (Gibco, Grand Island, New York, USA) in a humidified chamber incubator at 37°C and 5% (v/v) CO_2.

A non-secreting mouse myeloma cell line, P3X653-AG8.653 (ATCC) was used as a fusion partner for the production of hybridomas by cell fusion. This cell line was kept in culture in RPMI 1640 (Gibco) supplemented with 2.5 µg/ml Fungizone (Gibco), 1 mM MEM sodium pyruvate (Gibco) and 50 µg/ml gentamicin (Gibco). Cells were kept in culture in a humidified chamber incubator at 37°C and 5% (v/v) CO_2.

3. Virus

Both virus strains HCV-229E and HCV-OC43 were obtained from the ATCC. The third passage of HCV-229E (P3, 19-01-94) in susceptible cell line L132, and the fourth passage of HCV-OC43 (P4, 21-04-94) in susceptible cell line HRT-18 from the laboratory stocks stored at -90 °C were used for all experiments described herein. The titer of the P3 stock of HCV-229E was $5.5x10^5$ $TCID_{50}$/ml or $2.1x10^6$ PFU/ml and the titer of the P4 stock of HCV-OC43 was $5.15x10^5$ $TCID_{50}$/ml or $3.6x10^5$ PFU/ml.

4. Production and purification of HCV-OC43

Petri dishes, 150x20 mm (Nunc, Roskilde, Denmark), were seeded with 50 ml of a 75,000 cells/ml suspension of HRT-18 cells in MEM Earle : M199 Hanks medium (1:1; v/v) supplemented with 10% (v/v) FBS (Gibco), 50 µg/ml gentamicin (Gibco) and 0.13% (w/v) sodium bicarbonate (Gibco). After 4 days of incubation at 37°C, in a humidified incubator containing 5% (v/v) CO_2 (at which time the cells were at about 80% confluence), the growth medium was removed and replaced with 3 ml of an inoculum containing 1/10 (v/v) OC43 (MOI of 0.02), and 1/500 (v/v) TPCK-trypsin (Sigma, St. Louis, Missouri, USA) (10 U/ml) in cell growth medium. The Petri dishes were gently shaken manually every 10 min. for about 2 hrs to ensure proper contact of the cell layer with the viral inoculum. Two hours later, 12

ml of growth medium was added and the cells were incubated at 33°C, 5% (v/v) CO_2 in a humidified chamber incubator for 4 days. The supernatant was collected and centrifuged for 20 min. at 10,000 x *g*. The supernatant was brought to a final concentration of 0.5 M NaCl (Anachemia, Montreal, Quebec, Canada) and 10% (w/v) PEG-8000 (Sigma, St. Louis, Missouri, USA). The solution was placed on a magnetic plate and stirred overnight at 4°C. The solution was then centrifuged at 10,000 x *g* for 30 min. at 4°C and the pellet was resuspended in TMEN, pH 6.2 to a final volume of between 1/100 and 1/50 of the initial volume. The TMEN buffer contained 0.05 M Tris-base (Boehringer Mannheim, Laval, Quebec, Canada), 0.58% (w/v) maleic acid (Sigma), 0.038% (w/v) EDTA (Sigma), 0.58% (w/v) NaCl (Anachemia), with the pH adjusted to 6.2 with 5 M NaOH. The virus was purified on a Nycodenz® (Nycomed, Oslo, Norway) discontinuous gradient prepared by adding 3 ml of 50% (w/v) Nycodenz® in TMEN, pH 6.2 and 28.5 ml of 10% (w/v) Nycodenz® in TMEN, pH 6.2 solution in a Beckman "Ultra clear" 13x51 mm centrifuge tube (Beckman, Palo Alto, California, USA). The viral solution was layered on top of the gradient. The gradient was ultracentrifuged at 4°C and at 83,000 x *g* for 4 hrs. The gradient was then fractionated from the bottom (1 ml/fraction) in a fraction collector. The viral sample was detected at the interface between the two Nycodenz® concentrations as a dense band. The fractions containing the viral sample were dialyzed against TMEN, pH 6.2. For further purification, a continuous gradient was prepared by stacking 2 ml of 50%, 40%, 30%, 20%, and 10% (w/v) Nycodenz® respectively in TMEN, pH 6.2. The viral solution was

layered on top, and the gradient was ultracentrifuged at 100,000 x *g* overnight (15 hrs). The gradient was fractionated into 500 µl fractions. Again, a dense band containing virus was present. The fractions that contained it were collected and then analyzed by electron microscopy after negative staining. To achieve this, 50 µl of 1/2 dilution of every sample was centrifuged for 5 min. at 20 PSI in a Beckman Airfuge centrifuge in conjunction with an electron microscopy grid. The grid was then immersed in a solution of 3% (w/v) phosphate tungsten acid (Mecalab, Montreal, Quebec, Canada) for 1 min., then dried at room temperature. The fractions containing the virus were dialyzed against TMEN, pH 6.2 and a protein assay was performed.

5. Infection of cells

Prior to all infections, the virus inoculum was thawed in a 37°C water bath and sonicated for 30 seconds in a B-12 ultrasonic cleaner (Branson, Shelton, Connecticut, USA) to disintegrate possible clusters formed during freezing. Cells were inoculated in either in 60x15 mm or 100x15 mm Petri dishes or in 16 well Lab-Tek® dishes (Nunc). Petri dishes were used when cells were seeded in micro discs. The micro discs were carefully and sterilely transferred to the Petri dish and enough inoculum was added to cover the discs. In the Lab-Tek® dishes (Nunc), the culture medium was discarded and replaced with inoculum. An HCV-229E and HCV-OC43 inoculum of 1:9 (v/v) and 1:1 (v/v), respectively, was prepared in DMEM (Gibco) supplemented with

5% (v/v) FBS (Gibco), 10 µg/ml gentamicin (Gibco). Incubation took place in a humidified chamber incubator for 2, 4 or 7 days at 37°C and 5% (v/v) CO_2. Infections were performed at a multiplicity of infection (MOI) of 4 or 8 depending on the type of culture dish used.

$$MOI = \frac{Vv \times Vt}{C}$$

Vv: Viral volume (ml)

Vt: Viral titer (PFU/ml)

C: Number of cells

6. Purification of antibody

Protein A-Sepharose CL-4B or Protein G-Sepharose 4 Fast Flow (Pharmacia, Uppsala, Sweden) were used for column chromatography. A protein G column was an alternative when the protein A column failed to give a good yield of antibody. Protein A was used to purify anti-c-myc monoclonal antibody (mAb) and Protein G was used to purify antiviral mAb 4-E11.3 and mAb 5-11H.6. All solutions were stored at 4°C and all procedures were performed in a cold room at 4°C. The beads were washed for 15 to 30 min. with the appropriate buffer; 0.05 M Tris-HCl (Boehringer Mannheim) buffer, pH 8.5 for Protein A and 0.02 M phosphate buffer, pH 7.0 for Protein G. Monoclonal antibody stocks were derived from ascites fluids. In order to adjust

the pH, they were dialyzed against the buffer used to wash the beads. The antibody sample was centrifuged in a high speed centrifuge (Savant, Farmingdale, New York, USA) for 5 min. at 10,000 x *g* to avoid cell debris blocking the column. The supernatant was passed through the column and a 30 min. adsorption was allowed to let the antibodies bind properly to the beads. The column was then washed until the optical density of the effluent was back to zero indicating that all undesirable proteins were rinsed off. Bound antibodies were then eluted with 0.05 M citrate buffer, pH 3.0 for Protein A and 0.1 M glycine-HCl buffer, pH 2.7 for Protein G. The purified antibody was recovered with a fraction collector (Gilson, Middleton, Wisconsin, USA). To each fraction, 100 µl of 2 M Tris-HCl (Boehringer Mannheim), pH 8.5 buffer was added to restore a neutral pH to avoid protein denaturation. For the same reason, the column was afterwards washed with a high pH buffer. If necessary, the recovered antibody solution was then concentrated in a disposable ultrafiltration Centriprep-100 device (Amicon, Beverly, Massachusetts, USA). By centrifuging at 700 x *g* for 30 min. the Centriprep-100 filter allows the free flow of all molecules less than 100 kDa, leaving the immunoglobulins of 150-160 kDa trapped in a smaller volume.

7. Preparation of F(ab')$_2$ fragments of antibody

A solution of 1 mg/ml of pepsin (Sigma) was prepared in 0.1 M citrate buffer, pH 3.5. The Ab solution was then acidified to pH 3.5 with 0.1 M citrate buffer, pH 3.0. After adding 0.031 mg of pepsin per mg of Ab, the solution was placed in a water bath at 37°C. The optimal digestion time was determined by a pilot experiment where samples where taken at timed intervals. The digestion was verified by differences in molecular mass between the whole antibody, 150-160 kDa, and the F(ab')$_2$ fragments, 110 kDa, by resolution in a 12% polyacrylamide SDS (Bio-Rad) Coomasie blue stained gel with protein molecular mass standards (Pharmacia). The separating gel consisted of a solution of 25% (v/v) of 1.5 M Tris-HCl (Boehringer Mannheim), pH 8.8, 0.1% (w/v) SDS (Bio-Rad), 12% (w/v) acrylamide/Bis (Bio-Rad), 0.05% (w/v) ammonium persulfate (Anachemia), 0.5% (v/v) TEMED (Bio-Rad). The stacking gel consisted of 25% (v/v) 0.5 M Tris-HCl (Boehringer Mannheim), pH 6.8, 0.1% (w/v) SDS (Bio-Rad), 3.9% (w/v) acrylamide/Bis, 0.05% (w/v) ammonium persulfate, 0.1% (v/v) TEMED. The gel was stained for 30 min. in 0.1% (w/v) Coomassie blue R-250 (Bio-Rad), 40% (v/v) methanol, 10% (v/v) acetic acid and then destained with 40% (v/v) methanol, 10% (v/v) acetic acid. To purify the F(ab')$_2$ fragments the digest was then repassed through the protein A or protein G column. This time the F(ab')$_2$ fragments were recovered in the wash while the Fc portions or the remaining undigested Abs bound to the column. The F(ab')$_2$ fragments were then

concentrated in a Centriprep-30 device (Amicon, Beverly, Massachusetts, USA) at 1,000 x *g*. Centriprep-30 filter allow molecules under 30 kDa to flow through, leaving the $F(ab')_2$ fragments trapped in a smaller volume.

8. Production of polyclonal antibody to HCV-OC43

A Harkley guinea pig was used for the production of an anti-OC43 polyclonal serum. The guinea pig was bled prior to immunization in order to obtain pre-immune serum. The animal was immunized subcutaneously with 300 µg of purified virus in a 1:1 solution in complete Freund's adjuvant. The animal was challenged 4 times, at 2 week intervals, with a subcutaneous injection of 300 µg of semi-purified virus in a 1:1 solution in incomplete Freund's adjuvant. At each injection, the animal was bled to verify, by immunofluorescence, if the serum contained antibodies to OC43 and to determine if their concentration had reached a plateau. When the plateau was reached, the animal was bled out via a heart puncture to collect serum.

9. Production of monoclonal antibody to HCV-OC43

A BALB/c mouse (Charles River, St. Constant, Quebec, Canada) was immunized intraperitoneally with 100 µg of semipurified HCV-OC43 (see section 4) emulsified in 1:1 (v/v) complete Freund's adjuvant (Difco, Detroit, Michigan, USA). The mouse received 3 subsequent booster injections. The first booster was with 100 µg semipurified HCV-OC43 (see section 4) emulsified in 1:1 (v/v) incomplete Freund's adjuvant (Difco) injected intraperitoneally 6 months prior to the fusion. The last two boosts were 200 µg of HCV-OC43 P4 (see section 3) by intravenous injection at 20 and 3 days prior to the fusion, respectively. Five days before the fusion the 653 myeloma cell line (see section 2), was expanded. Expansion consisted in daily splitting of the cells at a 1:1 ratio with growth medium. A cell count was done to verify a cell survival rate of at least 90%. A cell solution of 1:1 in 0.1% (w/v) Trypan Blue (Sigma) was made and unstained viable cells were counted in a hemacytometer (Reichert, Buffalo, New York, USA). The mouse was bled from the retroorbital plexus with a heparinized capillary tube in order to save the plasma as a source of polyclonal antibodies against HCV-OC43. The mouse was sacrificed by cervical dislocation. The spleen was removed and teased in a Petri dish with 2.5 ml of RPMI until a homogenous single cell suspension was obtained. The solution was transferred to a 50 ml tube with 7.5 ml of RPMI. The Petri dish was rinsed with 2 ml of medium and this was added to the 50 ml tube. The whole solution

was filtered through a sterile gauze in a funnel. The filtrate was centrifuged at 100 x *g* (700 rpm, Beckman GS-6R) for 10 min. The supernatant was discarded and the pellet resuspended in 1.5 ml of cold erythrocyte lysis buffer, containing 0.83% (w/v) ammonium chloride (Anachemia), and 1% (w/v) HEPES (Gibco), pH 7.6-7.8 (adjusted with HCl or NaOH), and filtered through a 0.22 µm Millex-GV device (Millipore, Bedford, Massachusetts, USA). After 10 min. of incubation on ice, 5 ml of RPMI were added, and the solution was transferred to a second 50 ml tube containing 2 ml of FBS and centrifuged at 100 x *g* for 10 min. The supernatant was discarded and the pellet resuspended in 10 ml of RPMI (Gibco) containing 10% (v/v) FBS (Gibco), and 20 mM HEPES (Gibco). The solution was placed in a 100x15 mm sterile Petri dish and left for 30 min. at 37°C to allow adsorption of macrophages and fibroblasts to the plastic. The supernatant was recovered and the Petri dish carefully washed twice with 5 ml of RPMI. The washes were combined with the supernatant the cells were pelleted at 100 x *g* for 10 min. The supernatant was discarded and the pellet resuspended in 5 ml of RPMI. The cells were rinsed two times in this manner. After being resuspended, the cells were counted in a hemacytometer. A volume of 0.06 ml of the suspension of spleen cells were kept on ice in a tube containing 0.94 ml of RPMI (Gibco)-HAT supplemented with 20% (v/v) FBS (Gibco). RPMI (Gibco)-HAT is RPMI (Gibco) with 100 µM hypoxanthine (Sigma), 0.4 µM aminopterin (Sigma) and 16 µM thymidine (Sigma). In parallel with the last two centrifugations mentioned above, the 653 cells were simultaneously centrifuged under the same conditions. A volume of 1

ml containing $2.4x10^5$ cells in RPMI (Gibco)-HAT with 20% (v/v) FBS (Gibco) was kept on ice. In a 50 ml tube the spleen cells were combined with the myeloma cells at a 5:1 ratio. The solution was centrifuged at 100 x *g* for 7 min. The supernatant was discarded, leaving approximately 0.1 ml of medium in the tube to resuspend the pellet. During the next 45 seconds, 0.5 ml of 50% (w/v) PEG-8000 dissolved in RPMI was added dropwise. At the end of the first minute the tube was agitated very slowly in a circular motion for 15 seconds. The solution was left for 1 min., and 17.5 ml of RPMI was added dropwise in three consecutive steps while agitating the tube; 0.5 ml in one min., 2 ml in 1 min. and 15 ml in 3 min. The solution was centrifuged twice at 100 x *g* for 7 min., the supernatant was discarded, the pellet was resuspended in the volume left after decantation, and 10 ml of RPMI (Gibco)-HAT with 20% (v/v) FBS (Gibco) was added. The solution was split in two and transferred to a 50 ml tube with 20 ml of RPMI (Gibco)-HAT with 20% (v/v) FBS (Gibco). β-mercaptoethanol (Bio-Rad) was added to one of the tubes to reach a final concentration of 50 mM. Each solution was sterilely and evenly distributed with a micro pipette in a 96-well plate (Flow, McLean, Virginia, USA) (100 µl in each well). For controls, spleen and myeloma cells were also plated. Plates were placed in an incubator with humidified atmosphere at 37°C, 7% (v/v) CO_2. Four days later, 100 µl of RPMI (Gibco)-HAT with 20% (v/v) FBS (Gibco) were added. Twice a week, hybridomas were nourished taking away half of the supernatant and replacing it with new medium. After 3 weeks, the medium was changed to RPMI (Gibco) with 20% (v/v) FBS (Gibco).

Hybridomas were then tested for antiviral antibodies in a single immunofluorescence (see section 10). The hybridoma was cloned if positive for HCV-OC43. To clone, a limiting dilution was performed and plated a 96-well plate (Flow) one third of which contained 3 cells per well, 1 cell per well, or 0.3 cell per well, respectively. The single clones obtained were then retested in single immunofluorescence (see section 10). If positive, they were centrifuged at 200 x *g* for 7 min. The pellet was resuspended in cold RPMI (Gibco) containing 20% (v/v) FBS (Gibco) and 10% (v/v) dimethyl sulfoxide (Sigma) to reach a final concentration of 1.5-4x10^6 cells/ml. The solution was aliquoted in 1.5 ml tubes and kept at -20°C for 6 hrs. Then kept at -70°C for 24 hrs and finally placed in liquid nitrogen for storage.

10. Single immunofluorescence (SIF)

The goal of the single indirect immunofluorescence was to detect viral antigens in an infected cell. Cells (infected or not) were fixed in 70% (v/v) ethanol for 15 min. at room temperature. The primary antibody (anti-virus or control), was added to the fixed cells and incubated in a humidified chamber at room temperature for 45 min. Three washes in PBS followed the incubation. A fluorescein-conjugated antibody against the same animal species from which the primary antibody was obtained, was then added to the monolayer and incubated for 45 min. in the same conditions. After 3 washes in PBS, the slides were mounted with Gelvatol and stored at -20°C. Gelvatol was prepared by mixing 4 g of glycerol with 2 g of polyvinylalcohol

(Sigma), the solution was left at room temperature for 15 to 20 min. Fourteen ml of 0.1 M Tris-HCl (Boehringer Mannheim), pH 8.0-8.3 was added and the solution was placed on a magnetic stirrer and allowed to mix well for 10 min. The solution was then incubated at 37°C for 20 to 24 hrs. After incubation it was centrifuged at 3,000 rpm for 20 min. The supernatant (Gelvatol) was recovered and kept at 4°C. Slides were examined under ultraviolet light with a Reichert immunofluorescence microscope at a magnification of 250 times, using fluorescein and rhodamine filters.

11. Double immunofluorescence (DIF)

The goal of the double immunofluorescence was to obtain simultaneous staining of a viral antigen and a cellular marker in order to detect the infectability of a particular type of human neural cell.

Cells (infected or not) were fixed in 70% (v/v) ethanol for 15 min. at room temperature. The primary antibody (anti-virus or control), was added to the fixed cells and incubated in a humidified chamber at room temperature for 45 min. Three washes in PBS followed the incubation. A fluorescein-conjugated antibody against the same animal species from which the primary antibody was obtained was then added to the monolayer and incubated for 45 min. at the same conditions. After 3 washes in PBS the antibody to the appropriate cell marker was added to the monolayer and incubated for 45 min. After 3 washes in PBS, the rhodamine-conjugated

antibody against the same animal species in which the antibody to the cell marker was produced, was added and incubated for 45 min. After three more washes in PBS, Hoechst dye 10 mg/ml in the form of Nuclear Yellow was added and incubated for 20 min. After three more washes in PBS, and one wash in double distilled and deionized water the cell slides were mounted in Gelvatol (see above) and kept at -20°C, until they could be examined for fluorescence.

If the cell marker antibody required live cells for staining, the fixation step was omitted and the anti-marker antibody incubation was done first. After incubation with the appropriate fluorochrome-conjugated antibody against the animal species in which the antibody to the marker was obtained, the cells were fixed and a SIF for the virus was performed. The animal species in which the antiviral and cell marker antibody were produced, were different in order to avoid recognition of both antibodies by the fluorochrome-conjugated antibody. Preliminary experiments were also performed to make sure that there were no inter-species cross-reactivities of the fluorochrome-conjugated antibodies. Three types of controls were used. The first was a DIF with non-infected cells to verify virus-free samples. The second was a replacement of the antiviral antibody with the antibody dilution buffer in order to detect overlap in the wavelengths of the fluorescein and rhodamine fluorochromes. The third control was a substitution of the antiviral antibody with an isotypic control in the case of a mAb or by a pre-immune serum in the

case of a polyclonal antibody. This was to verify that there was no non-specific binding of antibodies to the cells.

12 Antibodies used in immunofluorescence

To detect HCV-229E, we used a mouse mAb (5-11H.6), directed against the S protein and a rabbit polyclonal antibody. The mouse antibody was produced in our laboratory and was of the IgG1 isotype, the polyclonal antibody was graciously provided by Dr. Serge Dea, Institut Armand-Frappier, Laval, Quebec, Canada. To detect HCV-OC43, we used three different antibodies. The first one was a mouse mAb (4-E11.3) of the IgG1 isotype, directed against the N protein of HEV. There is a high homology between the N protein of HEV and OC43 and the antibody shows cross-reactivity with the human virus antigen in infected cells. . The second was a rabbit polyclonal antibody. Both antibody were graciously provided by Dr. Serge Dea. The third antibody was a guinea pig polyclonal antibody produced in our laboratory. All antiviral antibodies could be used on fixed cells. In order to stain a specific cell type we used antibodies to specific cell markers. To detect astrocytes, we used a rabbit anti-cow glial fibrillary acidic protein (GFAP) that reacts strongly with human GFAP in fixed cells. The antibody was obtained from DAKO, Carpinteria, California, USA. For oligodendrocytes we used two markers. The first was a mouse mAb, of the IgG3 isotype, against galactocerebroside (H8H9). Monoclonal antibody H8H9 had to be used on live cells. The second was an affinity purified rabbit polyclonal antibody against

cyclic nucleotide phosphodiesterase (CNP) that recognizes CNP1 and CNP2 in fixed cells. It was graciously provided by Dr. Peter Braun, McGill University, Montreal, Quebec, Canada. To detect microglial cells, we used three antibodies. The first was mouse mAb Leu-M5 used on fixed cells. It is specific for the alpha subunit of the CD11c heterodimer present on monocytes, granulocytes and natural killer cells. It could be used on fixed cells and was of the IgG2b isotype. The second was a mouse mAb against lymphocyte function antigen (LFA). It recognized the CD11c marker on fixed cells and was of the IgG1 isotype. It was obtained from Boehringer Mannheim. The third was a mouse mAb against the CD68 marker of macrophage (KP1) that stained fixed cells and was of the IgG1 isotype. To detect neurons we used a rabbit anti-bovine neuron specific enolase (NSE) that recognized the alpha-subunit of this enzyme expressed primarily in neurons. It was obtained from DAKO. It stained fixed cells and was of the IgG1 isotype. As a nuclear marker we used Nuclear Yellow (NY). All antibodies, unless specified, were graciously provided by Dr. Voon Wee Yong. Five fluorochrome-conjugated antibodies were used as secondary antibodies. The first one was fluorescein-conjugated goat $F(ab')_2$ fragments to guinea pig IgG (FITCgp) (Organon Teknika Corporation, Durham, North Carolina, USA). The second was fluorescein-conjugated goat affinity purified $F(ab')_2$ fragments to mouse IgG (FITCm) (Organon Teknika Corporation). The third was fluorescein-conjugated $F(ab')_2$ fragments of affinity purified anti-rabbit IgG (FITCr) (Organon Teknika Corporation). The fourth was a rhodamine-conjugated goat IgG fraction to mouse IgG, IgA, IgM

(TRITCm) (Organon Teknika Corporation). The fifth was a rhodamine-conjugated goat affinity purified antibody to rabbit IgG (TRITCr) (Organon Teknika Corporation).

13. RNA extraction

The RNA was extracted by a boilate method. The supernatant of the infected or non-infected cells was discarded and the cells washed three times with PBS. The PBS buffer contained 0.8% (w/v) sodium chloride, 0.02% (w/v) potassium chloride (Anachemia), 0.115% (w/v) dibasic sodium phosphate (Anachemia), and 0.02% (w/v) potassium phosphate (Anachemia). The cells were trypsinized with 1 or 2 ml of 0.25% (w/v) trypsin, depending on the size of the culture plate. The enzyme was added and left at 37°C for 5 min. The cells were gently scrapped off by pipetting several times with the help of a Pipet-Aid (Drummond Scientific, Broomall, Philadelphia, USA). The solution was placed in a 1.5 ml Eppendorf tube and spun down in a 5415C centrifuge (Eppendorf, Hamburg, Germany) at 9,000 rpm (5,900 x *g*) for 10 min. The pellet was resuspended in 200 µl aliquot of 1% (w/v) diethyl pyrocarbonate (Sigma). In order to obtain a more concentrated solution of RNA, each pellet from the same cell batch was resuspended in the same 200 µl of 1% (w/v) diethyl pyrocarbonate. The solution was boiled for 5 min. and then stored at -20 °C.

14. Reverse transcription (RT) and polymerase chain reaction (PCR)

The set of primers used for the RT-PCR was previously reported by Stewart *et al.*, (1992). The set was composed of primers E7 and E9. E7 was an oligonucleotide used for PCR amplification that corresponded to bases 964-982 on mRNA 7 of HCV-229E, with a sequence of 5'-AACTTTGGAAGTGCAGGTGTTGTG-3'. E9 was an oligonucleotide used for RT and PCR amplification that corresponded to bases 1242-1265 on mRNA 7 of HCV-229E, with a sequence of 5'-TGGTTCAGCAGTTGCAGGTGAAGT-3'.

For RT, 76 µl of RNA solution were combined with 4 µl of primer in a PCR reagent cup with integrated volume limitation (Sarstedt, Ville St. Laurent, Quebec, Canada), and placed in a DNA thermal cycler (Perkin Elmer, Norwalk, Connecticut, USA) for an incubation of 5 min. at 65°C, followed by a slow cool down to 22°C (to break secondary structures and allow annealing of the primer oligo). After cooling, 16 µl of a reverse transcription master mix was added. The master mix contained 12.5% (v/v) of "RNA guard" RNase inhibitor (Pharmacia), 62.5% (v/v) of 10X Moloney RT Buffer, 12.5% (v/v) of 20 mM DNA polymerization mix (Pharmacia) and 18.75% (v/v) of Moloney Murine Leukemia Virus Reverse Transcriptase (Pharmacia, Uppsala, Sweden). The 10X Moloney Buffer contained 500 mM Tris-HCl (Boehringer Mannheim), pH 8.0, 625 mM potassium chloride (Anachemia), 30 mM

magnesium chloride (Anachemia) and 100 mM dithiotreitol (Pharmacia). An incubation in the thermal cycler at 42°C for 90 min. was performed and then the solution was kept at 4°C. For the PCR, 50 µl of the cDNA were used in combination with 50 µl of a PCR master mix. The master mix contained 20% (v/v) of 10X Taq Buffer (Bio/Can Scientific, Mississauga, Ontario, Canada), 5 mM magnesium chloride (Bio/Can Scientific), 4% (v/v) of 20 mM dNTP (Pharmacia), and 4% (v/v) of each primer (10 pmol/µl). The solution was placed in the thermal cycler for an incubation at 94°C for 5 min., and 5 min. at 60°C. Then, 1 µl of a solution of 1:1 Taq (Pharmacia) :Moloney 1X Buffer was added and the thermal cycler was set for 30 cycles of 2 min. at 72°C, 1 min. at 94°C, and 2 min. at 60°C. At the end, a 10 min. incubation at 72°C was done, and the solution was stored at 4°C.

15. Southern blotting

DNA samples were separated by electrophoresis in a 5% (w/v) SeaKem agarose (FMC, Rockland, Maine, USA) gel with 1 mg/ml of ethidium bromide using TAE as solvent and running buffer. The TAE buffer contained 0.04 M Tris-acetate and 0.001 M EDTA (Sigma). The gel was run at 100 volts for 90 min. After migration, the gel was denatured for 35 min. in a solution of 1.5 M sodium chloride, and 0.5 M NaOH, then neutralized by two 15 min. rinses in a solution of 1.5 M sodium chloride, 0.5 M Tris-HCl (Boehringer Mannheim), pH 7.2, and 1 mM EDTA (Sigma). The gel was transferred to a positively charged nylon membrane (Hybond-N+, Amersham, Oakville, Ontario, Canada)

overnight by capillary action in 20X SSC buffer at room temperature. This buffer contained 3 M sodium chloride, and 0.3 M sodium citrate dihydrate (Anachemia). The membrane was rinsed with 2X SSC and the DNA on the membrane fixed with ultraviolet light (Fotodyne, New Berlin, Wisconsin, USA) for 5 min. The membrane was either stored at -20°C or used immediately for hybridization. The membrane was incubated with a pre-hybridization solution in a rotatory hybridization oven (Bio/Can Scientific) at 42°C for 2 hrs. The pre-hybridization solution contained 6X SSC, 5X Denhardt's reagent (0.02% (w/v) Ficoll (Pharmacia), 0.02% (w/v) polyvinylpyrrolidone (Sigma), 0.02% (w/v) bovine serum albumin (Sigma), 0.5% SDS (Bio-Rad), and 50% (w/v) formamide (Fisher, Nepean, Ontario, Canada). and 100 µg/ml denatured, fragmented salmon sperm DNA. The solution was then replaced by a hybridization solution containing a radioactively labeled probe. The hybridization solution was obtained by incubating a solution of 1.5% (v/v) 10X Kinase buffer (Pharmacia) (0.5 M Tris-HCl (Boehringer Mannheim), pH 9.5, 0.1 M magnesium chloride (Anachemia), 50 mM dithiothreitol (Sigma), 30% (v/v) glycerol (Anachemia), 5.1% (w/v) Tris-HCl spermidine, 1.5% (v/v) of a 10 pmol/µl probe solution, 1.3% (v/v) T4 kinase (Pharmacia), and 7.7% (w/v) [γ-^{32}P]ATP (ICN, Mississauga, Ontario, Canada), at 37°C for 2 hrs. The solution was then incubated at 68°C for 5 min., and the reaction was stopped with 50 µl of TEN buffer containing 0.1 M Tris-HCl (Boehringer Mannheim), pH 8.0, 0.01 M EDTA (Sigma) and 1 M NaCl (Anachemia). The solution was then passed through a Sephadex G50 (Pharmacia) column to remove the unincorporated radiolabeled

nucleotides. The probe was eluted in 100 µl of TEN and stored at -20°C. A probe, previously published by Stewart *et al.*, (1992) was used for hybridization. The probe, designated E2, was an oligonucleotide that corresponded to bases 1080-1103 on the mRNA 7 of HCV-229E, with a sequence of 5'-GAGTCAGGCAACACTGTGGTCTTG-3'.

Hybridization of the probe with the filter proceeded overnight at 42°C for at least 12 hours. The membrane was washed twice for 15 min. with 2X SSC and once for 30 min. with 2X SSC with 1% (w/v) SDS (Bio-Rad), covered with Saran Wrap and exposed to a Kodak X-OMAT autoradiography film for 2 to 48 hrs at -70°C.

16. Micro protein assay

A 96-well Linbro® plate was used to determine protein concentration. All samples were tested in duplicate. Depending on the protein to be tested we used a 50 µg/ml IgG standard (Bio-Rad) for immunoglobulins or a 50 µg/ml bovine serum albumin standard (Bio-Rad) for other proteins. The standards were used at 0.5, 1, 2, 3, 4, and 5 µg/ml in PBS. A sample containing only PBS was used for control. The solution to be tested was also diluted as needed. The final volume to be tested in each well was 100 µl. Then, 100 µl of a 40% (w/v) solution of the dye reagent, Bio-Rad Protein-assay were added and the plate was incubated at room temperature for 10 min. The plate was read in an Easy Reader (SLT-Lab Instruments, Salzburg, Austria) at a wavelength of 600 nm. A standard curve was drawn, and the

absorbance of the test sample intrapolated within it, to obtain the protein concentrations of the samples analyzed.

17. Electron microscopy (EM)

The cells were fixed with 2.5% (v/v) glutaraldehyde (Mecalab, Montreal, Quebec, Canada) in 0.1 M sodium cacodylate, pH 7.2 (Mecalab) buffer for 15 min. The solution was centrifuged at 12,000 x *g* for 3 min. and the pellet washed three times with 3% (w/v) sucrose (Mecalab) in sodium cacodylate buffer. After an incubation of 24 hrs, the sample was fixed with 1.33% (w/v) osmium tetraoxide (SPI-Chem, West Chester, Pennsylvania, USA) in collidine buffer (Mecalab) for 2 hrs at 21°C. The sample was then dehydrated by 30 min. incubations with 25, 50, 75, 95 and twice with 100% (v/v) acetone. The dehydrated sample was mixed 1:1 with Spurr resin (Mecalab) and incubated for 24 hrs. The resin block was cut in 90-100 nm sections in a microtome and the samples were stained with 5% (w/v) alcohol uranyl acetate (Mecalab), and with lead citrate (J.B. EM. Services, Dorval, Quebec, Canada), respectively. The electon microscopy was performed by Robert Alain at the Institut Armand-Frappier.

18. Indirect immunoperoxidase

The indirect immunoperoxidase test was used to detect infectious virus in the infected cell culture supernatants. Susceptible cells (L132 or HRT-18) at 80% confluence, were inoculated with infected cell culture supernatants in a 96-well Linbro® plate. Varying concentrations of the supernatants were used. After 4 to 5 days of incubation in a humidified chamber at 33°C and 5% (v/v) CO_2, the cells were washed with PBS and fixed with 0.3% (v/v) hydrogen peroxide (Sigma) in methanol for 30 min. The cells were washed with PBS and incubated for 2 hrs at 33°C and 5% (v/v) CO_2 with an antiviral antibody. The cells were washed five times with PBS and horseradish peroxidase-conjugated anti-mouse immunoglobulins (Cappell, Durham, North Carolina, USA) was added. After 2 hrs at 37°C without CO_2, the cells were washed five times with PBS, and the bound antibodies were detected by incubation with 0.025% (w/v) 3,3'-diaminobenzidine tetrahydrochloride (Bio-Rad), 0.01% (v/v) hydrogen peroxide (Sigma) in PBS. When the colorant was observed in the light microscope, the reaction was stopped with deionized water. The infectious titer was then obtained following the Kärber method, where

$$TCID_{50} = +\Delta - \delta(S - 0.5)$$

$TCID_{50}$:	Lethal tissue culture infective dose
Δ:	$\log_{10}$ of the sample where the dilution shows 100% of infected cells
δ:	$\log_{10}$ of dilution factor
S:	addition of the number of samples that show infected cells

19. Double immunodiffusion

A solution of 1% (w/v) agarose (FMC, Rockland, Maine, USA) in PBS was heated until the agarose was dissolved, 5 ml were then poured into a 5x5 cm. glass plate and allowed to solidify at room temperature for 45 min. With a punch, five holes were equally spaced around the diameter of a circle. A sixth hole was made in the center of the circle. To each peripheral hole, 10 µl of specific anti-serum for each immunoglobulin isotype (Organon Teknika Corporation) was added, and 10 µl of the monoclonal antibody to be tested was added in the central hole. The plate was incubated at 4°C until the precipitation lines could be observed in the agarose, this allowed determination of the immunoglobulin isotype of each mAb.

RESULTS

1. Virus Production

In order to obtain enough virus to immunize a guinea pig, 70 Petri dishes where plated with HRT-18 cells at passage 22. Human coronavirus OC43 from a laboratory stock was used to inoculate the cells. Four days post-inoculation, 910 ml of cell supernatant were collected. Proteins in the viral solution were precipitated with polyethylene glycol and virus particles were purified by centrifugation through a discontinuous and a continuous gradient of Nycodenz®. The refractive index was determined to verify the efficiency of the continuous gradient (Figure 1). Fractions 14 to 19 were analyzed by electron microscopy to verify the presence of viral particles. Fractions 15 to 18 showed the highest concentration of virus and the less cell debris. These fractions were pooled and dialyzed against TMEN buffer and then assayed for protein content. The protein concentration was 168 µg/ml, corresponding to a total of 336 µg of purified virus.

Figure 1: Profile of the refractive index of fractions collected from a continuous Nycodenz® gradient used for the purification of HCV-OC43.

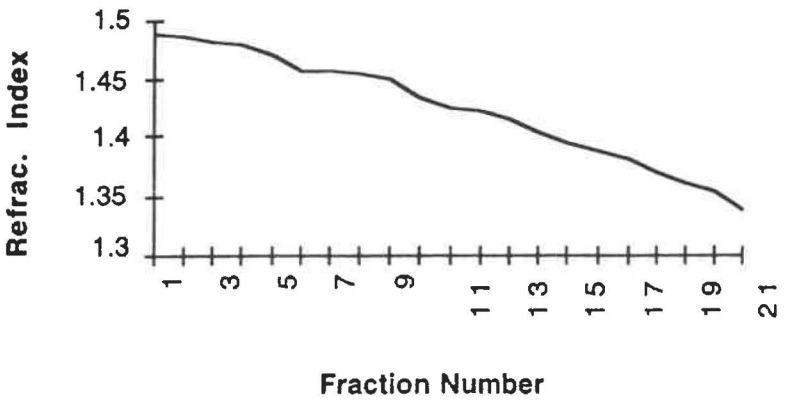
Refrac. Index
1.5
1.45
1.4
1.35
1.3
1
3
5
7
9
11
13
15
17
19
21
Fraction Number

2. Production of F(ab')$_2$ fragments of monoclonal antibodies

For immunofluorescence experiments with human coronavirus, it was previously found that whole immunoglobulins yielded high background. This background was eliminated by the use of F(ab')$_2$ fragments. This suggested that the cells used had Fc receptors (Talbot, personal communication). Therefore, we produced F(ab')$_2$ fragments for 3 mAbs to use in these studies.

2.1 5-11H.6

Two ml of ascites fluid containing 28 mg of HCV-229E specific mAb 5-11H.6 were run through a Sepharose Protein-G column to purify the antibody. After verification of the purity by SDS-PAGE in a 7.5% (w/v) acrylamide gel (Figure 2, lane 1), the recovered, purified antibody was concentrated by filtration in a Centriprep-100 ultrafiltration apparatus; a final concentration of 0.84 mg/ml was obtained, for a total of 8.4 mg. Therefore, the yield was 30%. The antibody was digested with 0.27 mg of pepsin for 2 hrs at 37°C. The time of digestion was previously optimized by performing a time course of digestion (Figure 3). The digested antibody was passed

Figure 2: Coomassie blue-stained 7.5% SDS-PAGE gel to detect pepsin digestion products of mAb 5-11H.6.

Lane M: Bio-Rad protein standards (molecular masses in kDa shown on the left)

Lane 1: Purified 5-11H.6

Lane 2: 5-11H.6 $F(ab')_2$ fragments (110kDa)

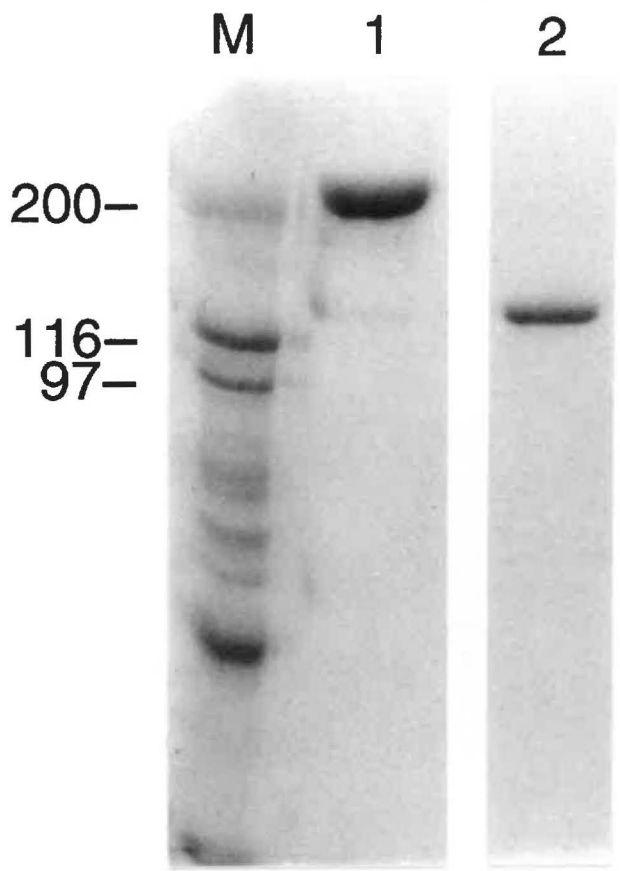
M
1
2
200–
116–
97–

Figure 3: Time course of digestion of mAb 5-11H.6 by pepsin, using a 12% SDS-PAGE Coomassie blue-stained gel.

Lane M: Pharmacia protein standards
Lane 1: Purified antibody (160kDa)
Lane 2: 0.5 hr digestion ($F(ab')_2$ fragments at 110kDa)
Lane 3: 1 " " "
Lane 4: 2 " " "
Lane 5: 3 " " (Fab fragments at 55 kDa)
Lane 6: 5 " " "
Lane 7: 7 " " "
Lane 8: 9 " " "
Lane 9: 12 " " "
Lane 10: 18 " " "
Lane 11: 24 " " "

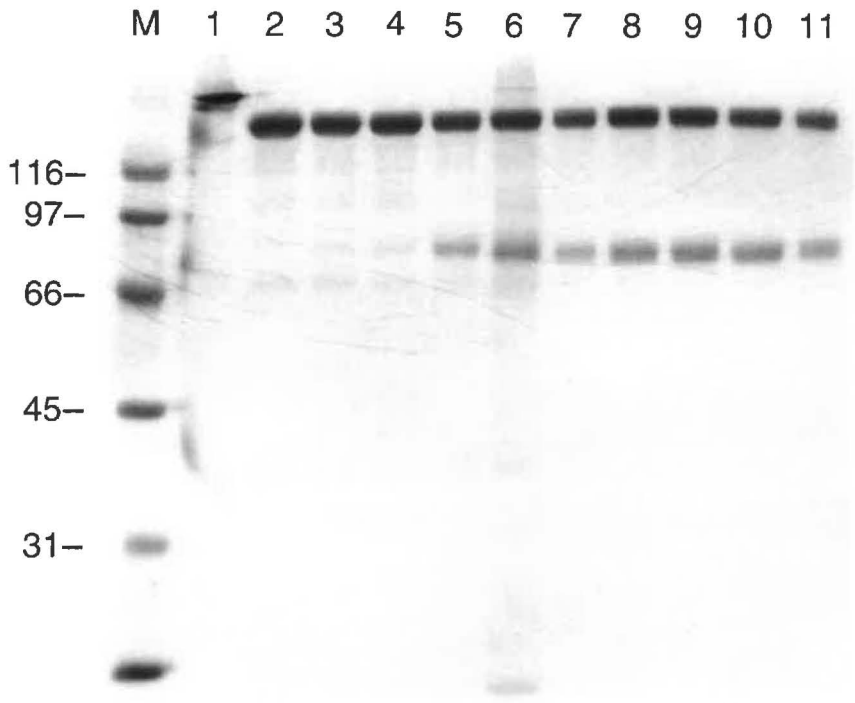
M 1 2 3 4 5 6 7 8 9 10 11
116–
97–
66–
45–
31–

through a protein-G column in order to eliminate any remaining undigested antibody. The purified $F(ab')_2$ fragments solution was concentrated by filtration in a Centriprep-30 ultrafiltration apparatus. Presence of the fragments were verified by SDS-PAGE in a 12% (w/v) acrylamide gel (Figure 2, lane 2). A protein assay revealed the final concentration to be 920 µg/ml, for a total 2.5 mg of 5-11H.6 $F(ab')_2$ fragments.

2.2 4-E11.3

Seven ml of ascites fluid containing 8.47 mg of HCV-OC43 specific mAb 4-E11.3 were run through a Sepharose Protein-G column to purify the antibody. After verification of the purity by SDS-PAGE in a 12% (w/v) acrylamide gel (Figure 4, lane 1), the recovered, purified antibody was concentrated by filtration in a Centriprep-100 ultrafiltration apparatus; a final concentration of 0.8 mg/ml was obtained, for a total of 5.3 mg. Therefore, the yield was 62.5%. The antibody was digested with 0.17 mg of pepsin for 1 hr at 37°C. The time of digestion was previously optimized by performing a timecourse of digestion (Figure 5). The digested antibody was passed through a protein-G column in order to eliminate any remaining undigested antibody. The purified $F(ab')_2$ solution was concentrated by filtration in a Centriprep-30 ultrafiltration apparatus. Presence of the fragments were verified by SDS-PAGE in a 12% (w/v) acrylamide gel (Figure 4, lane 2). Fab fragments and other digestion products were observed, but no complete Ab was present. For our purpose it

Figure 4: Coomassie blue-stained 12% SDS-PAGE gel to detect pepsin digestion products of mAb 4-E11.3.

Lane M: Bio-Rad protein standards (molecular masses in kDa shown on the left)

Lane 1: Purified 4-E11.3 (160 kDa)

Lane 2: 4-E11.3 $F(ab')_2$ fragments (110 kDa, with by products at 90 and 50 kDa)

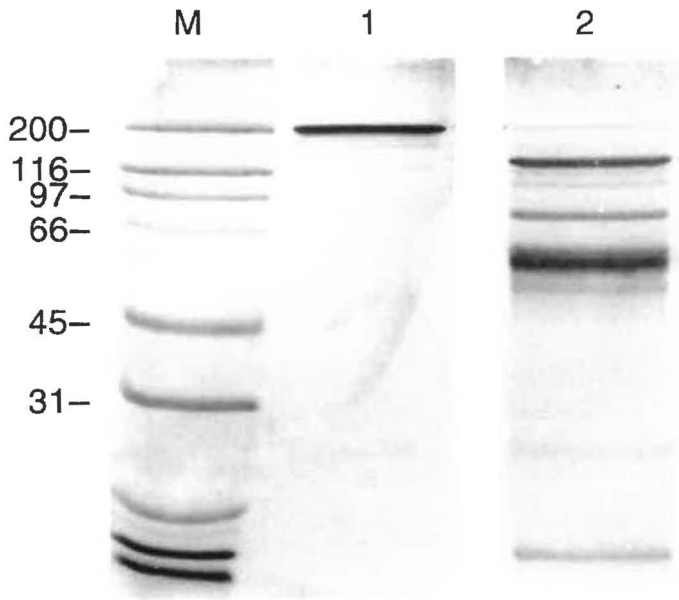
M
1
2
200–
116–
97–
66–
45–
31–

Figure 5: Time course of digestion of mAb 4-E11.3 by pepsin, using a 12% SDS-PAGE Coomassie blue-stained gel.

Top panel	Lane M:	Bio-Rad protein standards (molecular masses in kDa shown on the left)
	Lane 1:	Purified antibody (160 kDa)
	Lane 2:	5 min. digestion (whole antibody at 160 kDa and $F(ab')_2$ fragments at 110 kDa)
	Lane 3:	10 " " "
	Lane 4:	15 " " ($F(ab')_2$ fragments at 110 kDa)
	Lane 5:	25 " " "
	Lane 6:	35 " " "
	Lane 7:	45 " " "
	Lane 8:	1 hr " "
Bottom panel	Lane M:	Bio-Rad protein standards (molecular masses in kDa shown on the left)
	Lane 9:	Purified antibody (160 kDa)
	Lane 10:	1 hr 15 min. digestion ($F(ab')_2$ fragments at 110 kDa and Fab fragments at 50 kDa)
	Lane 11:	1 " 30 " " "
	Lane 12:	1 " 45 " " "
	Lane 13:	2 " " " "
	Lane 14:	2 " 15 " " "
	Lane 15:	2 " 30 " " "

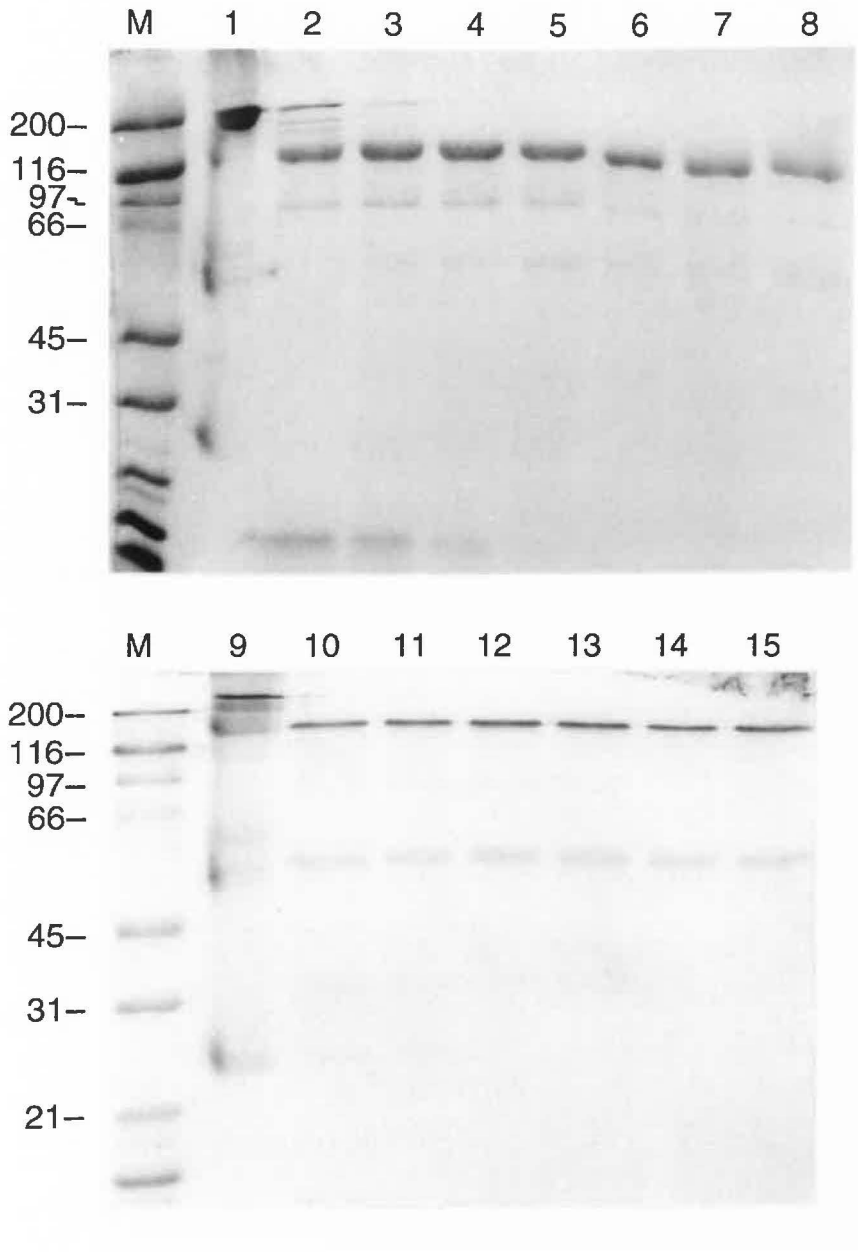
M 1 2 3 4 5 6 7 8
200–
116–
97–
66–
45–
31–
M 9 10 11 12 13 14 15
200–
116–
97–
66–
45–
31–
21–

was only important to remove the Fc part, the by-products of digestion would not interfere in our experiments. A protein assay revealed the final concentration to be 1.44 mg/ml, for a total 3 mg of 4-E11.3 $F(ab')_2$ fragments.

2.3 Anti-c-myc

One and a half ml of ascites fluid containing 21 mg of mouse c-myc specific mAb were run through a Sepharose Protein-A column to purify the antibody. After verification of the purity by SDS-PAGE in a 12% (w/v) acrylamide gel (Figure 6, lane 1), the recovered, purified antibody was concentrated by filtration in a Centriprep-100 ultrafiltration apparatus; a final concentration of 1.93 mg/ml was obtained, for a total of 11.76 mg. Therefore, the yield was 56%. The antibody was digested with 0.2 mg of pepsin for 30 min. at 37°C. The time of digestion was previously optimized by a time course of digestion (Figure 7). The digested antibody was passed through a protein-A column in order to eliminate any remaining undigested antibody. The purified $F(ab')_2$ fragments solution was concentrated by filtration in a Centriprep-30 ultrafiltration apparatus. Presence of the fragments were verified by SDS-PAGE in a 12% (w/v) acrylamide gel (Figure 6, lane 2). A protein assay revealed the final concentration to be 3.28 mg/ml, for a total 9 mg of anti-c-myc $F(ab')_2$ fragments.

Figure 6: Coomassie blue-stained 7.5% SDS-PAGE gel to detect pepsin digestion products of anti-c-myc mAb.
Lane M: Bio-Rad protein standards (molecular masses in kDa shown on the left)
Lane 1: Purified anti-c-myc (160 kDa)
Lane 2: anti-c-myc $F(ab')_2$ fragments (110 kDa)

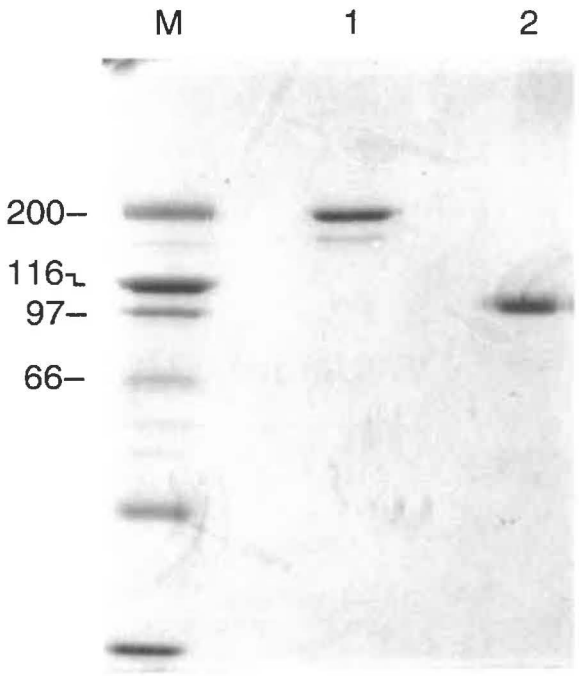
M
1
2
200–
116–
97–
66–

Figure 7: Time course of digestion of anti-c-myc mAb by pepsin using a 7.5% SDS-PAGE Coomassie blue-stained gel.

Top panel	Lane M:	Bio-Rad protein standards (molecular masses in kDa shown on the left)
	Lane 1:	Purified antibody (160 kDa)
	Lane 2:	10 min. digestion ($F(ab')_2$ fragments at 110 kDa)
	Lane 3:	20 " " "
	Lane 4:	30 " " "
	Lane 5:	40 " " "
	Lane 6:	50 " " "
	Lane 7:	1 hr " "
Bottom panel	Lane M:	Bio Rad protein standards (molecular masses in kDa shown on the left)
	Lane 8:	1 hr 15 min. digestion ($F(ab')_2$ fragments at 110 kDa and Fab fragments at 50 kDa)
	Lane 9:	1 " 30 ". " "
	Lane 10:	1 " 45 " " "
	Lane 11:	2 " " "
	Lane 12:	2 " 30 " " "
	Lane 13:	3 " " "
	Lane 14:	3 " 30 " " "

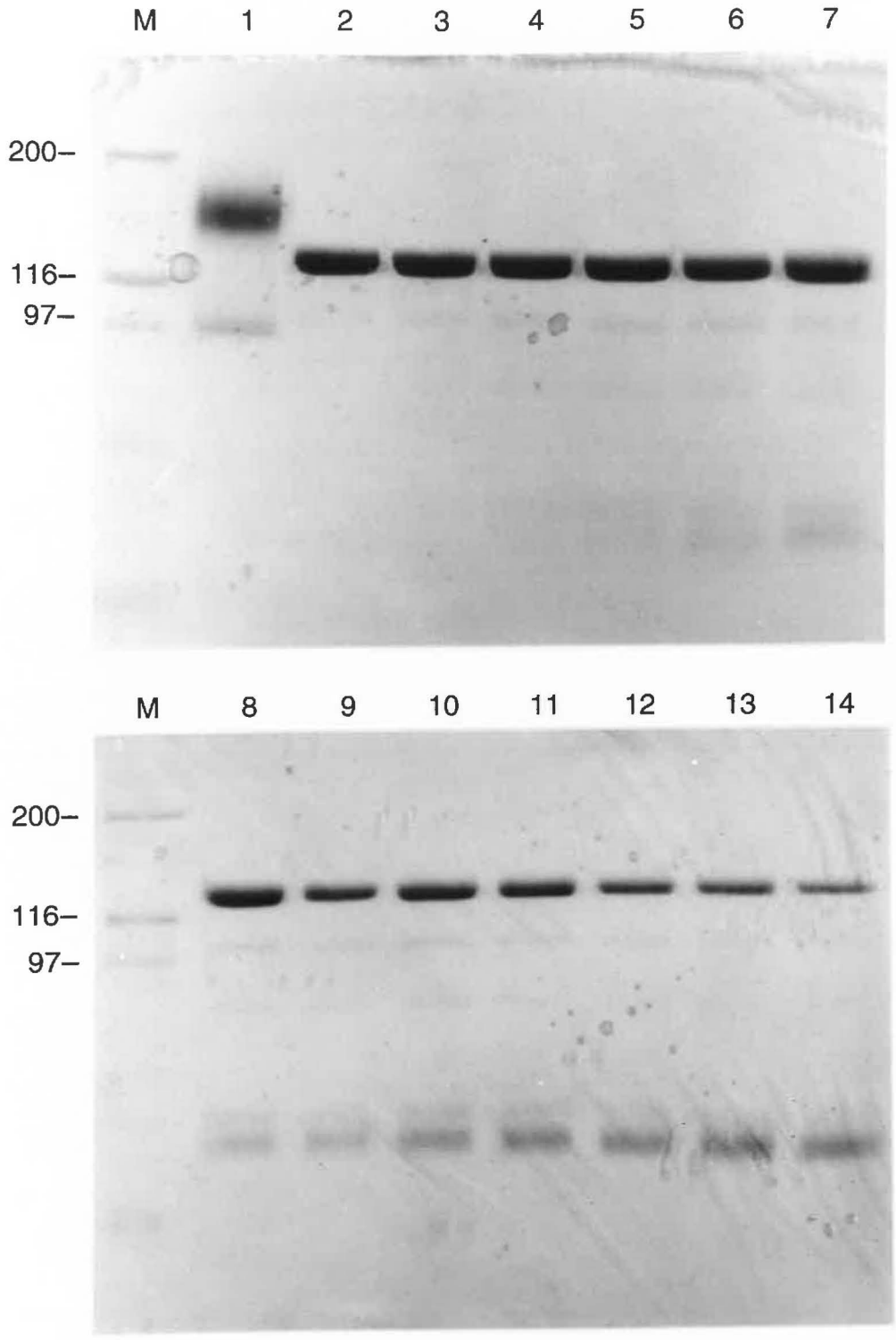
M 1 2 3 4 5 6 7
200–
116–
97–
M 8 9 10 11 12 13 14
200–
116–
97–

3. Immunofluorescence

3.1 Biological activity of $F(ab')_2$ fragments

After obtaining $F(ab')_2$ fragments by digesting the mAbs with pepsin, we tested them in an immunofluorescence assay to confirm their biological activity and to determine the best dilution to be used in future experiments.

3.1.1 5-11H.6 and anti-c-myc mAb

Immunofluorescence was performed in L132 cells infected with HCV-229E. $F(ab')_2$ fragments of mAb 5-11H.6 were active and the best dilution was 1/10. $F(ab')_2$ fragments of anti-c-myc mAb gave the best results at a dilution of 1/40 and showed that background fluorescence with whole antibody, due to a Fc receptor activity, was not a problem with $F(ab')_2$ fragments (Table 2). Immunofluorescence was also performed in non-infected cells and the results were all negative.

3.1.2 4-E11.3

Immunofluorescence was performed in HRT-18 cells infected with HCV-OC43. The $F(ab')_2$ fragments of mAb 4-E11.3 were active and the best dilution was 1/100 (Table 3). Immunofluorescence was also performed in non-infected cells and the results were all negative.

Table 2: Immunofluorescence in L132 cells inoculated with HCV-229E detected with FITC mouse at 1/100 dilution, to verify biological activity of mAb 5-11H.6 $F(ab')_2$ fragments and to verify lack of Fc receptor activity of anti-c-myc $F(ab')_2$ fragments.
When stated "background" refers to an unacceptable level of background fluorescence that interferes with the differentiation of viral specific vs. non-viral fluorescence.

Ab	1/Dilution	Concentration (mg/ml)	Results
5-11H.6	100	0.15	+ background
	250	0.06	+ background
	500	0.03	+ background
anti-c-myc	100	0.14	- background
	250	0.056	- background
	500	0.028	- background
5-11H.6 $F(ab')_2$	6	0.15	+
	15	0.06	+
	30	0.03	+
anti-c-myc $F(ab')_2$	20	0.15	-
	55	0.06	-
	110	0.03	-

Table 3: Immunofluorescence in HRT-18 cells inoculated with HCV-OC43 detected with FITC mouse at 1/100 dilution, to verify biological activity of mAb 4-E11.3 $F(ab')_2$ fragments.

Ab	1/Dilution	Concentration (mg/ml)	Results
4-E11.3 $F(ab')_2$	10	0.144	+
	50	0.028	+
	100	0.014	+
	200	0.007	+
	400	0.003	+
anti-c-myc $F(ab')_2$	40	0.075	-

3.2 Optimization of fluorochrome-conjugated antibodies

3.2.1 FITC guinea pig

To determine the best dilution of FITC guinea pig (fluorescein-conjugated goat $F(ab')_2$ fragments anti-guinea pig IgG) to be used in the IF tests, an IF was performed in HRT-18 cells infected with HCV-OC43. The serum used was the one recovered after four immunizations of a guinea pig with semi-purified virus (Table 4). The best dilution was 1/200.

3.2.2 TRITC rabbit

In order to determine the dilution of TRITC rabbit (rhodamine-conjugated goat anti-rabbit IgG) to be used in the IF tests, an IF was conducted in L132 cells infected with HCV-229E. The best dilution was 1/50 (Table 5). The same experiment was performed in non-infected cells and the results were all negative.

3.2.3 TRITC mouse

In order to determine the dilution of TRITC mouse (rhodamine-conjugated goat anti-mouse IgG, IgA, IgM) to be used in the IF tests, an IF was conducted in HRT-18 cells infected with HCV-OC43 and mAb 4-E11.3. The best dilution was 1/50 (Table 6). The same experiment was performed in non-infected cells and the results were all negative.

Table 4: Immunofluorescence in HRT-18 cells inoculated with HCV-OC43 to determine the optimal dilution of FITC guinea pig to be used in the IF tests.
When stated "background" refers to an unacceptable level of background fluorescence that interferes with the differentiation of viral specific vs. non-viral fluorescence.
n.a. : not applicable

1/Dilution of antibody reagents			
guinea pig serum anti-OC43	guinea pig pre-immune serum	FITC guinea pig	Results
100	n.a.	50	+ background
400	n.a.	50	+ background
800	n.a.	50	+ background
1200	n.a	50	+ background
1600	n.a.	50	+ background
2000	n.a	50	+ background
n.a.	200	50	- background
100	n.a.	100	+ background
400	n.a	100	+ background
800	n.a.	100	+ background
1200	n.a	100	+ background
1600	n.a.	100	+ background
2000	n.a	100	+ background
n.a.	200	100	- background
1000	n.a.	100	+ background
4000	n.a	100	+ background
8000	n.a.	100	+ background
n.a.	200	200	-
1000	n.a.	200	+ background
4000	n.a	200	+
8000	n.a.	200	+

Table 5: Immunofluorescence in L132 cells inoculated with HCV-229E to determine the optimal dilution of TRITC rabbit to be used in the IF tests.
When stated "background" refers to an unacceptable level of background fluorescence that interferes with the differentiation of viral specific vs. non-viral fluorescence.
n.a. : not applicable

1/Dilution of antibody reagents			
rabbit anti-229E	rabbit pre-immune serum	TRITC rabbit	Results
50	n.a.	50	+ background
100	n.a.	50	+ background
200	n.a.	50	+ background
400	n.a.	50	+
n.a.	50	50	-
n.a.	100	50	-
50	n.a.	75	+ background
100	n.a.	75	+ background
200	n.a.	75	+ background
400	n.a.	75	+ background
n.a.	50	75	-
n.a.	100	75	-
50	n.a.	100	+ background
100	n.a.	100	+ background
200	n.a.	100	+ background
400	n.a.	100	+ background
n.a.	50	100	-
n.a.	100	100	-
50	n.a.	150	-
100	n.a.	150	-
200	n.a.	150	-
400	n.a.	150	-
n.a.	50	150	-
n.a.	100	150	-

Table 6: Immunofluorescence in HRT-18 cells inoculated with HCV-OC43 to determine the optimal dilution of TRITC mouse to be used in the IF tests.
When stated "background" refers to an unacceptable level of background fluorescence that interferes with the differentiation of viral specific vs. non-viral fluorescence.
n.a. : not applicable

1/Dilution of antibody reagents			
4-E11.3 $F(ab')_2$	Anti-c-myc $F(ab')_2$	TRITC mouse	Results
100	n.a.	10	+ background
100	n.a.	50	+
100	n.a.	100	-
100	n.a.	200	-
n.a.	40	50	-
n.a.	40	100	-

3.3 Optimization of guinea pig polyclonal antiviral antibody

To determine the optimal concentration of the guinea pig anti-OC43 polyclonal antibody to be used in the IF experiments, an IF test was performed on HRT-18 infected cells with HCV-OC43 (Table 7). The optimum combination was guinea pig polyclonal antibody at a dilution of 1/10 000 and guinea pig pre-immune serum at 1/2,000. The same experiment was performed in non-infected cells and the results were all negative.

3.4 Characterization of antibodies to cell markers

It was important to show that the antibodies against cell markers did not show Fc receptor activity in order to avoid any non-viral fluorescence from these reagents in the IF tests. The markers were tested in L132 cells infected with HCV-229E (Table 8). The same experiment was performed on non-infected cells as controls and the results were all negative. The results proved that these antibodies did not unexpectedly recognize other proteins and that they could be used as cell markers.

Table 7: Immunofluorescence in HRT-18 cells inoculated with HCV-OC43 to determine the optimal dilution of guinea pig polyclonal antibody to be used in the IF tests.
When stated "background" refers to an unacceptable level of background fluorescence that interferes with the differentiation of viral specific vs. non-viral fluorescence.
n.a. : not applicable

1/Dilution of antibody reagents			
guinea pig serum anti-OC43	guinea pig pre-immune serum	FITC guinea pig	Results
1000	n.a.	200	+ background
5000	n.a.	200	+
10000	n.a.	200	+
15000	n.a.	200	+
20000	n.a.	200	+
n.a.	500	200	- background
n.a.	1000	200	-
n.a.	2000	200	-
n.a.	5000	200	-

Table 8: Immunofluorescence in HRT-18 cells inoculated with HCV-229E to characterize antibodies to cell markers.

3.5 Cross-reactivity of species-specific fluorochrome-conjugated anti-immunoglobulins

In order to avoid a cross-reactivity between a fluorochrome-conjugated antibody and species-specific antibodies from another species in the double immunofluorescence tests we tested the appropriate conjugates, for any interspecies cross-reactivities.

3.5.1 FITCgp vs. mouse Ab

An IF test was performed in HRT-18 cells infected with HCV-OC43. FITC guinea pig recognized mouse immunoglobulins (Table 9); therefore, it could not be used as secondary fluorochrome-conjugated antibody in the double immunofluorescence tests.

3.5.2 FITCm vs. guinea pig Ab

An IF test was performed in HRT-18 cells infected with HCV-OC43. FITC mouse did not recognize guinea pig immunoglobulins (Table 10).

3.5.3 TRITCr vs. mouse Ab

An IF test was performed in HRT-18 cells infected with HCV-OC43. TRITC rabbit did not recognize mouse immunoglobulins (Table 11).

Table 9: Immunofluorescence to verify any cross-reactivity between FITC guinea pig and mouse Abs.
n.a. : not applicable

1/Dilution of antibody reagents					
mouse anti-OC43 serum	mouse pre-immune serum	guinea pig serum anti-OC43	guinea pig pre-immune serum	FITCgp	Results
100	n.a.	n.a.	n.a.	200	+
n.a.	100	n.a.	n.a.	200	-
n.a.	n.a.	10000	n.a.	200	+
n.a.	n.a.	n.a.	2000	200	-
n.a.	n.a.	n.a.	n.a.	200	-

Table 10: Immunofluorescence to verify any cross-reactivity between FITC mouse and guinea pig Abs.
n.a. : not applicable

1/Dilution of antibody reagents					
mouse serum anti-OC43	mouse pre-immune serum	guinea pig serum anti-OC43	guinea pig pre-immune serum	FITCm	Results
100	n.a.	n.a.	n.a.	100	+
n.a.	100	n.a.	n.a.	100	-
n.a.	n.a.	10000	n.a.	100	-
n.a.	n.a.	n.a.	2000	100	-
n.a.	n.a.	n.a.	n.a.	100	-

Table 11: Immunofluorescence to verify any cross-reactivity between TRITC rabbit and mouse Abs.
n.a. : not applicable

1/Dilution of antibody reagents			
4-E11.3 $F(ab')_2$	**TRITCr**	**TRITCm**	**Results**
100	50	n.a.	-
100	n.a.	50	+

3.5.4 FITCgp vs. rabbit Ab and FITCr vs. guinea pig Ab

An IF test was performed in HRT-18 cells infected with HCV-OC43. FITC guinea pig did not recognize rabbit immunoglobulins and FITC rabbit did not recognize guinea pig immunoglobulins (Table 12).

3.6 Detection of viral antigens

3.6.1 HCV-229E

A rabbit anti-229E polyclonal antibody and $F(ab')_2$ fragments of mAb 4-E11.3 were used to detect HCV-229E viral antigens in infected human primary cultured neural cells by DIF. The immunofluorescence test was performed at 2, 4, and 7 days post-infection. None of the cells cultured were positive for viral antigens when assayed by immunofluorescence. Each experiment was repeated at least twice to verify reproducibility (data not shown).

3.6.2 HCV-OC43

A guinea pig anti-OC43 polyclonal antibody and $F(ab')_2$ fragments of 4-E11.3 mouse monoclonal antibody were used to detect HCV-OC43 antigens in infected human primary cultured neural cells by DIF. The immunofluorescence test was performed at 2, 4, and 7 days post-infection. Each experiment was repeated at least twice to verify reproducibility. Human fetal astrocytes, adult human microglia and adult astrocytes were shown to be infectable through the

Table 12: Immunofluorescence to verify any cross-reactivity between FITC guinea pig and rabbit Abs, and FITC rabbit and guinea pig Abs.
n.a. : not applicable

1/Dilution of antibody reagents						
rabbit serum anti-OC43	guinea pig serum anti-OC43	rabbit pre-immune serum	guinea pig pre-immune serum	FITCgp	FITCr	Results
100	n.a.	n.a.	n.a.	200	n.a.	-
n.a.	10000	n.a.	n.a.	n.a.	n.a.	-
100	n.a.	n.a.	n.a.	n.a.	100	+
n.a.	10000	n.a.	n.a.	200	n.a.	+
n.a.	n.a.	100	n.a.	n.a.	100	-
n.a.	n.a.	n.a.	2000	200	n.a.	-

detection of intracellular viral antigens in amounts that are consistent with viral replication (Figure 8 to 14). At 2 days post-infection 10% of the human fetal astrocytes were infected, at 4 days 50 to 70% and at 7 days 90 to 100%. For the human adult microglia, 10% of the culture was infected at 2 days post-infection, 40% at 4 days and 80 to 100% at 7 days Human fetal neurons (data not shown) and human adult oligodendrocytes were negative in immunofluorescence. Although it remains possible that some oligodendrocyte could be infected (Figure 14), this was not proven due to technical problems with the antibody against the oligodendrocyte markers.

4. Genome detection

Since the immunofluorescence tests may not have been sensitive enough to detect a low level infection of several cells with HCV-229E, we used a more sensitive test for detection of viral RNA, RT-PCR Southern Blotting.

4.1 Adsorption test

In order to rule out the possibility of detecting virus adsorbed in the cell surface but not internalized, an experiment using HeLa cells (permissive for HCV-229E infection (Talbot, personal communication)) was conducted where adsorption of the virus was allowed for 2 hrs. at 4°C. The RNA was extracted from non-infected HeLa cells, HeLa cells plus virus at 4°C, and HeLa cells at 7 days post-inoculation, and used

Figure 8: Human fetal astrocytes at 2 days post-inoculation with HCV-OC43.

A) Viral antigen detected with anti-OC43 mAb 4-E11.3 and FITCm

B) Astrocytes detected with anti-GFAP and TRITCr

C) Negative control: non-infected cells adsorbed with anti-OC43 mAb 4-E11.3 and FITCm

D) Negative control: isotypic antibody control anti-c-myc mAb detected with FITCm

E) Negative control: primary antibody replaced with dilution buffer detected with FITCm

F) Nuclear marker

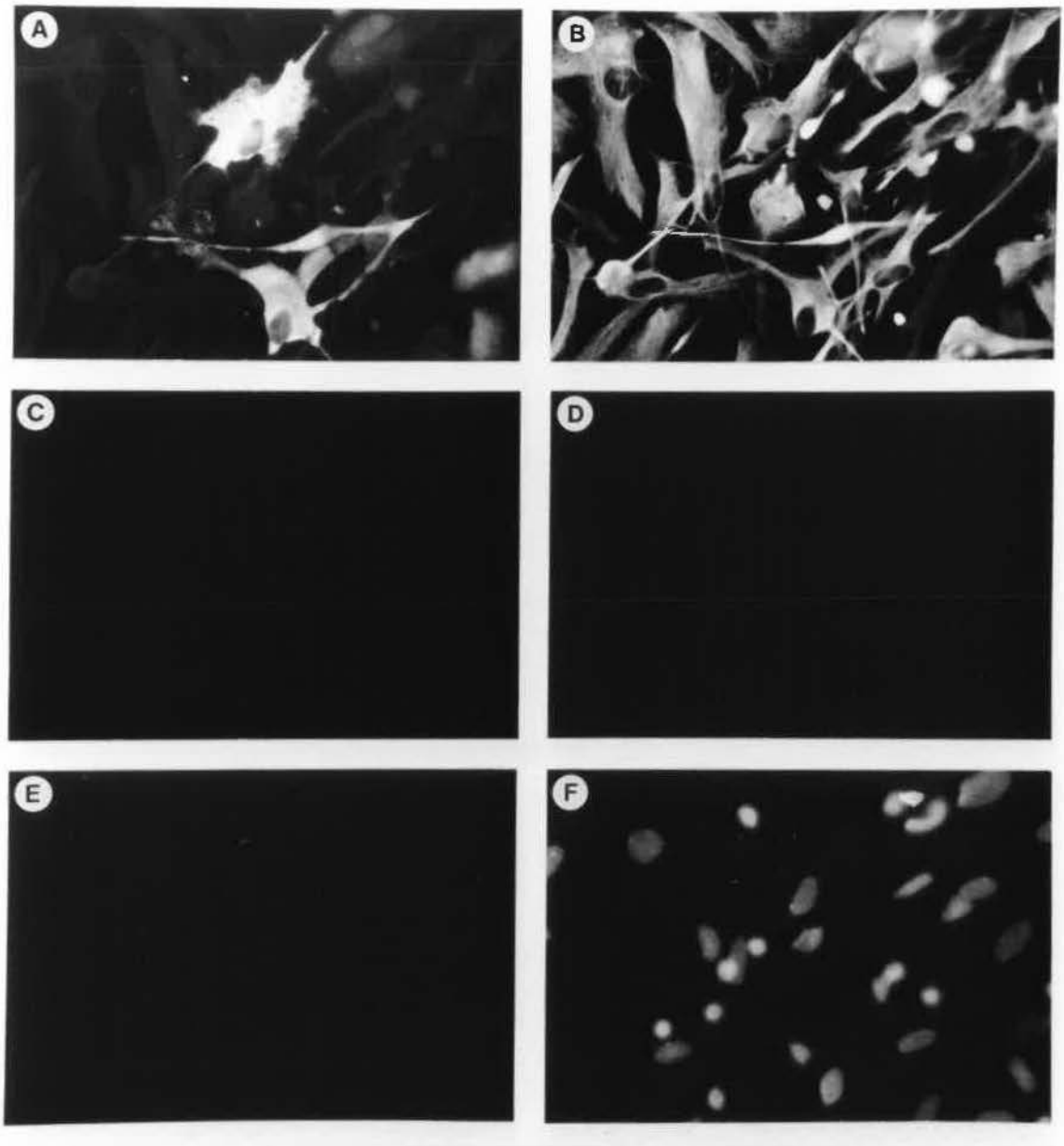
A
B
C
D
E
F

Figure 9: Human fetal astrocytes at 4 days post-inoculation with HCV-OC43.

A) Viral antigen detected with anti-OC43 mAb 4-E11.3 and FITCm
B) Astrocytes detected with anti-GFAP and TRITCr
C) Negative control: non-infected cells adsorbed with anti-OC43 mAb 4-E11.3 and FITCm
D) Negative control: isotypic antibody control anti-c-myc mAb detected with FITCm
E) Negative control: primary antibody replaced with dilution buffer detected with FITCm
F) Nuclear marker

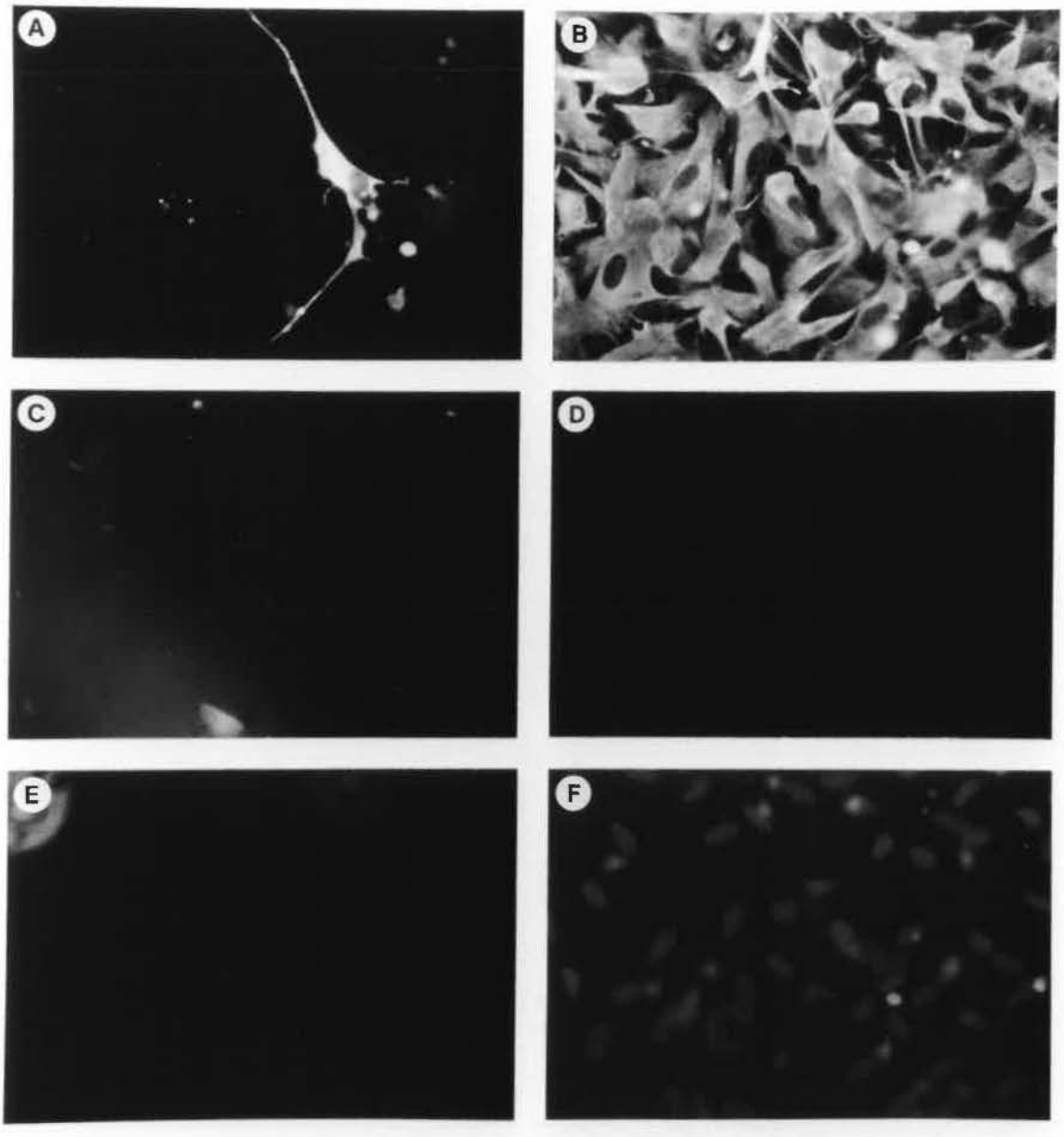
A
B
C
D
E
F

Figure 10: Human fetal astrocytes at 7 days post-inoculation with HCV-OC43.

A) Viral antigen detected with anti-OC43 mAb 4-E11.3 and FITCm

B) Astrocytes detected with anti-GFAP and TRITCr

C) Negative control: non-infected cells adsorbed with anti-OC43 mAb 4-E11.3 and FITCm

D) Negative control: isotypic antibody control anti-c-myc mAb detected with FITCm

E) Negative control: primary antibody replaced with dilution buffer detected with FITCm

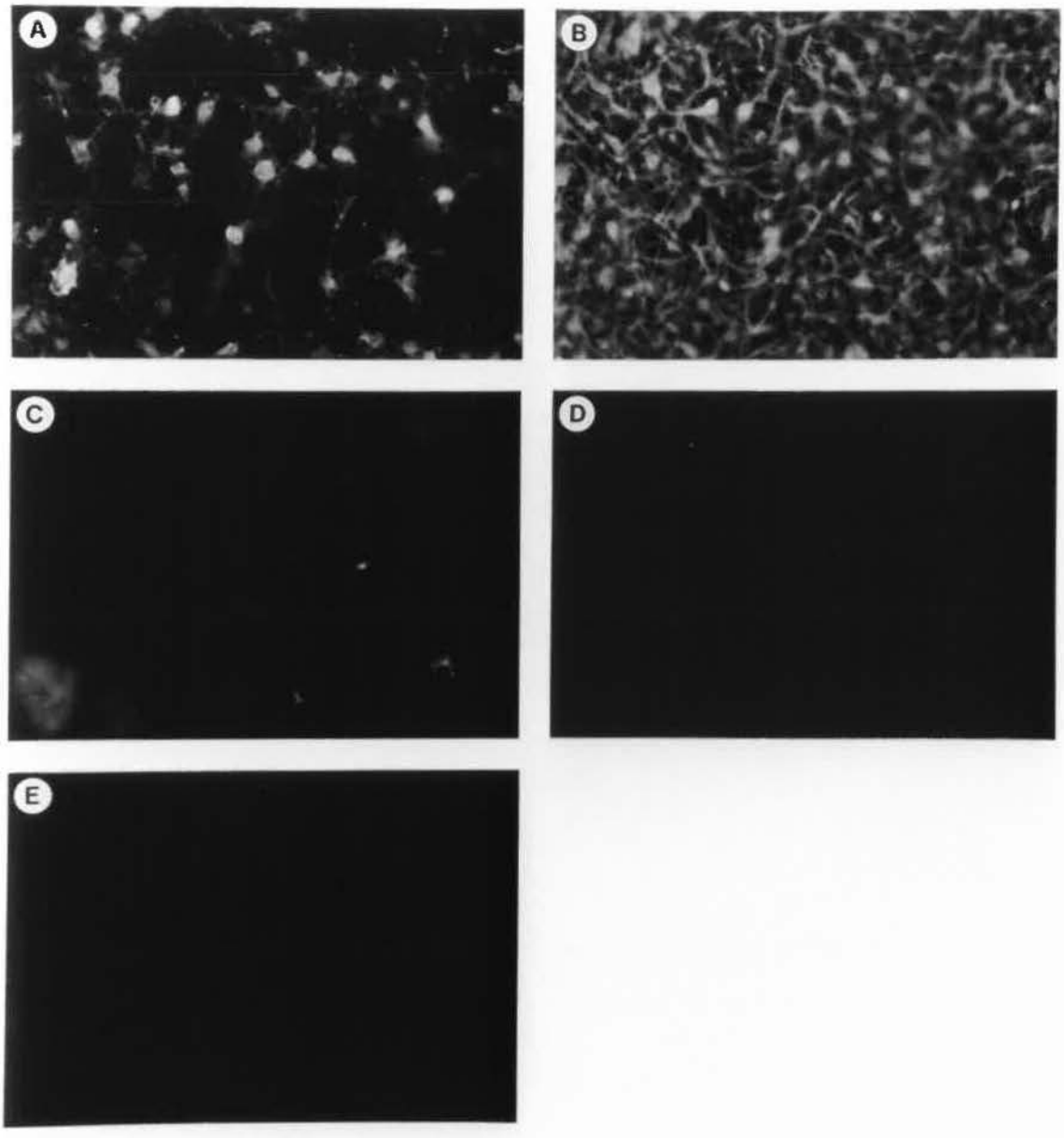
A
B
C
D
E

Figure 11: Human adult microglia at 2 days post-inoculation with HCV-OC43.

A) Viral antigen detected with anti-OC43 guinea pig polyclonal antibody and FITCgp

B) Microglia marked with KP-1 detected with TRITCm

C) Negative control: non-infected cells adsorbed with anti-OC43 guinea pig polyclonal antibody and FITCgp

D) Negative control: pre-immune guinea pig serum detected with FITCgp

E) Negative control: primary antibody replaced with dilution buffer detected with FITCgp

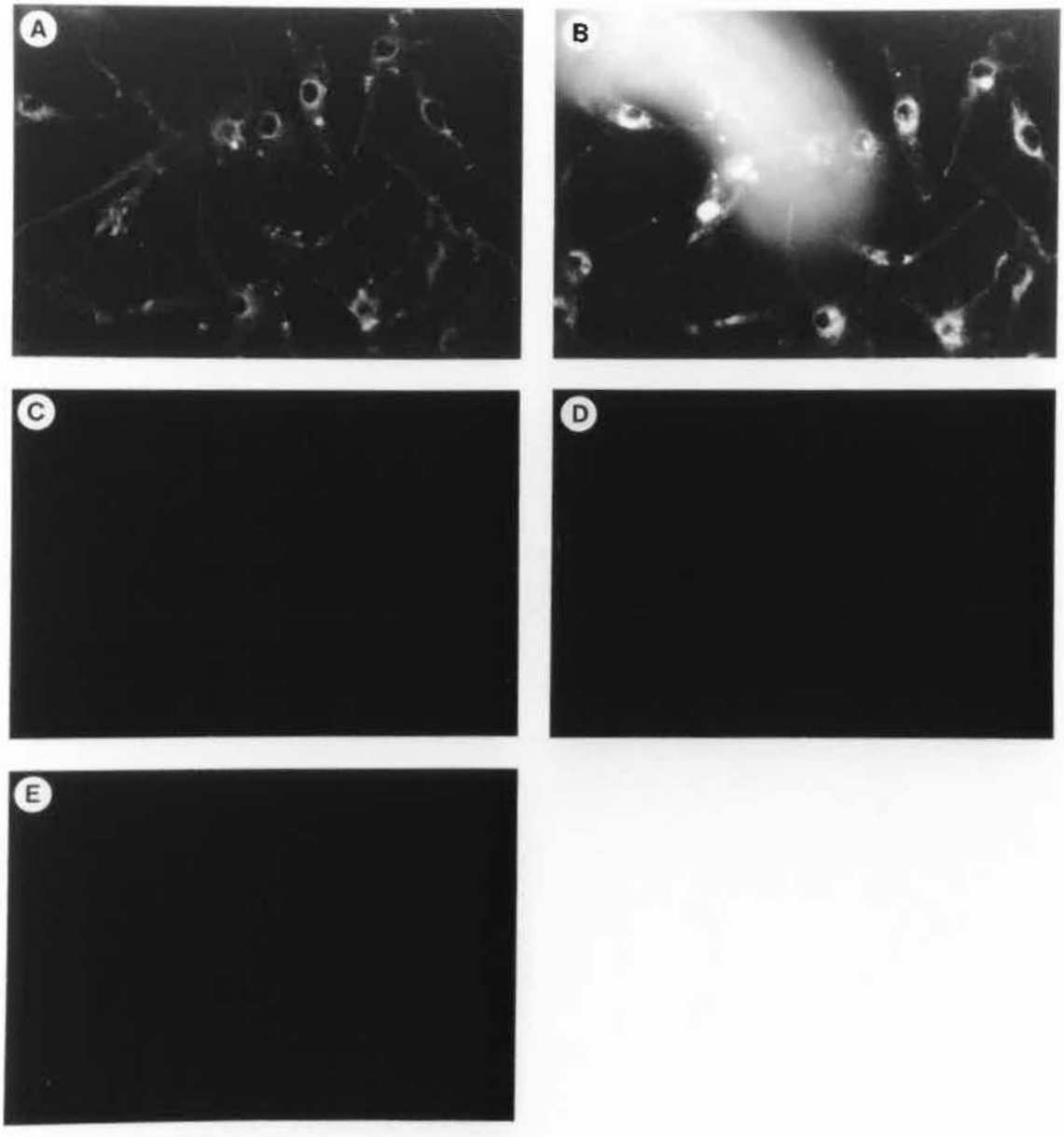
A
B
C
D
E

Figure 12: Human adult microglia at 4 days post-inoculation with HCV-OC43.

A) Viral antigen detected with anti-OC43 guinea pig polyclonal antibody and FITCgp
B) Microglia marked with KP-1 detected with TRITCm
C) Negative control: non-infected cells adsorbed with anti-OC43 guinea pig polyclonal antibody and FITCgp
D) Negative control: pre-immune guinea pig serum detected with FITCgp
E) Negative control: primary antibody replaced with dilution buffer detected with FITCgp
F) Nuclear marker

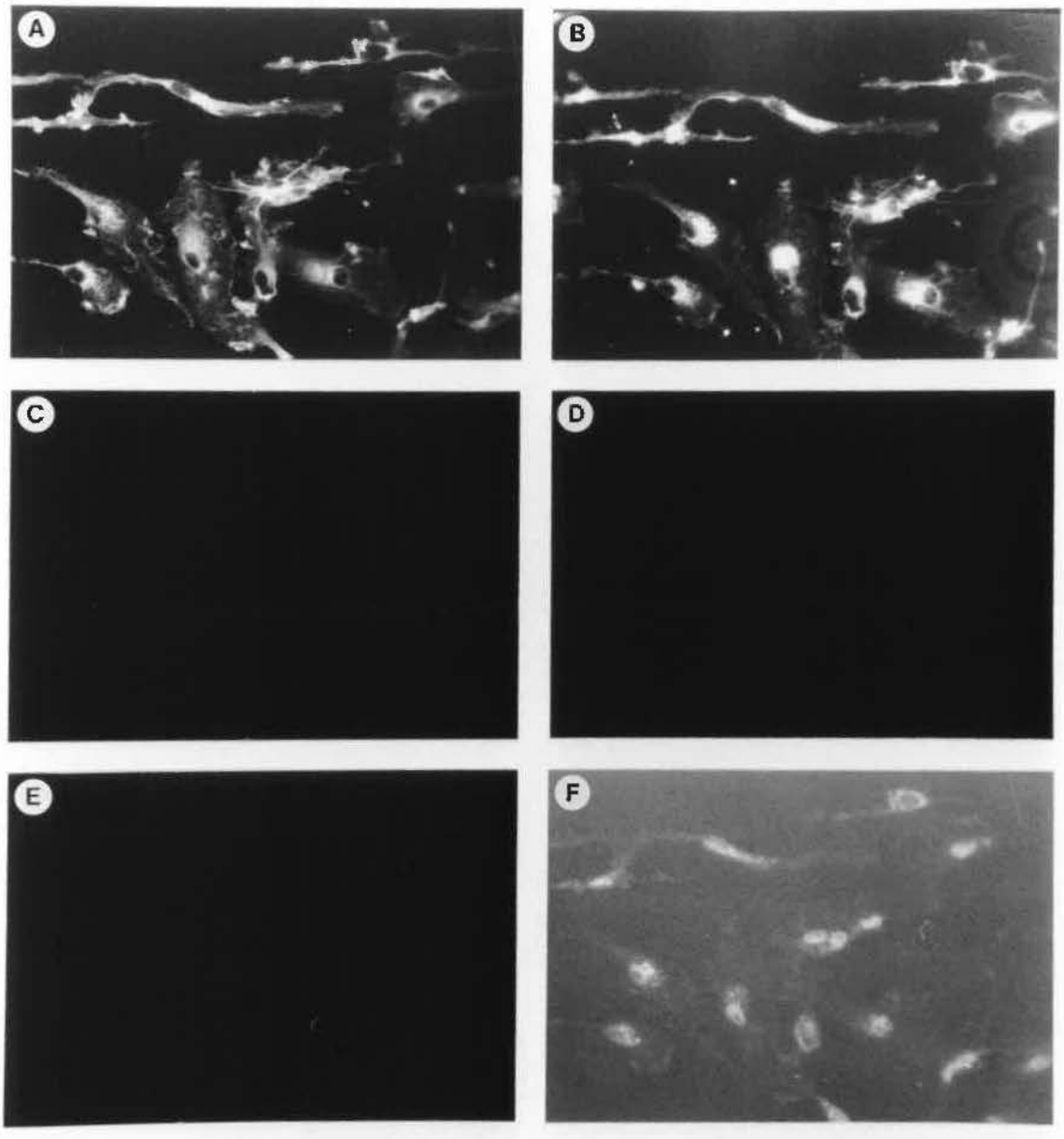
A
B
C
D
E
F

Figure 13: Human adult microglia at 7 days post-inoculation with HCV-OC43.

A) Viral antigen detected with anti-OC43 guinea pig polyclonal antibody and FITCgp
B) Microglia marked with KP-1 detected with TRITCm
C) Negative control: non-infected cells adsorbed with anti-OC43 guinea pig polyclonal antibody and FITCgp
D) Negative control: pre-immune guinea pig serum detected with FITCgp
E) Negative control: primary antibody replaced with dilution buffer detected with FITCgp
F) Nuclear marker

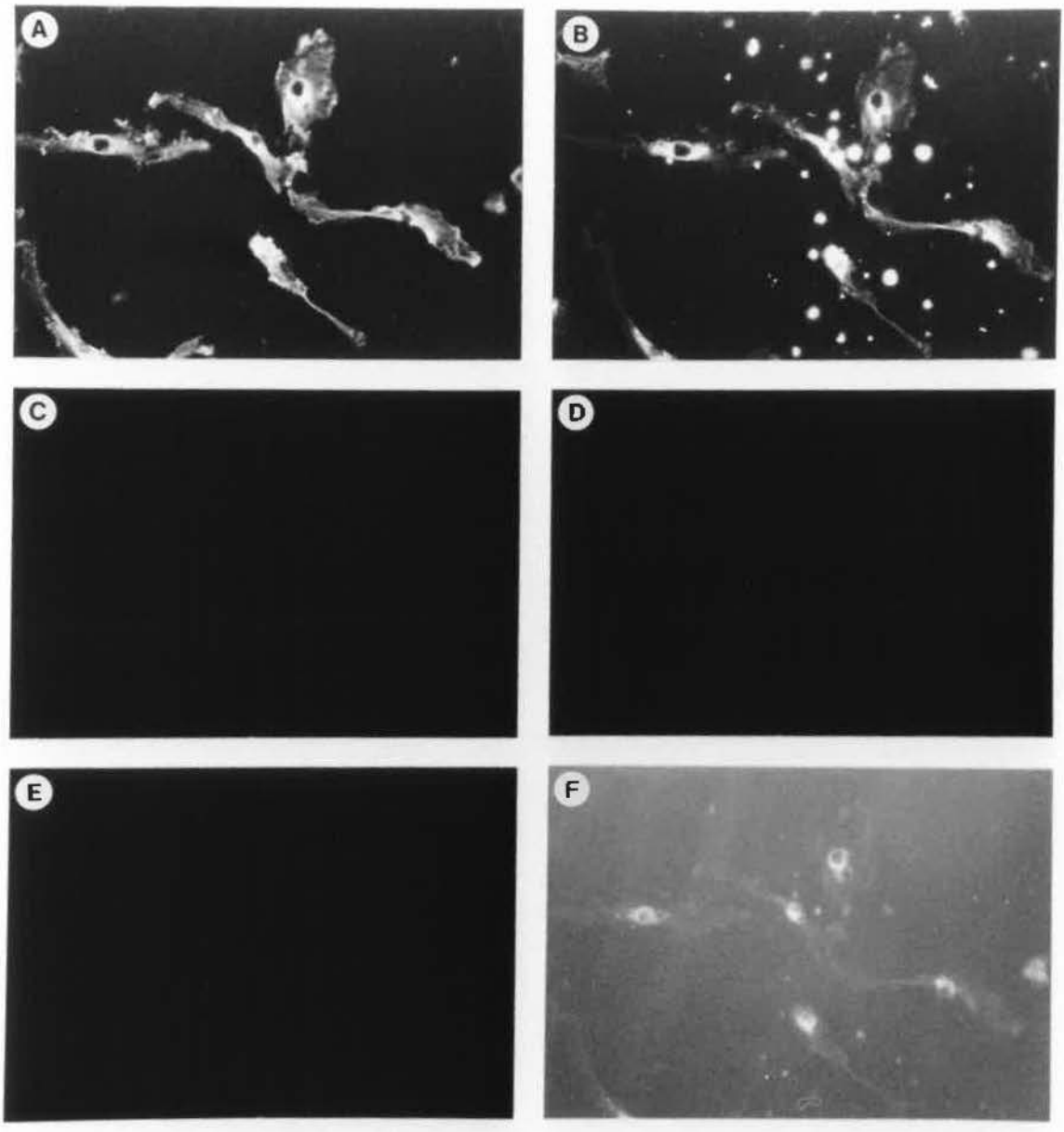
A
B
C
D
E
F

Figure 14: Mix of human adult oligodendrocytes and astrocytes at 7 days post-inoculation with HCV-OC43.

A) Viral antigen detected with anti-OC43 guinea pig polyclonal antibody and FITCgp

B) Astrocytes marked with anti-GFAP detected with TRITCr

C) Negative control: non-infected cells adsorbed with anti-OC43 guinea pig polyclonal antibody and FITCgp

D) Negative control: pre-immune guinea pig serum detected with FITCgp

E) Negative control: primary antibody replaced with dilution buffer detected with FITCgp

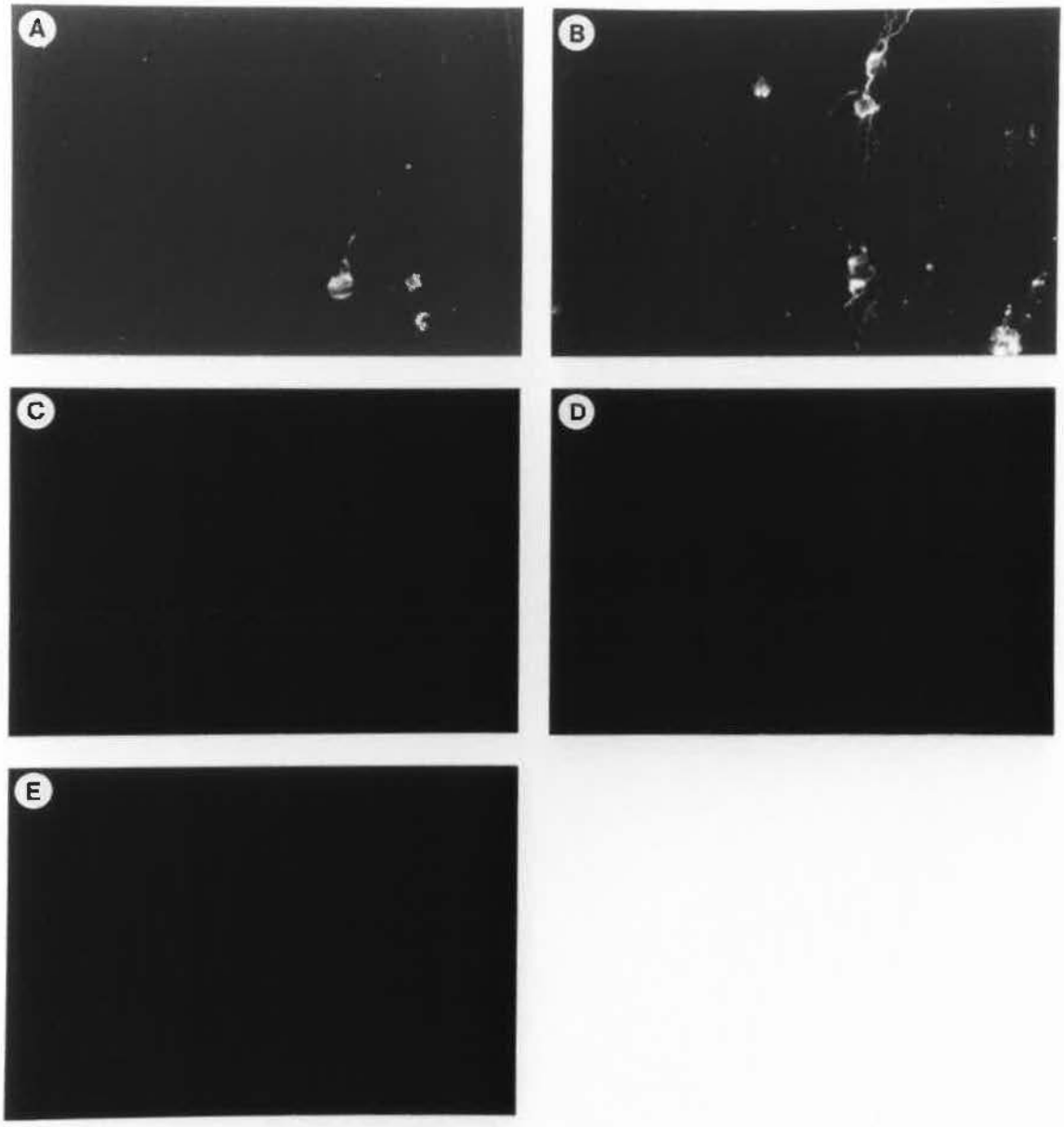
A
B
C
D
E

for RT-PCR using viral specific primers. Positive results were only seen for the 7 days post-inoculation sample by Southern blot analysis, showing that no adsorbed viral particles were detected by this method (Figure 15, lanes 14,15,20,21,22).

4.2 Detection of HCV-229E

Primary cultured human neural cells were inoculated with HCV-229E. The RNA was extracted at 4 or 7 days post inoculation and RT-PCR was performed. Southern blot analysis showed the presence of viral RNA in human fetal astrocytes, human adult microglia, and for the mix of adult oligodendrocytes and adult astrocytes. One batch of human fetal astrocytes gave negative results (Figure 15, lane 19). Since the experiments with other sources of these cells were positive, we can conclude that HCV-229E infects human fetal astrocytes. All the non-infected cells gave negative results (Figure 15).

4.3 Minimal RNA needed for detection

To determine the minimal amount of RNA needed in our experiments to detect viral RNA in infected cells, an RT-PCR was performed with dilutions of the RNA extracted from L132 cells at 20 hrs. post-inoculation with HCV-229E. Viral RNA amplified from 7.1×10^{-7} μg of total cellular RNA could be detected in a 1.5% (w/v) agarose gel stained with ethidium bromide (Figure 16). Using Southern blotting hybridization, viral RNA could be detected with as

Figure 15: Autoradiograph of a Southern blot of RT-PCR products generated from RNA extracted from different cells.

1) Positive control, L132 cells 2 days post-inoculation with HCV-229E
2) Human fetal astrocytes
3) Human fetal astrocytes 4 days post-inoculation with HCV-229E
4) Human adult microglia
5) Adult oligodendrocytes and astrocytes mix 4 days post-inoculation with HCV-229E
6) Adult oligodendrocytes and astrocytes mix
7) Human adult microglia
8) Human adult microglia 4 days post-inoculation with HCV-229E
9) Positive control, L132 cells 2 days post-inoculation with HCV-229E
10) Adult oligodendrocytes and astrocytes mix
11) Adult oligodendrocytes and astrocytes mix 7 days post-inoculation with HCV-229E
12) Human fetal astrocytes
13) Human fetal astrocytes 7 days post-inoculation with HCV-22E
14) HeLa cells
15) HeLa cells 2 hrs adsorption with HCV-229E at 4°C
16) Human fetal astrocytes
17) Positive control, L132 cells 2 days post-inoculation with HCV-229E
18) Human fetal astrocytes 2 hrs adsorption with HCV-229E at 4°C
19) Human fetal astrocytes 7 days post-inoculation with HCV-229E
20) HeLa cells
21) HeLa cells 2 hrs adsorption with HCV-229E at 4°C
22) HeLa cells 7 days post-inoculation with HCV-229E
23) Negative control, sample devoid of DNA
24) Negative control, sample devoid of DNA

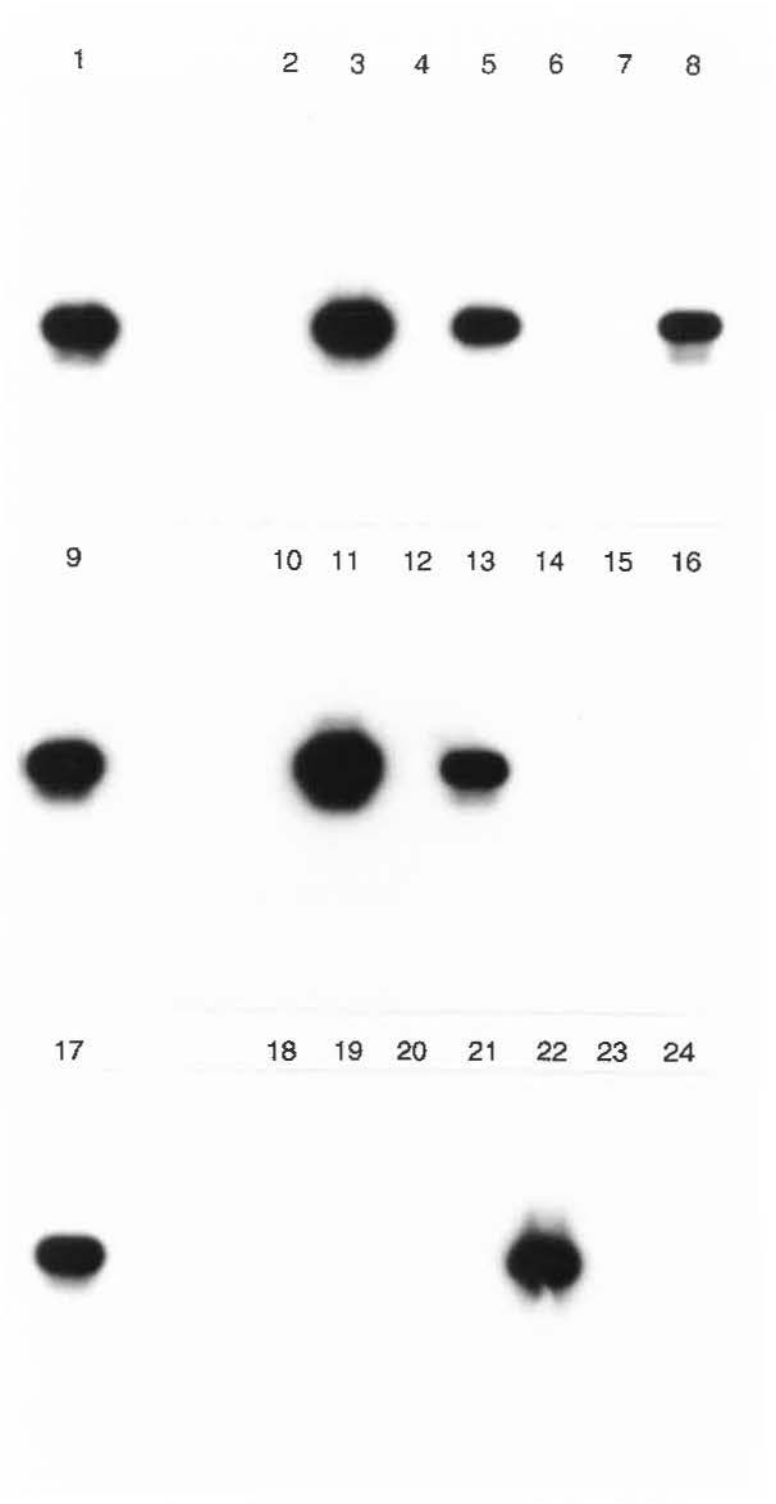
1
2
3
4
5
6
7
8
9
10
11
12
13
14
15
16
17
18
19
20
21
22
23
24

Figure 16: Ethidium bromide stained 1.5% (w/v) agarose gel showing RT-PCR amplification products using different amounts (in µg) of total RNA from L132 cells inoculated with HCV-229E.

M) Pharmacia 100 bp ladder
1) Positive control, RNA from L132 cells infected with HCV-229E
2) Negative control, sample devoid of DNA
3) 7.1
4) $7x10^{-1}$
5) $7x10^{-2}$
6) $7x10^{-3}$
7) $7x10^{-4}$
8) $7x10^{-5}$
9) $7x10^{-6}$
10) Positive control, RNA from L132 cells infected with HCV-229E
11) $7x10^{-7}$ (Limit of detection)
12) $7x10^{-8}$
13) $7x10^{-9}$
14) $7x10^{-10}$
15) $7x10^{-11}$
16) $7x10^{-12}$
17) $7x10^{-13}$
18) $7x10^{-14}$

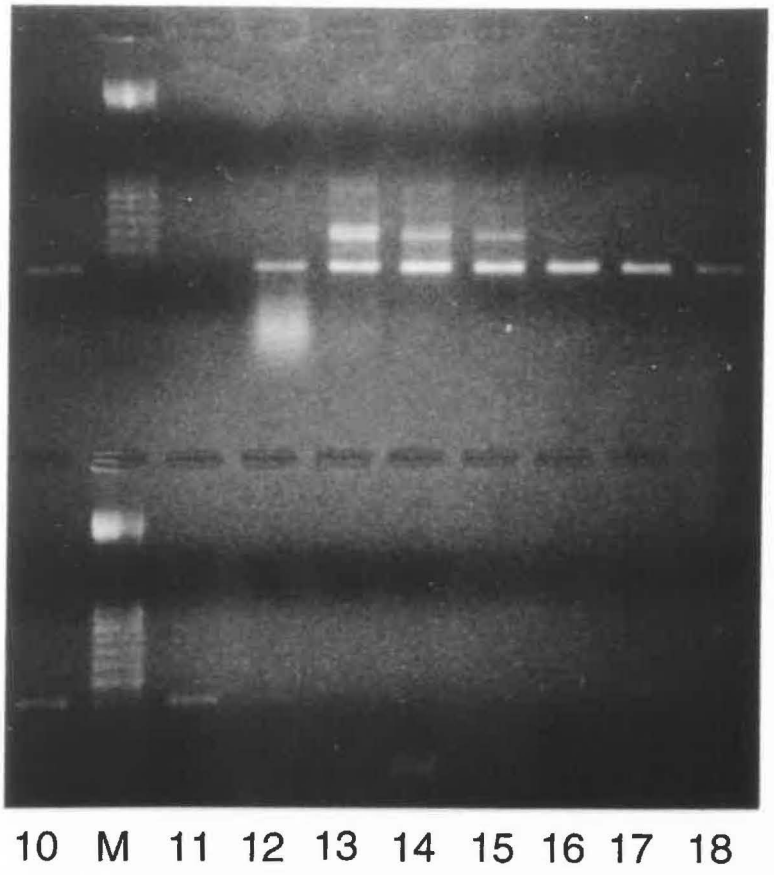
1 M 2 3 4 5 6 7 8 9
10 M 11 12 13 14 15 16 17 18

little as 7.1×10^{-9} µg of total cellular RNA (Figure 17), showing the technique of hybridization to be 100-fold more sensitive. However, since we do not know the proportion of viral RNA in these samples, it is not possible to quantitate viral RNA detected in infected neural cells.

5. Electron microscopy

Cultures of human fetal astrocytes were analyzed by electron microscopy. No coronavirus particles were observed in the extracellular medium. Cells infected with HCV-OC43 revealed inclusions of viral particles in vacuoles (Figure 18) however no viral particles were observed in cells infected with HCV-229E (Figure 19).

6. Detection of infectious virus

In order to detect the production of infectious viral particles from the primary cultured neural cells inoculated with HCV, we used the indirect immunoperoxidase test. The culture supernatants of theinoculated cells were used to inoculate cells susceptible to human coronavirus. The infection of these cells could then be detected with an anti-virus monoclonal antibody and horseradish peroxidase-conjugated anti-mouse immunoglobulins. From cells infected with HCV-229E, only human fetal astrocytes produced infectious virus (Table 13). However, the titers obtained were very low. With HCV-OC43, infectious virus was produced by fetal astrocytes, and the titers increased with time of infection from 3,163 to 31,623 $TCID_{50}$/ml at 2,

Figure 17: Autoradiograph of a Southern blotting with products of a RT-PCR using different amounts (in µg) of RNA from L132 cells infected with HCV-229E.

M) Pharmacia 100 bp ladder (top panel)
1) Positive control, RNA from L132 cells infected with HCV-229E
2) Negative control, sample devoid of DNA
3) 7.1
4) $7x10^{-1}$
5) $7x10^{-2}$
6) $7x10^{-3}$
7) $7x10^{-4}$
8) $7x10^{-5}$
9) $7x10^{-6}$
10) $7x10^{-7}$
11) $7x10^{-8}$
12) $7x10^{-9}$ (Limit of detection)
13) $7x10^{-10}$
14) $7x10^{-11}$
15) $7x10^{-12}$
16) $7x10^{-13}$
17) $7x10^{-14}$
18) $7x10^{-15}$
19) $7x10^{-16}$


1 M 2 3 4 5 6 7 8 9
10 11 12 13 14 15 16 17 18 19


1 M 2 3 4 5 6 7 8 9
10 11 12 13 14 15 16 17 18 19

Figure 18: Electron microscopy of ultra-thin sections of human fetal astrocytes inoculated with HCV-OC43 at 7 days post-inoculation. Arrows show HCV-OC43 virions.

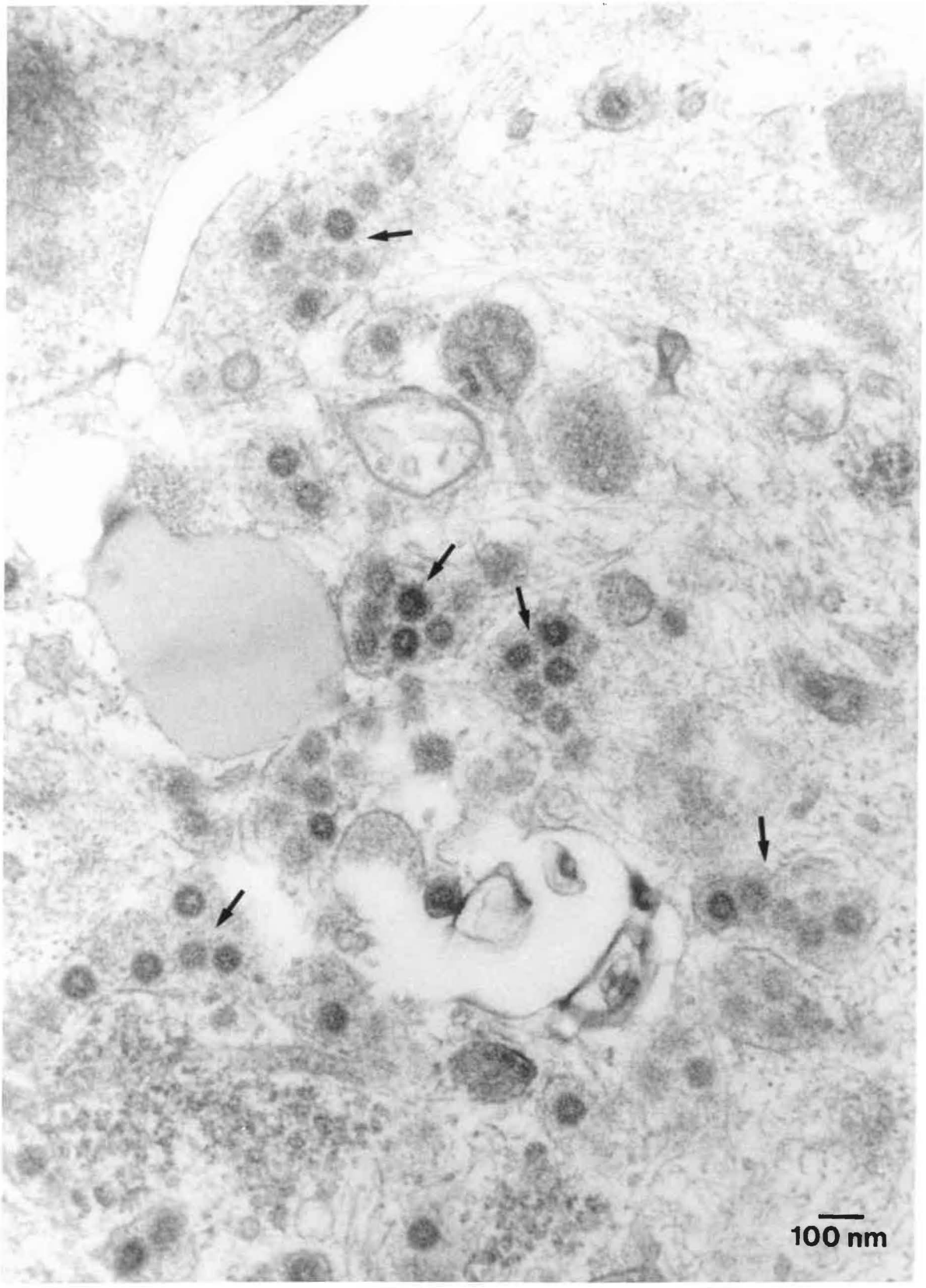
100 nm

Figure 19: Electron microscopy of ultra-thin sections of human fetal astrocytes inoculated with HCV-229E at 7 days post-inoculation. No virions were detected.

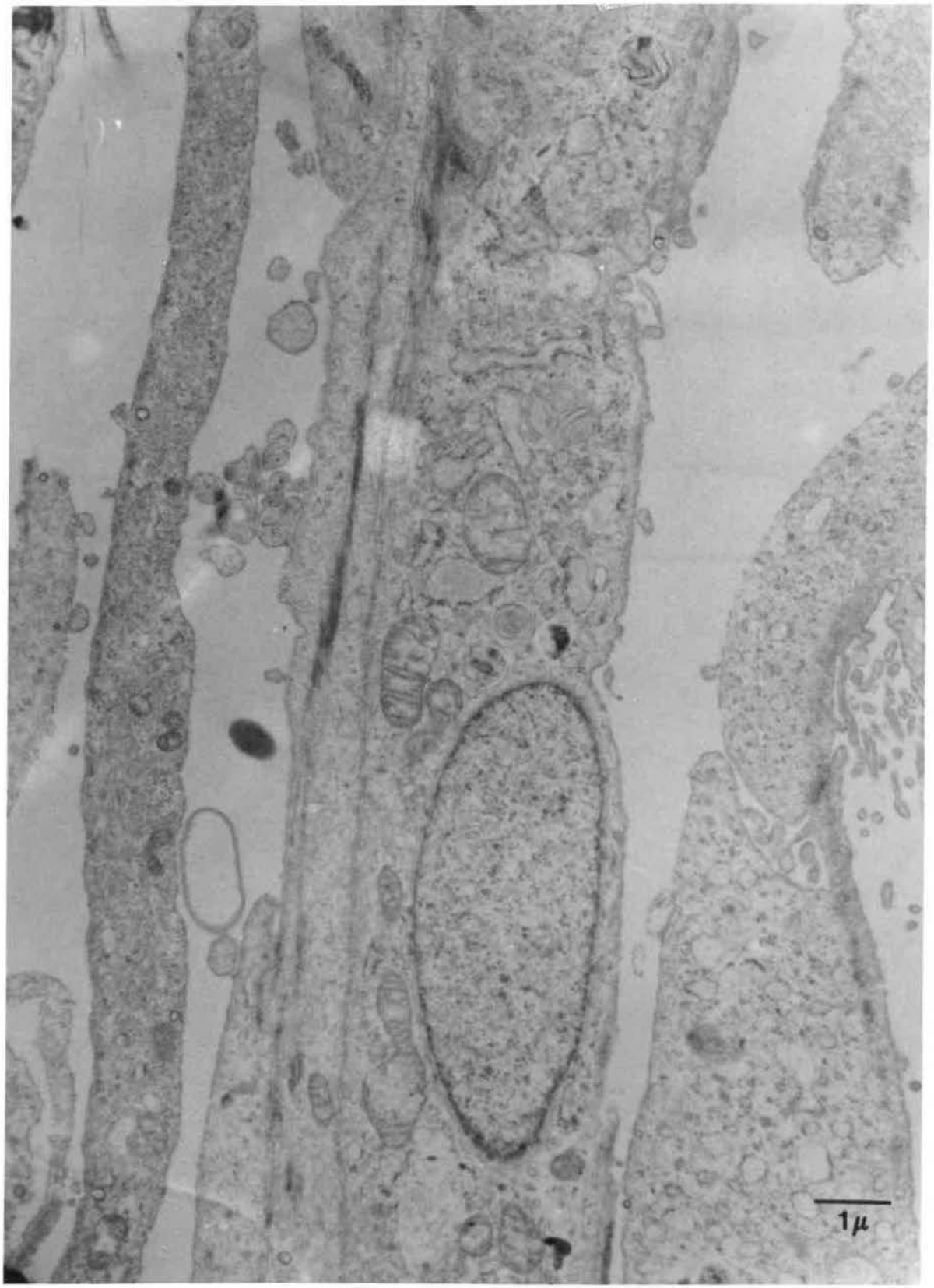
1μ

Table 13: Infectious viral particles in extracellular medium of cultures of cells inoculated with HCV-229E.

Cell type	Time post-inoculation (days)	Infectious titer $TCID_{50}$/ml
Fetal astrocytes	2	< 10
	4	32
	7	56
Adult microglia	4	< 3
	7	< 3
Adult astrocytes and oligodendrocytes	4	< 3
	7	< 3
Fetal neurons	4	< 32

4 and 7 days post-infection. Very low titers, in the order of 56 to 100 $TCID_{50}$/ml were found for the mix of adult oligodendrocytes and astrocytes, and in adult microglia 2 days after inoculation, suggesting that the reduced population of infectable astrocytes was in fact producing some virus, as were the microglia. However, as with fetal neurons, these low titers, only observed at 2 days post-infection, may represent the viral inoculum. Therefore we can only conclude that virus productively infects fetal astrocytes (Table 14).

7. Hybridomas

In order to produce mouse monoclonal antibodies against HCV-OC43 a BALB/c mouse was immunized intraperitoneally with 100 µg of semi-purified HCV-OC43. The mouse was boosted with an intraperitoneal injection of 100 µg of semi-purified virus and two intravenous injections of 200 µl of HCV-OC43 P4. The spleen was extracted and $4.9x10^7$ cells were used in conjunction with $5.4x10^7$ myeloma cells. After fusion, the hybridomas obtained were cloned by limiting dilution. The supernatants were screened by IF on HRT-18 cells infected with OC43. Immunofluorescence was also performed in non-infected cells to discard hybridomas that reacted with non-infected cells. We obtained 4 clones and two hybridomas that are in stock to clone in the future. The immunoglobulin isotypes were determined by a double immunodiffusion test (Table 15). Ascites fluids were produced from the 3-2B.2 clone and the concentration of

Table 14: Infectious viral particles in extracellular medium of cultures of cells inoculated with HCV-OC43.

Cell type	Time post-inoculation (days)	Infectious titer $TCID_{50}$/ml
Fetal astrocytes	2	3163
	4	3163
	7	31623
Adult microglia	2	100
	4	< 3
	7	< 3
Adult astrocytes and oligodendrocytes	2	56
	4	< 6
	7	< 10
Fetal neuron	4	18

Table 15: List of immunoglobulin isotypes of the produced mouse anti-OC43 monoclonal antibodies.

Clones	IgG Isotype
3-2B.2	2a
2-3C.1	2b
2-3C.2	2b
1-7G.3	2a
Hybridomas	
2-7B	1
1-5G	2a

17.6 mg/ml was determined by a protein assay. Further characterization of these antibodies is in progress.

DISCUSSION

The fact that murine respiratory coronaviruses cause a demyelinating disease in mice suggested a possible equivalent in humans. Furthermore, several studies have reported the finding of human coronaviruses in the central nervous system of patients with multiple sclerosis (Tanaka *et al.*, 1976; Murray *et al.*, 1990; 1992b; Stewart *et al.*, 1992), a demyelinating disease. This suggests a possible neurotropism of human respiratory coronaviruses. Although the neurotropism of human coronaviruses has not yet been proven, studies in immortalized human neural cell lines have shown that these cells can be infected in vitro by HCV, and that the infection can be persistent and productive (Collins and Sorensen, 1986; Talbot *et al.*, 1994; Talbot, personal communication). There is usually a correlation between the *in vitro* and *in vivo* systems, however, there is always a possibility of cell alteration in the *in vitro* cell immortalization process which could modify the virus/host interactions. In order to use the closest model to *in vivo*, we used primary cultured human neural cells to verify infectability by human coronaviruses. A study reported that astrocytes in a primary culture of embryo brain cells were infectable with OC43 (Pearson and Mims, 1985). Unfortunately, there was no description of the methodology used and no controls of any kind were mentioned.

To detect viral antigens in *in vitro* inoculated human neural primary cultured cells, we used an indirect immunofluorescence test. To determine the infected cell type, we used the indirect double immunofluorescence technique where the viral antigen and the cell

marker were labeled in the same field. The indirect labeling required two antibodies produced in different animal species in order to avoid recognition of both antibodies by the fluorochrome-conjugated secondary antibody. In the case of HCV-OC43, due to the animal species in which the commercial markers were produced, we needed to use an anti-OC43 antibody produced in an animal species other than mouse or rabbit. For this purpose we produced a guinea pig polyclonal antibody.

In preliminary experiments to optimize detection techniques, we observed non-viral specific fluorescence with the monoclonal antibodies, most likely due to their attachment to cells by their Fc portions (Oleszak and Leibowitz, 1990). To solve this problem we digested the monoclonal antibodies with pepsin and purified $F(ab')_2$ fragments devoid of the Fc portion. The biological activity of the fragments was verified in an immunofluorescence test. Antibodies to cell markers were also tested. All the antibodies chosen, that is anti-virus, cell marker, or fluorochrome-conjugated were tested in immunofluorescence at different dilutions to determine the optimal dilution to be consistently used in the immunofluorescence tests.

Even though we chose antibodies to cell markers and anti-viral antibody made in different species, we wanted to make sure that the fluorochrome-conjugated antibodies were specific to their species and did not cross-react. To do this, we tested all possible combinations that could be encountered in the immunofluorescence tests. There

was only one antibody that cross reacted, the FITC guinea pig was shown to recognize the mouse immunoglobulins. Therefore no experiments were designed where these two antibodies interacted. Once all the antibodies where checked and the technique was optimized, we proceeded with the immunofluorescence tests of the infected primary cultured neural cells.

To ensure that the immunofluorescence observed in the inoculated primary cells was specific to viral antigens, we used a set of controls in each experiment. The first control chosen was a double immunofluorescence in non-infected cells to verify viral-free samples and any possible non viral-specific fluorescence. The second was a replacement of the antiviral antibody with the dilution buffer in order to detect a possible overlapping in the wavelengths of the fluorochromes (fluorescein and rhodamine). The third was a replacement of the antiviral antibody with an isotypic control in the case of mAb or by a pre-immune serum in the case of a polyclonal antibody to verify that there was not a non-specific binding of antibodies to the cells. All inoculations were done at a high MOI, 4 or 8, to make sure that there was enough virus to infect all cells. Because we used an anti-virus monoclonal antibody, we were sacrificing sensitivity for specificity. The mAb would only recognize one epitope of a single viral protein, so we decided to include an anti-virus polyclonal antibody to broaden the spectrum of viral detection.

For HCV-229E, there were no positive results in immunofluorescence. In the case of HCV-OC43, we found that human fetal astrocytes, adult microglia, and adult astrocytes were infectable. At 2 days post-inoculation 10% of the human fetal astrocytes were infected, at 4 days, 50 to 70% and at 7 days, 90 to 100%. For the human adult microglia, 10% of the culture was infected at 2 days post-inoculation, 40% at 4 days, and 80 to 100% at 7 days. Quantitation of infected cells was made possible by the double labeling, the non-infected cells were positive for the cell marker but negative for the viral antigen. The fluorescence observed was typical of coronaviral infection, that is strictly cytoplasmic since the viral replication cycle takes place only in the cytoplasm (Holmes, 1990). We also observed a concentration of antigens in vacuole-like formations. This was corroborated by electron microscopy of thin sections of infected cells, where accumulation of HCV was observed in vacuoles of human fetal astrocytes. Human adult neurons and oligodendrocytes were not infectable.

Results obtained with HCV-229E were somewhat surprising because it has been reported that viral RNA of this HCV strain could be detected in brains of some MS patients. This suggested that perhaps the immunofluorescence technique was not sensitive enough to detect the viral antigens. As an alternative we used RT-PCR/Southern-blotting to detect viral RNA in the infected cells. Because the amount of cells present in the discs of primary cultured cells was very low compared to continuous cells lines where the RT-PCR was optimized,

we were concerned that we would not have enough viral RNA for amplification and detection. To determine the limits of detection, we ran an RT-PCR with ten-fold serial dilutions of RNA extracted from L132 cells at 20 hrs. post-inoculation with HCV-229E. We were able to detect the amplification of viral genome from as little as $7.1x10^{-7}$ µg of total RNA in an agarose gel stained with ethidium bromide (Figure 16) and from as little as $7.1x10^{-9}$ µg of total RNA in hybridization (Figure 17). These results showed that we had enough neural cell specific RNA to detect viral RNA. We obtained positive results for human fetal astrocytes, human adult microglia, and for a mix of adult oligodendrocytes and adult astrocytes. Unfortunately, because the latter sample was a mix of cells, we cannot conclude as to which cell type is infected. We could not test fetal neurons by RT-PCR due to a shortage of samples.

To make sure that the viral RNA detected was in fact the genome of internalized or newly produced viral particles in inoculated cells and not from adsorbed virus on the cell surface we ran a control test. We used HeLa cells that are susceptible to 229E infection, and we allowed the virus to adsorb for 2 hours at 4°C. An RT-PCR/Southern blotting was performed with the RNA of non-infected, cell-adsorbed virus and cells at 7 days post-inoculation. We only obtained positive results for the 7 days post-inoculation sample, which proved that the viral RNA amplified was produced in the infected cells.

The use of enriched primary human neural cell cultures enabled us in most cases to determine which cell type was infectable and also to determine which cell type could produce infectious virus. All the previous reports on infection of primary cultures besides the one of Sharpless *et al.* (1992) with HIV used cell mixes. These results are also important since molecular data of viral RNA detection by RT-PCR in CNS tissue from human patients only indicates the presence of virus in the CNS but cannot define in which cell the virus is found and if this virus has been produced there or elsewhere, unless *in situ* hybridization is used (Murray *et al.*, 1992b).

To verify the productivity of the infection, an indirect immunoperoxidase test was conducted on the cell culture supernatants from coronavirus-susceptible cells. With HCV-229E, only human fetal astrocytes were shown to produce infectious virus. The titers obtained were very low, which could explain the negative results obtained in immunofluorescence and at the same time the positive results in RT-PCR/Southern-blotting. That is, the cells are infected but they produce low levels of progeny virus. As for HCV-OC43, adult microglia and fetal neurons did not produce significant amounts of infectious virus. On the other hand, fetal astrocytes produced a significant titer of infectious virus and there was a clear increase in titer with time after infection. This was also seen using the immunofluorescence technique. We also obtained low titers of HCV-OC43 in the mix of adult oligodendrocytes and astrocytes. Since it was a mix we cannot conclude which cell type produced the virus, but we are inclined to

think that the virus comes from infected astrocytes. This is supported by the fact that the mixed cell cultures were 80-90% oligodendrocytes and by the results from an immunofluorescence assay in which the only fluorescent cells in the mix, were all positive for GFAP staining, the astrocytes marker. It is important to note that we could not label the oligodendrocytes in our immunofluorescence assay. Another aspect to consider is that we did not have control over the number of cells plated in each culture dish, which may reflect in the difference in viral titers obtained from different cultures.

The difference in the degree of infectability of the two strains is not a surprise since this phenomena has been reported in the mouse model with murine coronavirus (Dubois-Dalcq *et al.*, 1982; Gagneten *et al.*, 1995). It is hard at this point to speculate why strain HCV-229E infects poorly when compared to HCV-OC43 since there is not enough molecular data available for both strains. It may be due to a difference in receptors expressed in the neural cells. Again, the receptor for OC43 is not yet known so it is only a hypothesis. Another explanation could be the presence of an intracellular factor used by one of the strains which facilitates infection. The infectability pattern of the virus found in the present study is similar to the one observed in mouse neural primary cultured cells infected with HCV-OC43 as well as in the study with primary human embryo brain cell culture (Pearson and Mims, 1985). Similarly, studies with murine coronaviruses have shown that all neural cells can be infected but each strain has a different pattern of infection (Dubois-Dalcq *et al.*,

1982; Suzumura *et al.*, 1986; Gagneten *et al.*, 1995). It is interesting to see that in the murine model, as well as, in the human one there are overlapping results; a low or nil infectability of neurons and a very high infectability of astrocytes. On the other hand, the results with continuous cell lines do not correlate with those from primary cell lines, where both HCV strains -229E and -OC43 show high infectability, high infectious titers and where all the immortalized cell types are infectable (Talbot *et al.*, 1994; Talbot personal communication). Although our study provides more detailed information on the characterization of the infection of human neural cells by human coronaviruses, there is a need of further investigation to understand the neurotropism of coronavirus.

It is difficult to compare coronavirus infection of neural cells to other viral systems because there are very few reports of *in vitro* infection of human neural cells. From the data available it can be seen that neurotropic viruses usually target a specific neural cell type. For example, it is suggested that HSV and JC virus infect astrocytes, although these studies are not conclusive. In a more complete study, HIV-1 has been shown to selectively infect microglia (Brynmor *et al.*, 1990; Sharpless *et al.*, 1992; Lee *et al.*, 1993). It is very important to understand which neural cell type is susceptible to infection by human coronaviruses to make the link between a neurological disease and this agent.

CONCLUSION

The goal of this project was to characterize the infectability of primary cultured human neural cells by human coronaviruses 229E and OC43.

We have demonstrated that fetal astrocytes, adult microglia, and a mix of adult oligodendrocytes and astrocytes are infectable by HCV-229E. The infection seems to occur at a low level, since viral RNA could only be detected in inoculated cells using a RT-PCR/Southern blotting technique, but no viral antigens could be detected using indirect immunofluorescence and only fetal astrocytes produced very low titers of infectious virus. Viral antigens could not be detected in neurons but these cells could not be tested in RT-PCR due to a lack of samples.

We have demonstrated by indirect immunofluorescence that fetal astrocytes, adult astrocytes, and adult microglia are susceptible to infection by HCV-OC43, while adult oligodendrocytes are not. Adult microglia did not produce infectious virus while fetal astrocytes produced high titers which increased with time of infection. The mix of adult oligodendrocytes and astrocytes produced low titers of infectious virus. The virus from these cells could have been produced by the astrocytes since they were positive in immunofluorescence and the oligodendrocytes were not. Viral antigens could not be detected in neurons and these cells did not produce infectious virus, suggesting that they are not infectable. This could be verified in the future with

the availability of more cells for testing with the more sensitive RT-PCR/Southern-blotting technique.

The results obtained in this project are consistent with the hypothesis of the neurotropism of human coronaviruses and their possible implication in a neurological disease such as multiple sclerosis. However, the use of *in situ* techniques on brain or spinal cord sections will be needed to clearly demonstrate the neurotropism of human respiratory coronaviruses.

ACKNOWLEDGMENTS

I would like to express my appreciation to each member of the "Les Talbotins" team who contributed in this project with their ideas, technical or moral support.

I would like to thank Dr. Voon Wee Yong for the interest showed in the research and for all the help given.

I would also like to thank Dr. Robin Levis for proofreading the manuscript.

I dearly want to thank Dr. Thomas Fisher and Bruna Bonavia-Fisher for helping me in such trying times...

BIBLIOGRAPHY

ALLEN, I., AND BRANKIN, B. 1993. Pathogenesis of multiple sclerosis-the immune diathesis and the role of viruses. J. Neuropathology & Experimental Neurology, 52(2):95-105

ALMEIDA, J. D., AND TYRRELL, D. A. J. 1967. The morphology of three previously uncharacterized human respiratory viruses that grow in organ culture. J. Gen. Virol., 1:175-178

ALMEIDA, J. D., BERRY, D. M., CUNNINGHAM, C. H., HAMRE, D., HOFSTAD, M. S., MALLUCCI, L., McINTOSH, K., AND TYRRELL, D. A. J. 1969. Coronaviruses. Nature, 220:650

ALTER, M., LEIBOWITZ, U., AND SPEER, J. 1966a. Risk of multiple sclerosis related to age at immigration to Israel. Arch. Neurol., 15(3):234-237

ALTER, M., LEIBOWIZ, U., AND HALPERN, L. 1966b. Multiple sclerosis in European & Afro-Asian population of Israel. A clinical appraisal. Acta. Neurol. Scand., 42(Suppl 19):47-54

BARIC, R. S., STOHLMAN, S. A., AND LAI, M. M. 1983. Characterization of replicative intermediate RNA of mouse hepatitis virus: presence of leader RNA sequence on nascent chains. J. Virol., 48(3):633-640

BARIC, R. S., STOHLMAN, S. A., RAZAVI, M. K., AND LAI, M. M. 1985. Characterization of leader-related small RNAs in coronavirus-infected cells: further evidence for leader-primed mechanism of transcription. Virus Res., 31(1):19-33

BELL, T. M., CASPARY, E. A., COWSHALL, S., FIELD, E. J., NARANG, H. K., AND NOBLE, T. C. 1972. Measles virus associated with an unusual subacute encephalitis in an infant. J. Neurol. Sci., 16(4):455-463

BOERMAN, R. H., BAX, J. J., BEEKHUIS-BRUSSEE, J. A., MEDAER, R., AND BOLLEN, L. E. 1993. JC virus and multiple sclerosis: a refutation?. Acta Neurol. Scand., 87(5):353-355

BOYLE, J. F., WISMILLER, F. G., AND HOLMES, K. V. 1987. Genetic resistance to mouse hepatitis virus correlates with absence of virus-binding activitiy on target tissues. J. Virol. 61(1):185-189

BRADBURNE, A. F. 1969 Sensitivity of L132 cells to some "new" respiratory viruses. Nature, 221:85-86

BRADBURNE, A. F., AND SOMERSET, B. A. 1972. Coronavirus antibody titres in sera of healthy adults and experimentally infected volunteers. J. Hyg., Cam., 70:235-245

BROKSTAD, K. A., KALLAND, K. H., PAGE, M., NYLAND, H., AND HAAHEIM, L. 1994. Serum antibodies from MS patients do not recognize HTLV-I, HIV-1, HIV-2 and SIV. APMIS, 102(7):514-520

BROWN, T. D., BOURSNELL, M. E., AND BINNS, M. M. 1984. A leader sequence is present on mRNA A of avian infectious bronchitis virus. J. Gen. Virol., 65(8):1437-1442

BRUCKOVA, M., McINTOSH, K., KAPIKIAN, A. Z., AND CHANOCK, R. M. 1970. The adaptation of two human coronavirus strains (OC38 and OC43) to growth in cell monolayers. Proc. Soc. Exp. Biol. Med., 135(2):431-435

BUCKLE, G. J., GODEC, M. S., RUBI, J. U., TORNATORE, C., MAJOR, E. O., GIBBS, C. J. Jr., GAJDUSEK, D. C., AND ASHER, D. M. 1992. Lack of JC viral genomic sequences in multiple sclerosis brain tissue by polymerase chain reaction. Ann. Neurol., 32(6):829-831

BUCKNALL, R. A., KING, L. M., KAPIKIAN, A. Z., AND CHANOCK, R. M. 1972. Studies with human coronaviruses. II. Some properties of strains 229E and OC43. Proc. Soc. Exp. Biol. Med., 139(3):722-727

BUDZILOWICZ, C. J., WILCZYNSKI, S. P., AND WEISS, S. R. 1985. Three intergenic regions of coronavirus mouse hepatitis virus strain A59 genome RNA contain a common nucleotide sequence that is homologous to the 3' end of the viral mRNA leader sequence. J. Virol., 53(3):834-840

BURKS, J. S., DEVALD, B. L., JANKOVSKI, L. D., AND GERDES, J. C. 1980. Two coronaviruses isolated from central nervous system tissue of two multiple sclerosis patients. Science, 209:933-934

CAVANAGH, D. 1983. Coronavirus IBV: structural characterization of the spike glycoprotein. J. Gen. Virol., 64:2577-2583

CHAMBON, M., LAVERAN, H., L'HARIDON, R., PEIGUE-LAFEUILLE, H., TRIMOLET, M., AND BEYTOUT, D. 1987. Enquête sérologique par immunofluorescence indirecte sur les infections à coronavirus OC43. Ann. Insti. Pasteur/Virol., 138:263-268

COLLINS, A. R., KNOBLER, R. L., POWELL, H., AND BUCHMEIER, M. J. 1982. Monoclonal antibodies to murine hepatitis virus-4 (strain JHM) define the viral glycoprotein responsible for attachment and cell-cell fusion. Virology, 119:358-371

COLLINS, A. R., AND SORENSEN, O. 1986. Regulation of viral persistence in human glioblastoma and rhabdomyosarcoma cells infected with coronavirus OC43. Microb. Pathog., 1(6):573-582

CONRAD, A. J., CHIANG, E. Y., ANDEEN, L. E., AVOLIO, C., WALKER, S. M., BAUMHEFNER, R. W., MIRZAYAN, R., AND TOURTELLOTTE, W. W. 1994. Quantitation of intrathecal measles virus IgG antibody synthesis rate: subacute sclerosing panencephalitis and multiple sclerosis. J. Neuroimmunol., 54(1-2):99-108

COSBY, S. L., McQUAID, S., TAYLOR, M. J., BAILEY, M., RIMA, B. K., MARTIN, S. J., AND ALLEN I. V. 1989. Examination of eight cases of multiple sclerosis and 56 neurological and non-neurological controls for genomic sequences of measles virus, canine distemper virus, simian virus 5 and rubella virus. J. Gen. Virol., 70(8):2027-2036

DANIEL, C., AND TALBOT, P. J. 1990. Protection from lethal coronavirus infection by affinity-purified spike glycoprotein of murine hepatitis virus, strain A59. Virology, 174:87-94

DAVID-FERREIRA, J. F., AND MANAKER, R. A. 1986. An electron microscope study of the development of a mouse hepatitits virus in tissue culture cells. J. Cell Biol., 24:57-58

DEAN, G., AND KURTZKE, J. F. 1971. On the risk of multiple sclerosis according to age at immigration to South Africa. Br. Med. J., 3(777):725-729

DOWLING, P. C., BLUMBERG, B. M., KOLAFOFSKY, D., COOK, P., JOTKOWITZ, A., PRINEAS, J. W., AND COOK, S. D. 1986. Measles virus nucleic acid sequences in human brain. Virus Res., 5(1):97-107

DUBOIS-DALCQ, M. E., DOLLER, E. W., HASPEL, M. V., AND HOLMES, K. V. 1982. Cell tropism and expression of mouse hepatitis viruses (MHV) in mouse spinal cord cultures. Virology, 119:317-331

DUQUETTE, P., PLEINES, J., AND GIRARD, M. 1992. The increased susceptibility of women to multiple sclerosis. Can. J. Neurol. Sci., 19(4):466-471

EBERS, G. C., AND SADOVNICK, A. D. 1993. The geographic distribution of multiple sclerosis: a review. Neuroepidemiology, 12:1-5

GAGNETEN, S., GOUT, O., DUBOIS-DALCQ, M., ROTTIER, P., ROSSEN, J., AND HOLMES, K. V. 1995. Interaction of mouse hepatitis virus (MHV) spike glycoprotein with receptor glycoprotein MHVR is required for infection with an MHV strain that expresses the hemagglutinin-esterase glycoprotein. J. Virol., 69:889-895

GERDES, J. C., KLEIN, I., DeVALD, B. L., AND BURKS, J. S. 1981. Coronavirus isolates SK and SD from multiple sclerosis patients are serologically related to murine coronaviruses A59 and JHM and human coronavirus OC43 but not to human coronavirus 229E. J. Virol., 38:231-238

GODEC, M. S., ASHER, D. M., SWOVELAND, P. T., ELDADAH, Z. A., FEINSTONE, S. M., GOLDFARB, L. G., GIBBS, C. J., AND GAJDUSEK, D. C. 1990. Detection of measles virus genomic sequences in SSPE brain tissue by the polymerase chain reaction. J. Med. Virol., 30(4):237-244

HAAHR, S., SOMMERLUND, M., CHRISTENSEN, T., JENSEN, A. W., HANSEN, H. J., AND MOLLER-LARSEN, A. 1994. A putative new retrovirus associated with multiple sclerosis and the possible involvement of Epstein-Barr virus in the disease. Ann. NY. Acad. Sci., 724:148-156

HAASE, A. T., VENTURA, P., GIBBS, C. J. Jr., TOURTELLOTTE, W., W. 1981a. Measles virus nucleotide sequences: detection by hybridization in situ Science, 212(4495):672-675

HAASE, A. T., SWOVELAND, P., STOWRING, L., VENTURA, P., JOHNSON, K. P., NORRBY, E., AND GIBBS, C. J. Jr. 1981b. Measles virus genome in infections of the central nervous system. J. Infect. Dis., 144(2):154-160

HAMRE, D., AND PROCKNOW, J. J. 1966. A new virus isolated from the human respiratory tract. Proc. Soc. Exp. Biol. Med., 121:190-193

HAUSER, S. L. 1994. Multiple sclerosis and other demyelinating diseases. In: Harrisson's principles of internal medicine. McGraw Hill eds., New York, USA

HEROLD, J., RAABE, T., AND SIDDELL, S. G. 1993. Characterization of the human coronavirus 229E (HCV-229E) gene 1. Adv. Exp. Med. Biol., 342:75-79

HILLERT, J., AND OLERUP, O. 1993. Multiple sclerosis is associated with genes within or close to the HLA-DR-DQ subregion on a normal DR15, DQ6, DW2 haplotype. Neurology, 43(1):163-168

HILTON, D. A., LOVE, S., FLETCHER, A., AND PRINGLE, J. H. 1994. Absence of Epstein-Barr virus RNA in multiple sclerosis as assessed by in situ hybridization. J. Neurol. Neurosurg. Phsychiatry, 57(8):975-976

HOFFMAN, P. M., DHIB-JALBUT, S., MIKOVITS, J. A., ROBBINS, D. S., WOLF, A. L., BERGEY, G. K., LOHREY, N. C., WEISLOW, O. S., AND RUSCETTI, F. W. 1992. Human T-cell leukemia virus type I infection of monocytes and microglial cells in primary human cultures. Proc. Natl. Acad. Sci. USA, 89(24):11784-11788

HOGUE, B. G., AND BRIAN, D. A. 1986. Structural proteins of human respiratory coronavirus OC43. Virus Research, 5:131-134

HOLLSBERG, P., MOLLER-LARSEN, A., SKOU PEDERSEN, F., JUSTESEN, J., HANSEN, H. J., AND HAAHR, S. 1989. Search for a retrovirus in long-term cultured cerebrospinal fluid cells and peripheral blood mononuclear cells from patients with multiple sclerosis. Acta Neurol. Scand., 80(6):603-609

HOLMES, K. V., DOLLER, E. W., AND BEHNKE, J. N. 1981. Analysis of the functions of coronavirus glycoproteins by differential inhibition of synthesis with tunicamycin. Adv. Exp. Med. Biol., 142:133-142

HOLMES, K. V., FRANA, M. F., ROBBINS, S. G., AND STURMAN, L. S. 1984. Coronavirus maturation. Adv. Exp. Med. Biol., 173:37-52

HOLMES, K. V., WILLIAMS, R. K., STEPHENSEN, C. B. 1989. Coronavirus receptors. In: Notkins A, Oldstone MBA, eds. Concepts in viral pathogenesis III. New York: Springer-Verlag, pp. 106-113

HOLMES, K. V. 1990. Coronaviridae and their replication. In: B N Fields, Virology. D M Knipe et al., Raven Press, New York.

HOLMES, K. V., DVEKSLER, G., GAGNETEN, S., YEAGER, C., LIN, S-H., BEAUCHEMIN, N., LOOK, A. T., ASHMUN, R., AND DIEFFENBACH, C. 1994. Coronavirus receptors specificity. Adv. Exp. Med. Biol., 342:261-266

HOVANEC, D. L., AND FLANAGAN, T. D. 1983. Detection of antibodies to human coronavirus 229E and OC43 in the sera of multiple sclerosis patients and normal subjects. Infection and Immunity, 41(1):426-429

JOHNSON, R. T. 1985. Viral aspects of multiple sclerosis. In: Handbook of clinical neurology. J C Koetsier ed. Elsevier Science Publishers

JOUVENNE, P., RICHARDSON, C. D., SCHREIBER, S. S., LAI, M. M. C., AND TALBOT, P. J. 1990. Sequence analysis of the membrane protein gene of human coronavirus 229E. Virology, 174:608-612

JOUVENNE, P., MOUNIR, S., STEWART, J. N., RICHARDSON, C. D., AND TALBOT, P. J. 1992. Sequence analysis of human coronavirus 229E mRNA 4 and 5: evidence for polymorphism and homology with myelin basic protein . Virus Res., 22:125-141

JOUVENNE, P. ARPIN, N., AND TALBOT, P. J. 1994. Characterization and antigenicity of the M glycoprotein of human coronavirus 229E. Mol. Biol. (Life. Sci. Adv.), 13:113-123

KAMAHORA, T., SOE, L. H., AND LAI, M. M. C. 1989. Sequence analysis of nucleocapsid gene and leader RNA of human coronavirus OC43. Virus Res., 12:1-9

KAPIKIAN, A. Z., JAMES H. D. Jr., KELLY, S. J., DEES, J. H., TURNER, H. C., McINTOSH, K., KIM, H. W., PARROTT, R. H., VINCENT, M. M., AND CHANOCK, R. M. 1969. Isolation from man of "avian infectious bronchitis virus-like" viruses (coronaviruses) similar to 229E virus, with some epidemiological observations. J. Infect. Dis., 119(3):282-290.

KAPIKIAN, A. Z., JAMES, H. D. Jr., KELLY, S. J., KING, L. M., VAUGHN, A. L., AND CHANOCK, R. M. 1972. Hemadsorption by coronavirus strain OC43. Proc. Soc. Exp. Biol. Med., 139(1):179-186

KAPIKIAN, A. Z., JAMES, H. D., KELLY, S. J., AND VAUGHN, A. L. 1973. Detection of coronavirus strain 692 by immune electron microscopy. Infect. Immun., 7:111-116

KENDALL, E. J. C., BYNOE, M. L., AND TYRRELL, D. A. J. 1962. Virus isolation from common colds occurring in a residential school. Brit. Med. J., 2:82-86

KENNEDY, D. A., AND JOHNSON-LUSSENBURG, C. M. 1975. Isolation and morphology of the internal component of human coronavirus, strain 229E. Intervirology, 6(4-5):197-206

KENNEDY, D. A., AND JOHNSON-LUSSENBURG, C. M. 1978. Inhibition of coronavirus 229E replication by actinomycin D. J. Viro., 29(1):401-404

KENNEDY, P. G. E., CLEMENTS, G. B., AND BROWN, S. M. 1983. Differential susceptibility of human neural cell types in cultures to infection with Herpes Simplex Virus. Brain, 106:101-119

KING, B., AND BRIAN, D. A. 1982. Bovine coronavirus structural proteins. J. Virol., 42(2):700-707

KIRA, J., KOYANAGI, Y., YAMADA, T., ITOYAMA, Y., TATEISHI, J., AKIZUKI, S., KISHIKAWA, M., BABA, E., NAKAMURA, M., SUZUKI, J., NAKAMURA, T., NAKAMURA, N., YAMAMOTO, N., AND GOTO, I. 1994. Sequence heterogeneity of HTLV-I proviral DNA in the central nervous system of patients with HTLV-I associated myelopathy. Ann. Neurol., 36(2):149-156

KOOI, C. M., CERVIN, M., AND ANDERSON, R. 1991. Differentiation of acid-pH-dependent and -nondependent entry pathways for mouse hepatitis virus. Virology, 180(1):108-119

KORNER, H., SCHLIEPHAKE, A., WINTER, J., ZIMPRICH, F., LASSMANN, H., SEDGWICK, J., SIDDELL, S., AND WEGE, H. 1991. Nucleocapsid or spike protein-specific CD4+ T lymphocytes protect against coronavirus-induced encephalomyelitis in the absence of CD8+ T cells. J. Immunol., 147(7):2317-2323

KRZYSTNYNIAK, K., AND DUPUY, J. M. 1984. Entry of mouse hepatitis virus 3 into cells. J. Gen. Virol., 65(1):227-231

KÜNKEL, F., AND HERRLER, G. 1993. Structural and functional analysis of the surface protein of human coronavirus OC43. Virology 195:195-202

KURTZKE, J. F. 1980. Epidemiological contributions to multiple sclerosis: an overview. Neurology, 30(7):61-79

KURTZKE, J. F., AND HYLLESTED, K. 1986. Multiple sclerosis in the Faroe Islands. II. Clinical update, transmission, and the nature of MS. Neurology, 36(3):307-328

KURTZKE, J. F. 1991. Multiple sclerosis: changing times. Neuroepidemiology, 10(1):1-8

LAI, M. M., PATTON, C. D., AND STOHLMAN, S. A. 1982a. Replication of mouse hepatitis virus: negative-stranded RNA and replicative form RNA are of genome length. J. Virol., 44(2):487-492

LAI, M. M., PATTON, C. D., AND STOHLMAN, S. A. 1982b. Further characterization of mRNA's of mouse hepatitis virus: presence of common 5' end nucleotides. J. Virol., 41(2):557-565

LAI, M. C. C. 1986. Coronavirus leader-RNA-primed transcription: an alternative mechanism to RNA splicing. BioEssays 5(6):257-260

LAMARRE, A., AND TALBOT, P. J. 1989. Effect of pH and temperature on the infectivity of human coronavirus 229E. Can. J. Microbiol., 35:972-974

LECOMTE, J., CAINELLI-GEBARA, V., MERCIER, G., MANSOUR, S., TALBOT, P. J., LUSSIER, G., AND OTH, D. 1987. Protection from mouse hepatitis virus type 3-induced acute disease by an anti-nucleoprotein monoclonal antibody. Arch. Virol., 97:123-130

LEE, S. C., HATCH, C., LIU, W., KRESS, Y., LYMAN, W. D., AND DICKSON, D. W. 1993. Productive infection of human fetal microglia by HIV-1. American J. Pathol., 143(4):1032-1039

MADDEN, D. L., WALLEN, W. C., HOUFF, S. A., LEINIKKI, P. A., SEVER, J. L., HOLMES K. V., CASTELLANO, G. A., AND SHEKARCHI, I. C. 1981. Coronavirus antibodies in sera from patients with multiple sclerosis and matched controls. Arch. Neurol., 38:209-210

MAKINO, S., SHIEH, C. K., KECK, J. G., AND LAI, M. M. 1988. Defective-interfering particles of murine coronavirus: mechanism of synthesis of defective viral RNAs. Virology, 163(1): 104-111

MARTYN, C. N., CRUDDAS, M., AND COMPSTON, D. A. 1993. Symptomatic Epstein-Barr virus infection and multiple sclerosis. J. Neurol. Neurosurg. Psychiatry, 56(2):167-168

MASTERS, P. S., PARKER, M. M., RICARD, C. S., DUCHALA, C., FRANA, M. F., HOLMES, K. V., AND STURMAN, L. S. 1990. Structure and function studies of the nucleocapsid protein of mouse hepatitis virus. Adv. Exp. Med. Biol., 276:239-246

McINTOSH, K., DEES, J., BECKER, W. B., KAPIKIAN, A. Z., AND CHANOCK, R. M. 1967a. Recovery in tracheal organ cultures of novel viruses from patients with respiratory disease. Proc. Natl. Acad. Sci. USA, 57:933-940

McINTHOSH, K., BECKER, W. B., AND CHANOCK, R. M. 1967b. Growth in suckling-mouse brain of "IBV-like" viruses from patients with upper respiratory tract disease. Proc. Natl. Acad. Sci. USA, 58:2268-2273

McINTOSH, K., BRUCKOVA, M., KAPIKIAN, A. Z., CHANOCK, R. J., AND TURNER, H. 1970a. Studies on new virus isolates recovered in tracheal organ culture. Ann. N. Y. Acad. Sci., 174(2):983-989

McINTOSH, K, KAPIKIAN, A. Z., TURNER, H. C., HARTLEY, J. W., PARROTT, R. H., AND CHANOCK, R. M. 1970b. Seroepidemiologic studies of coronavirus infection in adults and children. Am. J. Epidemiol., 91(6):585-592

McINTOSH, K., CHAO, R. K., KRAUSE, H. E., WASIL, R., MOCEGA, H. E., AND MUFSON, M. A. 1974. Coronavirus infection in acute lower respiratory tract disease of infants. J. Infect. Dis., 130(5):502-507

McKAY, R. P., AND MYRIANTHOROULOS, N. C. 1966. Multiple sclerosis in twins and their relatives. Arch. Neurol., 15:449-462

MIZZEN, L. A., HILTON, A., CHELEY, S., AND ANDERSON, R. 1985. Attenuation of murine coronavirus infection by ammonium chloride. Virology, 142(2):378-388

MOUNIR, S., AND TALBOT, P. J. 1992. Sequence analysis of the membrane protein gene of human coronavirus OC43 and evidence for O-glycosylation. J. Gen. Virol., 73:2731-2736

MOUNIR, S., AND TALBOT, P.J. 1993a. Human coronavirus OC43 RNA 4 lacks two open reading frames located downstream of the S gene of bovine coronavirus. Virology 192:355-360

MOUNIR, S., AND TALBOT, P. J. 1993b. Molecular characterization of the S protein gene of human coronavirus OC43. J. Gen. Virol., 74:1981-1987

MOUNIR, S., LABONTÉ, P., AND TALBOT, P. J. 1994. Characterization of the nonstructural and spike proteins of the human respiratory coronavirus OC43: comparison with bovine enteric coronavirus. Adv. Exp. Med. Biol., 342:61-67

MURRAY, R. S., MacMILLAN, B., CABIRAC, G., AND BURKS, J. S. 1990. Detection of coronavirus RNA in CNS tissue of multiple sclerosis and control patients. Adv. Exp. Med. Biol., 342:505-510

MURRAY, R. S., CAI, G-Y., HOEL, K., ZHANG, J-Y., SOIKE, K. F., AND CABIRAC, G. 1992a. Coronavirus infects and causes demyelination in primate central nervous system. Virology, 188:274-284

MURRAY, R. S., BROWN, B., BRIAN, D., AND CABIRAC, G. F. 1992b. Detection of coronavirus RNA and antigen in multiple sclerosis brain. Ann. Neurol., 31:525-533

MYINT, S., HARMSEN, D., RAABE, T., AND SIDDELL, S. G. 1990. Characterization of a nucleic acid probe for the diagnosis of human coronavirus 229E infections. J. Med. Virol., 31(2): 165-72

MYINT, S. H. 1994. Human coronaviruses: a brief review. Rev. Med. Virol., 4:35-46

MYHR, K. M., FROST, P., GRONNING, M., MIDGARD, R., KALLAND, K. H., HELLAND, D. E., AND NYLAND, H. I. 1994. Absence of HTLV-I related sequences in MS from high prevalence areas in western Norway. Acta. Neurol. Scand., 89(1):65-68

NICOLL, J. A., KINRADE, E., AND LOVE, S. 1992. PCR-mediated search for herpes simplex virus DNA in sections of brain from patients with multiple sclerosis and other neurological disorders. J. Neurol. Sci., 113(2):144-151

OGER, J., SABOURAUD, O., AND ARNASON, B. 1987. Génétique de la sclérose en plaques. Médecine/Sciences, 3:13-18

OKSENBERG, J. R., MANTEGAZZA, R., SAKAI, K., BERNARD, C. C., AND STEINMAN, L. 1990. HTLV-I sequences are not detected in peripheral blood genomic DNA or in brain cDNA of multiple sclerosis patients. Ann. Neurol., 28(4):574-577

OLESZAK, E. L., AND LEIBOWITZ, J. L. 1990. Immunoglobulin Fc binding activity is associated with the mouse hepatitis virus E2 peplomer protein. Virology, 176:70-80

PANITCH, H., PETURSSON, G., GEORGSSON, G., PALSSON, P. A., AND NATHANSON, N. 1976. Pathogenesis of visna. III. Imune responses to central nervous system antigens in experimental allergic encephalomyelitis and visna. Lav. Invest., 35(5):452-460

PEARSON, J., AND MIMS, C. A. 1983. Selective vulnerability of neural cells and age-related susceptibility to OC43 virus in mice. Arch. Virol., 77:109-118

PEARSON, J., AND MIMS, C. A. 1985. Differential susceptibility of cultured neural cells to the human coronavirus OC43. J. Virol., 53, 1016-1019

PERRON, H., GENY, C., LAURENT, A., MOURIQUAND, C., PELLAT, J., PERRET, J., AND SEIGNEURIN, J. M. 1989. Leptomeningeal cell line from multiple sclerosis with reverser transcriptase activity and viral particles. Res. Virol., 140(6):551-561

POKORNY, J., BRUCKOVA, M., AND RYC, M. 1975. Biophysical properties of coronavirus strain OC43. Acta Virol., 19(2):137-142

RAABE, T., AND SIDDELL, S. G. 1989a. Nucleotide sequence of the gene encoding the membrane protein of human coronavirus 229E. Arch. Virol., 107:323-328

RAABE, T., AND SIDDELL, S. G. 1989b. Nucleotide sequence of the human coronavirus 229E mRNA 4 and mRNA 5 unique regions. Nucleic Acids Res., 17:6387

RAABE, T., SCHELLE-PRINZ, B., AND SIDDEL, S. G. 1990. Nucleotide sequence of the gene encoding the spike glycoprotein of human coronavirus 229E. J. Gen. Virol., 71:1065-1073

RASMUSSEN, H. B., AND CLAUSEN, J. 1992. Search for a retrovirus in multiple sclerosis by enzymatic amplification of DNA from brain capillaries, brain tissue and mononuclear cells from peripheral blood. Acta Neurol. Scand., 86(1):87-90

REDDY, E. P., SANDBERG-WOLLHEIM, M., METTUS, R. V., RAY, P.E., DeFREITAS, E., AND KOPROWSKI, H. 1989. Amplification and molecular cloning of HTLV-1 sequences fom DNA of multiple sclerosis patients. Science, 243(4890):529-533

RESTA, R., LUBY, J. P., ROSENFELD, C. R., AND SIEGEL, J. D. 1985. Isolation and propagation of a human enteric coronavirus. Science, 229:978-981

RICARD, C. S., AND STURMAN, L. S. 1985. Isolation of the subunits of the coronavirus envelope glycoprotein E2 by hydroxyapatite high-performance liquid chromatography. J. Chromatogr., 326:191-197

RISKI, H., AND HOVI, T. 1980. Coronavirus infections of man associated with diseases other than the common cold. J. Med. Virol., 6:259-265

RODGER-JOHNSON, P. E. 1994. Tropical spastic paraparesis/HTLV-I associated myelopathy. Etiology and clinical spectrum. Mol. Neurobiol., 8(2-3):175-179

ROTTIER, P. J., WELLING, G. W., WELLING-WESTER, S., NIESTERS, H. G., LENSTRA, J. A., AND VAN DER ZEIJST, B. A. 1986. Predicted membrane topology of the coronavirus protein E1. Biochemistry, 25(6):1335-1339

SADOVNICK, A., AND MACLEOD, P. M. 1981. The familial nature of multiple sclerosis: empiric recurrence risks from first, second and third degree relatives of patients. Neurology, 31:1039-1041

SALIER, J. P., GOUST, J. M., PANDEY, J. P., AND FUDENBERG, H. H. 1981. Preferential synthesis of GIM(1) allotype of IgG1 in the CNS of MS. Science, 213:1400-1402

SALMI, A., ZIOLA, B., HOVI, T., AND REUNANEN, M. 1982. Antibodies to coronaviruses OC43 and 229E in multiple sclerosis patients. Neurology, 32:292-295

SCHMIDT, O. W., AND KENNY, G. E. 1982. Polypeptides and functions of antigens from human coronaviruses 229E and OC43. Infect. Immun., 35:515-522

SCHREIBER, S. S., KAMAHORA, T., AND LAI, M. M. C. 1989. Sequence analysis of the nucleocapsid gene of human coronavirus 229E. Virology, 169:142-151

SHARPLESS, N., GILBERT, D., VANDERCAM, B., ZHOU, J. M., VERDIN, E., RONNETT, G., FRIEDMAN, E., AND DUBOIS-DALCQ, M. 1992. The restricted nature of HIV-1 tropism for cultured neural cells. Virology, 191:813-825

SHIEH, C. K., SOE, L. H., MAKINO, S., CHANG, M F., STOHLMAN, S. A., AND LAI, M. M. 1987. The 5'-end sequence of the murine coronavirus genome: implications for multiple fusion sites in leader-primed transcription. Virology, 156(2):321-330

SIDDELL, S., WEGE, H., AND TER MEULEN, V. 1982. The structure and replication of coronaviruses. Curr. Top. Microbiol. Immunol., 99:131-163

SIDDELL, S. G., ANDERSON, R., CAVANAGH, D., FUJIWARA, K., KLENK, H. D., MACNAUGHTON, M. R., PENSAERT, M., STOHLMAN, S. A., STURMAN, L., AND VAN DER ZEIJST, B. A. M. 1983. Coronaviridae. Intervirology 20:181-189

SINDIC, C. J., MONTEYNE, P., AND LATERRE, E. C. 1994. The intrathecal synthesis of virus-specific oligoclonal IgG in multiple sclerosis. J. Neuroimmunol., 54(1-2):75-80

SORENSEN, O., COLLINS, A., FLINTOFF, W., EBERS, G., AND DALES, S. 1986. Probing for the human coronavirus OC43 in multiple sclerosis. Neurology, 36:1604-1606

SPAAN, W., CAVANAGH, D., AND HORZINEK, M. C. 1988. Coronaviruses: structure and genome expression. J. Gen. Virol., 69:2939-2952

SPAAN, W., CAVANAGH, D., AND HORZINEK, M. C. 1990. Coronaviruses. In:Immunochemistry of viruses II. The basis for serodiagnosis and vaccines. M H V van Regenmortel and A R Neurath eds. Elsevier Science Publishers B V. pp. 359-379

STERN, D. F., AND KENNEDY, S. I. 1980. Coronavirus multiplication strategy. II. Mapping the avian infectious bronchitis virus intracellular RNA species to the genome. J. Virol., 36(2):440-449

STEWART, G. J., BASTEN, A., AND KIRK, R. L. 1979. Strong linkage disequilibrium in MS. Tissue Antigens, 14:86-97

STEWART, J. N., MOUNIR, S., AND TALBOT, P. 1992. Human coronavirus gene expression in the brains of multiple sclerosis patients. Virology 191:502-505

STOHLMAN, S. A., AND LAI, M. M. 1979. Phosphoproteins of murine hepatitis viruses. J. Virol., 32(2):672-675

STOHLMAN, S. A., BARIC, R. S., NELSON, G. N., SOE, L. H., WELTER, L. M., AND DEANS, R. J. 1988. Specific interaction between coronavirus leader RNA and nucleocapsid protein. J. Virol., 62(11):4288-4295

STONER, G. L. 1993. Polyomavirus models of brain infection and the pathogenesis of multiple sclerosis. Brain. Pathol., 3(3):213-227

STRAUSS, E. G., AND STRAUSS, J. H. 1983. Replication strategies of the single stranded RNA viruses of eukaryotes. Curr. Top. Microbiol. Immunol., 105:1-98

STURMAN , L. S., HOLMES, K. V., AND BEHNKE, J. 1980. Isolation of coronavirus envelope glycoproteins and interaction with the viral nucleocapsid. J. Virol., 33(1):449-462

STURMAN, L. S., AND HOLMES, K. V. 1983. The molecular biology of coronaviruses. Adv. Virus. Res., 28:35-112

STURMAN, L. S., RICARD, C. S., AND HOLMES, K. V. 1985. Proteolytic cleavage of the E2 glycoprotein of murine coronavirus: activation of cell-fusing activity of virions by trypsin and separation of two different 90K cleavage fragments. J. Virol., 56:904-911

SUZUMURA, A., LAVI, E., WEISS, S. R., AND SILBERBERG, D. H. 1986. Coronavirus infection induces H-2 antigen expression on oligodendrocytes and astrocytes. Science, 232:991-993

SVENNINGSSON, A., LYCKE, J., SVENNERHOLM, B, GRONOWITZ, S., AND ANDERSEN, O. 1992. No evidence for spumavirus or oncovirus infection in relapsing-remitting multiple sclerosis. Ann. Neurol., 32(5):711-714

SWEENEY, B. J., MILLER, R. F., AND HARRISON, M. J. 1993. Progressive multifocal leucoencephalopathy. Br. J. Hosp. Med., 50(4):187-192

SWOVELAND, P. T. 1991. Molecular events in measles virus infection of the central nervous system. Int. Rev. Exp. Pathol., 32:255-275

TALBOT, P. J., SALMI, A. A., KNOBLER, R. L., AND BUCHMEIER, M. J. 1984. Topographical mapping of epitopes on the glycoproteins of murine hepatitis virus-4 (strain JHM): correlation with biological activities. Virology, 132(2):250-260

TALBOT, P. J., ÉKANDÉ, S., CASHMAN, N. R., MOUNIR, S., AND STEWART, J. N. 1994. Neurotropism of human coronavirus 229E. Adv. Exp. Med. Biol., 342:339-346

TALBOT, P. 1995. Implication des virus dans la sclérose en plaques. Medecine-Sciences. Médecine/sciences, 11(6):827-8443.

TANAKA, R., IWASAKI, Y., AND KOPROWSKI, H. 1976. Intracisternal virus-like particles in brain of a multiple sclerosis patient. J. Neurol. Sci., 28:121-126

TOOZE, J., TOOZE, S., AND WARREN, G. 1984. Replication of coronavirus MHV-A59 in Sac(-) cells determination of the first site of budding of progeny virions. Eur. J. Cell. Biol., 33(2):281-293

TYRRELL, D. A. J., AND BYNOE, M. L. 1965. Cultivation of a novel type of common cold virus in organ cultures. Br. Med. J., 1:1467-1470

TYRRELL, D. A., ALMEIDA, J. D., CUNNINGHAM, C. H., DOWDLE, W. R., HOFSTAD, M. S., McINTOSH, K., TAJIMA, M., ZAKSTELSKAYA, L. Y., EASTERDAY, B. C., KAPIKIAN, A., AND BINGHAM, R. W. 1975. Coronaviridae. Intervirology, 5(1-2):76-82

VAGABOV, R. M., SKVORTSOVA, T. M., GOFMAN, YU, P., AND BARINSKY, I. F. 1982. Isolation of the tick-borne encephalitis virus from a patient with multiple slerosis. Acta Virol., 26(5):403

VLASAK, R., LUYTJES, W., SPAAN, W., AND PALESE, P. 1988. Human and bovine coronaviruses recognize sialic acid-containing receptors similar to those of influenza C viruses. Proc. Natl. Acad. Sci. USA, 85:4526-4529

WANG, F. I., STOHLMAN, S. A., AND FLEMING, J. O. 1990. Demyelination induced by murine hepatitis virus JHM strain (MHV-4) is immunological mediated. J. Neuroimmunol., 30(1):31-41

WATABE, K., SAIDA, T., AND KIM, S. 1989. Human and simian glial cells infected by T-lymphotropic virus type I in culture. J. Neuropat. Exp. Neuro., 48(6):610-619

WATKINS, B. A., DORN, H. H., KELLY, W. B., ARMSTRONG, R. C., POTTS, B. J., MICHAELS, F., KUFTA, C. V., AND DUBOIS-DALCQ, M. 1990. Specific tropism of HIV-1 for microgial cells in primary human brain cultures. Science, 249:549-553

WELSH, C. J., TONKS, P., BORROW, P., AND NASH, A. A. 1990. Theiler's virus: an experimental model of virus-induced demyelination. Autoimmunity, 6(1):105-112

WROBLEWSKA, Z., GILDEN, D., DEVLIN, M., HUANG, E. S., RORKE, L. B., HAMADA, T., FURUKAWA, T., CUMMINS, L., KALTER, S., AND KOPROWSKI, H. 1979. Cytomegalovirus isolation from a chimpanzee with acute demyelinating disease after inoculation of multiple sclerosis brain cells. Infect. Immun., 25(3):1008-1015

WROBLEWSKA,Z., KENNEDY, P. G. E., WELLISH, M. C., LISAK, R. P., AND GILDEN, D. 1982. Demonstration of JC virus by immunofluorescence in multiple cell types in experimentally infected adult human brain cell cultures. J. Neurol. Sci., 54:189-196

YEAGER, C. L., ASHMUN, R. A., WILLIAMS, R. K., CARDELLICHIO, C. B., SHAPIRO, L. H., LOOK, A. T., AND HOLMES, K. V. 1992. Human aminopeptidase N is a receptor for human coronavirus 229E. Nature, 357(6377):420-422

YONG, V. W., AND ANTEL, J. 1992. Culture of glial cells from human brain biopsies, in: Protocols for Neural Cell culture, S. Fedoroff and A. Richardson eds., pp81-96, Humana Press, New Jersey, USA.

YONG, V. W., TEJADA-BERGES, T., GOODYER, C. G., ANTEL, J. P., AND YONG F. P. 1992. Differential proliferative response of human and mouse astrocytes to gamma-interferon. Glia, 2:269-280

ZHANG, X. M., KOUSOULAS, K. G., AND STORZ, J. 1992. The haemagglutinin/esterase gene of human coronavirus strain OC43:

phylogenetic relationships to bovine and murine coronaviruses and influenza C virus. Virology, 186:318-323